Modelling the Transmission of Tuberculosis

Chacha M. Issarow

Supervisors: Prof Nicola Mulder and Prof Robin Wood

A thesis submitted in partial fulfillment of the requirements
for the degree of Doctor of Philosophy in the Department
of Integrative Biomedical Sciences at the Faculty
of Health Sciences, University of Cape Town

University of Cape Town, South Africa

August 15, 2016

Declaration

I, Chacha Marwa Issarow, hereby declare that the work contained in this thesis is my original work (except where acknowledgements indicate otherwise) and that neither the whole work nor any part of it has been, is being, or is to be submitted for another degree in this or any other University. I authorise the University to reproduce for the purpose of research either the whole or any portion of the contents in any manner whatsoever.

Signature: Date: August 15, 2016

Signed by candidate

Summary

Airborne infectious diseases, such as tuberculosis (TB), are spread by airborne infectious particles (viable particles with potential for TB infection) in exhaled air from infectious individuals in enclosed spaces, which have a high probability of deposition in the terminal airways. Exhaled air is the carrier of airborne infectious particles and carbon dioxide is used as a surrogate of this exhaled air. Respiratory activities such as talking, coughing, sneezing and singing could contribute to respiratory particle production. When susceptible individuals become exposed to the expelled airborne infectious particles by infectors, they may become infected, depending on the infectivity of the strains in the infectious particles, proximity to infectors, duration of exposure and the immune response of the host.

Using carbon dioxide as a surrogate for exhaled air, we modified the Wells-Riley model and prior modified versions of the model, and obtained a flexible but sensitive mathematical model that predicts the risks of airborne infectious diseases, such as TB under steady and non-steady state conditions, without assumptions of well mixed airspace and equilibrium conditions. In reality, airspace can never be well mixed because regions of high and low contaminant concentrations exist simultaneously within the same airspace. Furthermore, equilibrium conditions cannot be achieved consistently as the climate changes. From a biological point of view, not all airborne infectious particles reach the target infection site of the host to establish infection, some deposit in the upper airways without inducing infection. In our model, we take into consideration that alveolar deposition fraction determines the number and concentration of surviving airborne infectious particles that reach the alveolar to induce infection.

Applying experimental data from *in vivo* studies to the mathematical model developed in this study, we explored the probability of exposed guinea pigs acquiring infection in these *in vivo* studies and quantified the number of surviving airborne infectious particles (infective organisms) required to reach the alveolar to establish infection. Our study shows that the number of infective organisms demonstrated in the *in vivo* studies might have been markedly underestimated. We note that for a susceptible individual to be infected, the average number

of inhaled airborne infectious particles should attain a threshold level, which is the minimum number of airborne infectious particles required to deposit in the alveolar to induce infection, and infection cannot occur from a single infective organism as reported previously.

In this study, we investigated TB transmission in congregate settings, such as schools, households, public transport, prisons and health care settings and suggested preventive measures for TB control. TB transmission in these locations is attributable to numerous factors, including overcrowding and air pollution, which acts as a carrier of airborne infectious particles. Furthermore, high TB prevalence in these locations fosters the force of infection and a large number of susceptible individuals get infected as they share expired air with infectious individuals. Though human immunodeficiency virus (HIV) may be regarded as a key contributing factor to TB transmission, TB prevalence in high TB burden settings is influenced by many other factors, including poor diagnostic tools, incomplete doses of therapy, overcrowding in townships, ineffective air disinfection tools in congregate settings and poverty-induced malnutrition.

We explored the population impact of effective contact rate (β) on TB epidemiology by comparing the number of newly infected and reinfected individuals at stability point of a TB epidemic with increasing effective contact rate (ranging from 5 to $30\ yr^{-1}$). Furthermore, we examined the impact of post-treatment immune status by comparing the number of active TB cases when all treated individuals move to either a susceptible, newly infected or reinfected state at stability point of a TB epidemic. We found that the number of newly infected cases increases when $\beta = 5$ to $\beta = 10\ yr^{-1}$ then decreases with increasing effective contact rate, while that of reinfected individuals increases in all values of effective contact rate, implying that TB prevalence might be driven by reinfection, especially in high burden settings. Furthermore, we noted that the number of active TB becomes higher when all treated individuals move to a susceptible state than when they move to either a newly infected or reinfected state, probably because of immunological factors. Results show that post-treatment immunological memory reduces the risk of active disease by $7-16\%$ compared to susceptible individuals.

Using an age-structured mathematical model developed in this study that incorporates vaccination for the age groups [0 - 5) and [5 - 15) years, we explored TB disease progression in different age groups (from $[0-5)$ to ≥ 75 years). We found that TB disease progression is age dependent. High TB notification was detected for the age groups $[0-5)$, $[15-25)$, $[45-55)$ and $[55-65)$ years, and the lowest TB notification rate was detected in the age group $[5-15)$ years. Furthermore, we noted that vaccination decreases active disease progression for the age groups $[0-5)$ to $[15-25)$ years, while TB notification rates remain high for the age groups $[25-35)$ to ≥ 75 years. The findings in this study suggest that active disease progression depends on age and average duration of the waning of the vaccine effect.

Acknowledgements

My endless thanks goes to Almighty God for giving me strength and knowledge to accomplish this work. I would like to thank him for his blessing and everything he has done in my life.

I would like to express my sincere thanks to my research supervisors, professor Nicola Mulder (Computational Biology Group, University of Cape Town) and professor Robin Wood (The Desmond Tutu HIV Centre, University of Cape Town) for introducing and supervising me in the field of Bioinformatics and Infectious Disease Modelling Epidemiology. I would like to acknowledge their valuable support, guidance, suggestions and encouragement. From them, I learnt a lot, including writing high quality research papers, response to reviewers, to be precise and consistent in every point and so much more. Their scientific inspirational will remain in me throughout my scientific carrier, and I really feel blessed to have such incredible and gifted advisors.

Thanks to Dr Gaston K. Mazandu (Computation Biology Group, University of Cape Town) for his useful comments and suggestions, which increased value and robustness of the thesis. I would like to extend my gratitude thanks to Dr Jason R. Andrews (School of Medicine, Stanford University) for his valuable idea and suggestions in the design and development of an age-structured mathematical model that incorporates vaccination.

For the knowledge of data collection devices and data synchronisation, I would like to acknowledge and thank Dr Carl Morrow (The Desmond Tutu HIV Centre, University of Cape Town). Special thanks to Dr Sabine Hermans (The Desmond Tutu HIV Centre, University of Cape Town) for the data confirmation, helpful comments and suggestions.

With great honour, I would like to thank my colleague students and staff (Computational Biology Group, University of Cape Town) for their support and comments during the seminar presentations. Many thanks to the University of Cape Town administration for the support and useful academic facilities for the whole period of my academic years.

This project would not be possible without funding. I would like to acknowledge and thank the

South African Medical Research Council (MRC) with funds from National Treasury under its Economic Competitiveness and Support Package (Grant MRC-RFA-UFSP-01-2013-CCAMP). Furthermore, I would like to extend my sincere thanks to Deutscher Akademischer Austausch Dienst (DAAD), Bonn/Germany and the African Institute for Mathematical Sciences (AIMS), South Africa for funding this project.

Special thanks to my family for their support, suggestions, love and encouragement in the whole journey of my academic career. To my parents (mr & mrs Issarow) who raised me with inspiration and encouragement for me to be a scientist. To my young sister (Deborah) and brothers (Andrew and Benson), stay blessed. Words can never be enough to express my feeling, what I can say is that God bless everyone who supported me to accomplish this work.

Contents

List of Figures

List of Tables

Publications

The University authorises publication of the whole or part of the thesis depending on the project outputs and agreement between the candidate and supervisor(s). Based on this thesis, we therefore published some papers and submitted several others for publication as outlined below.

1. Issarow C. M., Mulder N. and Wood R. (2015) Modelling the risk of airborne infectious disease using exhaled air. Journal of Theoretical Biology 372: 100-106.

2. Wood R., Morrow C., Barry 3rd C. E., Bryden W. A., Call C. J., Hickey A. J., Rodes C. E., Scriba T. J., Blackburn J., Issarow C., Mulder N., Woodward J., Moosa A., Singh V., Mizrahi V. and Warner D. F. (2016) Real-Time Investigation of Tuberculosis Transmission: Developing the Respiratory Aerosol Sampling Chamber (RASC). PloS One 11(1): e0146658.

3. Issarow C. M., Wood R. and Mulder N. (2016) Seminal *Mycobacterium tuberculosis in vivo* transmission studies: Reanalysis using probabilistic modelling. Mycobact Dis 6: 217. doi:10.4172/2161-1068.1000217

4. Issarow C. M., Mulder N. and Wood R. Impact of effective contact rate and post treatment immune status on population tuberculosis infection and disease states using a mathematical model (under review).

5. Issarow C. M., Wood R. and Mulder N. Impact of vaccination on tuberculosis control (in preparation).

Chapter 1

Introduction

This chapter reviews tuberculosis (TB) transmission scenarios from the historical background of *Mycobacterium tuberculosis* discovery, TB global status and TB prevalence in South Africa. It describes TB transmission mechanisms, TB transmission from adults to children, factors associated with TB transmission, TB diagnosis and tools used for TB diagnosis. It provides an overview of TB infection progression to disease and factors attributable to infection and disease, including environmental, socio-economic conditions, biological and immunological factors. Furthermore, it explores factors attributable to TB transmission in congregate settings, such as schools, households, public transport, health care settings and prisons. Finally it explores the motivation for this project.

1.1 Tuberculosis historical trends

In 1882, a medical scientist in Germany, Robert Koch, discovered airborne infectious particles viable with potential for TB infection, known as tubercle bacilli (*Mycobacterium tuberculosis*), in his seminal line of thinking for the proof of tubercle bacilli as the main cause of TB [12]. He observed that infection began in the respiratory tract and concluded that tubercle bacilli were mostly spread through the air [12]. Subsequently, work done by William Firth Wells, in the $1930s$, at the Harvard School of Public Health provided additional knowledge about airborne transmission by suggesting that for the infectious agent to be transmissible, it should remain buoyant in the air. Collaborating with Wells on a project conducted in the hospital using a guinea pig model, Riley and colleagues provided more information to enhance our understanding of the TB transmission scenario than any other prior project [59].

Historically, it is believed that *Mycobacterium tuberculosis*, which causes TB, probably originated in Africa because the earliest branches of its phylogenetic tree (*Mycobacterium africanum* and *Mycobacterium bovis*) are organisms that are found in Africa, and the earliest fossil records of TB in human are from the continent. Additionally, it was noted that TB was highly established in Africa and started to spread globally about 9000 years ago as people started to move into different regions around the world, including America and Europe [8].

However, there is empirical evidence that TB was present in Europe during the middle ages and during the 18^{th} century, when a TB epidemic erupted in Western Europe. In 1740, the TB morbidity rate was very high in London with approximately 900 deaths per $100,000$ individuals in the population [12, 13]. Furthermore, in 1882, Robert Koch, who discovered the tubercle bacilli, reported that 1 in 7 deaths in Berlin was caused by TB.

In the 19^{th} century the burden of TB in European cities began to diminish. This was demonstrated by Davies and colleagues after obtaining British data from the General's annual report register. These data noted that in the mid-19^{th} century there were approximately 300 deaths per $100,000$ population with a decline of 1.7% per year throughout the remaining period of the century. Additionally, the same declining statistics were observed in the United States. However, according to TB historical data, Europe and North America might still have had a TB burden even though the prevalence was not well documented [13]. The TB burden in Europe and North America started to diminish after the industrial revolution, associated with improvement of social and economic conditions. Some scientists concluded that TB started to diminish in Europe and North America due to the presence of a new generation with strong immune systems which resisted TB. This hypothesis was opposed by other scientists who claimed that TB diminished rapidly, while the new generation took a long time to be established. On the other hand, McKeown postulated that TB diminished in Europe and North America because nutrition was improved. According to the TB transmission environment, it's commonly believed that the disease is associated with poverty, for example, in 1988, Brudney and Dobkin classified 224 patients who were discharged after 9 months from one of the hospitals in New York City [8]. Of these patients, 82% were unemployed, 68% were homeless, 53% were alcoholic and 40% were HIV-positive.

According to TB historical data and statistics, whatever reason could be given for the TB epidemic and decline, there is a contradictory debate in terms of empirical evidence, but TB has remained a burden thought history in Europe and North America. TB remains one of the most prevalent infectious diseases globally, which kills millions of people each year, especially in Sub-Saharan Africa and South-East Asia as discussed in Section 1.2. This is briefly how TB was discovered and started to spread globally while destroying the lives of millions of people

worldwide. Knowledge of TB history is crucial in TB epidemiological studies because it helps us to understand how TB infectious particles where discovered, how TB started to spread globally and how it started to decline in some areas. Additionally, knowing the TB burden globally is very important as it provides the big picture of the TB status worldwide and factors potentially influencing TB prevalence, as discussed in the following section.

1.2 Tuberculosis global status

Tuberculosis is the major global health airborne infectious disease epidemic, which causes morbidity and mortality for millions of people annually [84, 85]. While human immunodeficiency virus (HIV) was the leading cause of mortality from infectious disease with 1.2 million deaths in 2014, TB was the second worst with 1.1 million deaths globally [84]. According to the World Health Organization (WHO) statistics in 2014, there were approximately 9.6 million incident TB cases and 1.5 million deaths, of which 1.1 million were HIV-negative and 0.39 million HIV-positive co-infected with TB [84]. The latest estimate in 2015 shows that there were 10.4 million incident TB cases and 1.4 million TB deaths among HIV-negative and additional of 0.4 million TB deaths among HIV co-infected, showing that TB caused more deaths than HIV in 2015 [85]. Though most of this TB morbidity and mortality occurred among men, perhaps because of higher exposure, TB morbidity and mortality among women and children has also been noted to be high [84, 85]. The degree of involvement in social and public activities differs by gender in different countries and societies, which is why exposure probability to infectious individuals differs for men and women [12]. Of 9.6 million incident TB cases in 2014, there were approximately 5.4 million among men, 3.2 million among women and 1.0 million among children [84]. In 2015, of the estimated 10.4 million incident TB cases globally, there were 5.9 million among men, 3.5 million among women and 1.0 million among children [85].

The TB burden can be measured in terms of the number of new and relapsed cases of TB disease arising in a given period of time (incidence), the number of cases of TB in a given population over time (prevalence rate) and the number of deaths caused by TB in a given period of time (mortality rate). It can also be measured in terms of incidence of ill-health in a given period of time such as per year (morbidity rate) [85]. According to the WHO statistics in 2015, there were about 10.4 million incident TB cases (range, $8.7 - 12.2$ million) globally which equates to approximately 142 cases per $100,000$ population [85]. This was distributed as follows: 61% in Asia, 26% Africa, 7% Eastern Mediterranean Region, 3% European Region and 3% in the Americas [85].

The three countries with the highest number of incident cases worldwide in 2014, were India with 2.2 million, followed by Indonesia with 1.0 million and the third country was China with 0.93 million [84]. In 2015, India was still leading with 2.84 million of incident cases followed by Indonesia (1.02 million) and the third position was occupied by China (0.918 million) [85]. India, Indonesia and China are the leading TB burden countries and together accounted for 45% of the total number of incidence cases globally in 2015 [85]. In 2015, countries with the highest TB mortality rate globally were India (0.48 million), Nigeria (0.18 million) and Indonesia (0.1 million). The fourth position was taken by Bangladesh with 0.073 million deaths, while China seemed to be out of top four in terms of mortality rate (0.035 million) [85]. According to WHO statistics, the burden of TB infection is very high globally and it is endemic in developing countries, especially in South-East Asia and Sub-Saharan Africa [84, 85]. The estimated annual incidence rate in Sub-Saharan Africa was over 255 per 100,000 population in 2014, which shows that the TB burden is still high, though recent data demonstrates that the incidence has declined [84]. Efforts to reduce TB infection rates could be a critical to decrease the TB morbidity and mortality rates in regions with high rates of TB cases. Figure 1.1 shows estimated TB incidence rates globally in 2015.

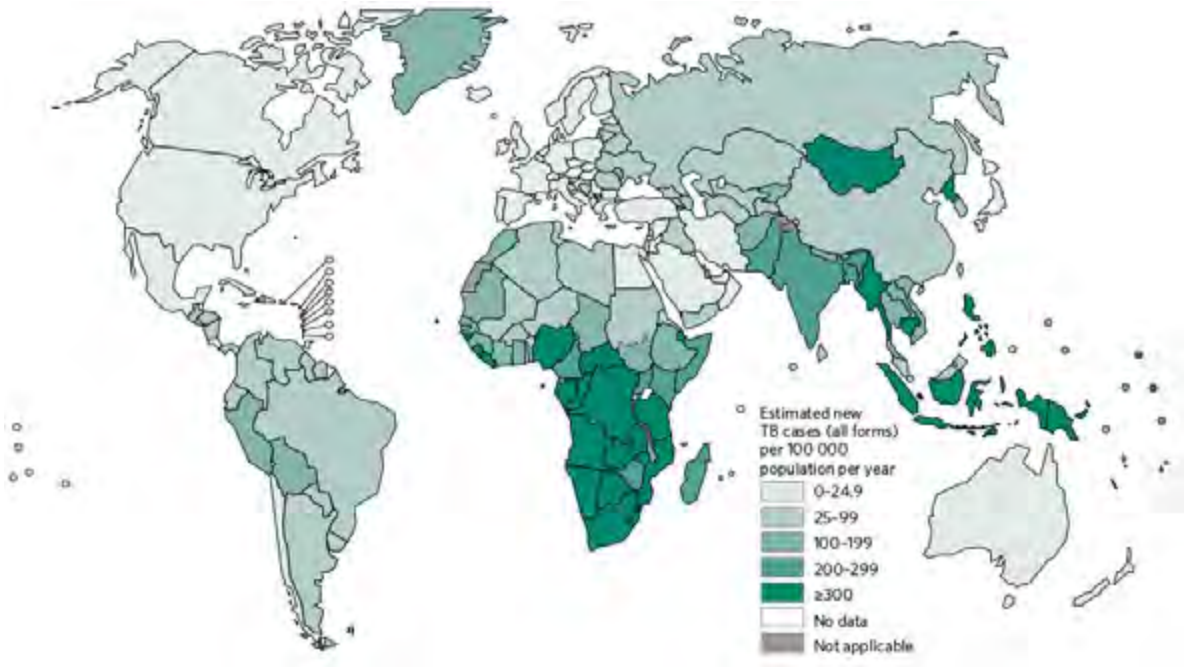

Figure 1.1: Estimated TB incidence rates in 2015 (*WHO global TB report* 2016*) [85].*

HIV infection is a big challenge and has been significantly associated with TB [58], it has increased the individual level risk of active TB incidence rate within the past few decades [70, 80]. Numerous studies have reported that the risk of active TB among HIV-positive individuals is higher than for HIV-negative individuals, due to high viral loads and low CD4

counts in the former. However, the correlation between HIV and TB strains is not clearly known and more research is needed. Currently it is estimated that the TB incidence rate is approximately 20% higher among HIV-positive than HIV-negative individuals [70]. This implies that the increase in HIV prevalence is highly associated with rapid increase in TB documentation rates, especially in high burden settings, including Sub-Saharan Africa and South-East Asia. The WHO estimated that 32% of TB cases were HIV co-infected in African countries in 2014 [84] and 31% in 2015 [85]. More than 50% of TB cases with HIV co-infection were from Southern Africa [83, 84, 85]. Overall, statistics show that the number of TB cases with HIV co-infection is extremely high in African regions. There is empirical evidence that patients with HIV-TB contribute to TB transmission in high burden settings, though they are less often sputum-positive. According to WHO data, in most of the countries with high TB prevalence, the high mortality rate is due to HIV associated with TB [80, 85]. The three main impacts of HIV on the TB burden, is that it is highly associated with endogenous reactivation if infected with MTB, it catalyses the progression from latent to active TB, and it acts as a reservoir for TB transmission in the community.

Multi-drug resistant tuberculosis (MDR-TB) is a great challenge that fosters the spread of TB and hampers the TB control effort globally [69, 78, 79]. Endemic transmission of MDR-TB is attributed to several factors, including: prolonged period of infectiousness due to delay in MDR-TB treatment, poor diagnosis and chemotherapy leading to improper MDR-TB treatment and a large number of MDR-TB patients are not yet identified due to insufficient chemotherapy susceptibility testing tools, which accelerates extensive drug resistance TB (XDR-TB) explosion. Additionally, MDR-TB increases the risk of morbidity and mortality globally especially for people living with HIV, due to compromised immune responses [79]. By definition, MDR-TB is resistant to the first line drugs Isoniazid and rifampicin while XDR-TB is resistance to Isoniazid, refampicin, and to any fluoroquinolone, as well as to at least one of the second line injectable drugs, including kanamycin, amikacin and kapreomycin. Countries with high prevalence of MDR-TB include India and China, which together account for about 50% of MDR-TB patients globally [69]. In 2015, it was estimated that there were $580,000$ $(520,000 - 640,000)$ incident cases of MDR-TB globally [85]. Furthermore, the WHO statistics show that there were $250,000$ $(160,000 - 340,000)$ deaths from MDR-TB in 2015 [85]. Generally, it shows that MDR-TB and HIV co-infection are among the barriers hindering TB control strategies towards the WHO target of eliminating TB [80, 82, 83, 84, 85].

1.3 TB transmission in Cape Town and South Africa in general

1.3.1 Cape Town

Cape Town is one of the major South African cities with a population of about 3.2 million residents in 2006, of which $27{,}000$ were TB cases [97]. Additionally, in 2006, TB annual notification rates where documented to exceed $1{,}500$ per $100{,}000$ population in urban high density settlements [55, 101]. In 2009, the city of Cape Town had approximately 3.4 million people, of which about $30{,}000$ were new TB cases as documented by the national TB control programme [102]. The TB notification rates in Cape Town are extremely high between the ages of 20 and 40 years, which might be fuelled by high prevalence of HIV in those age groups [29]. However, new TB cases among HIV-negative individuals were also found to be very high, at 386 per $100{,}000$ population. Children and young adults were found to be infected with the ratio 511 per $100{,}000$ population and 553 per $100{,}000$ population, respectively. Latent TB prevalence for children and adolescents in Cape Town is high at a prevalence of 20% for children of school going age. The annual rate of infection increases from approximately 4% per year in childhood to 7% per year in adolescence, and TB infection prevalence rises to 80% during the young adult age [103]. Childhood ($0-15$ years) TB notification rates in high burden Cape Townships have been noted to be 3.5 times the adult rate, where childhood TB accounts for 39% of the total prevalence [97]. Thus a large proportion of the population in Cape Town acquire TB infection and develop active TB before reaching adulthood [100]. It is not well understood in which specific locations TB transmission occurs, though empirical evidence shows that infections mostly occur in congregate locations outside of households [72, 111].

It has been noted that rebreathed air volume (RAV) that is associated with the transmission of airborne infectious diseases is very high in township adolescents [100]. A number of TB cases have been identified in townships with a high concentration of carbon dioxide as a surrogate for expired air, which reflects the dispersal of airborne infectious particles [98, 92]. According to a study conducted by the Desmond Tutu HIV Centre in Cape Town, when the concentration of carbon dioxide is high, the risk of acquiring airborne infectious disease, such as TB, increases [100]. The annual risk of children and adolescents in townships is remarkably high. Currently, it is estimated that 5% to 8% of adolescents become infected in townships annually [98, 100]. Since the concentration of exhaled air is reasonably high in townships, some of which is derived from infectious sources, it might be one of the key factors that accelerate TB transmission in

these areas [92].

Since Cape Town has high HIV and TB prevalence, the national programme launched antiretroviral therapy (ART) in the city for all HIV-infected individuals with CD4 counts below 200 cells/μl in 2004 [107]. ART reduces TB risk by two-third, depending on time and CD4 counts with the fact that the risk becomes high for individuals with low CD4 counts [28]. In 2013 ART became available for individuals with 350 cells/μl and 2015 for those with 500 cells/μl and currently, more than $130,000$ people in Cape Town have been initiated on ART [107]. Over the last 10 years, HIV control programme in the city of Cape Town has substantially advanced with identified HIV and TB co-infection notification rates. Furthermore, ART coverage has increased from 0 to 63% in nine years and TB notification rates continue to be high. Over the last three years, TB notification rates in Cape Town declined for approximately 16% in both the HIV-positive and the HIV-negative individuals after ART initialisation [107].

1.3.2 South Africa

South Africa has one of the highest TB notification rates in the world with approximately 1% of the population developing active TB annually [80, 100]. In 2011, WHO data demonstrated that South Africa had an incidence of $500,000$ cases of active TB. Hence, about 1% of the population of approximately 50 million people develop active TB disease each year, implying that the incidence has increased by 400% over the past 15 years [80]. Fuelled by high HIV prevalence, the TB notifications in South Africa have increased 6-fold over the last two decades [82]. It is estimated that South Africa accounts for 25% of HIV associated TB globally [80]. Of $500,000$ incident cases in South Africa, WHO estimated that about $330,000$ (66%) people have both HIV and TB infection. TB is the leading cause of death from infectious diseases in South Africa. In 2011, WHO estimated that there were $25,000$ deaths from TB in South Africa, excluding the death of people with both TB and HIV. This is because people who die of both TB and HIV, internationally are regarded as HIV deaths. One of the facts which identifies South Africa as among the countries with the highest burden of TB globally is that in 2007, there were $461,000$ new cases of TB infection while the total incidence rate was approximately 948 per $100,000$ population, of which the prevalence of HIV-positive associated TB infection was approximately 73% [98]. This implies that much of the burden of TB in South Africa can be attributed to HIV infection, which weakens the immune system, enabling airborne infectious particles to penetrate easily to the lungs, causing TB infection and active TB disease.

Though TB diagnosis and treatment have been improved, South Africa had an incidence greater than $1,000$ per $100,000$ people in 2012, which is highly associated with HIV prevalence

[113]. Besides the HIV epidemic in South Africa, TB transmission is highly associated with overcrowding, as the urban areas in the country, including the city of Cape Town, are extremely overcrowded. In this environment, many of the susceptible individuals become exposed and acquire TB infection easily [49]. In rural areas, most of the houses are poorly designed with inadequate natural ventilation, which creates a good environment for TB transmission [68].

Tobacco smoking is undoubtedly one of the risk factors influencing TB prevalence, and there is empirical evidence that smokers have a higher risk of developing and dying from TB than non-smokers [25, 30, 43, 70, 115]. Nicotine, carbon monoxide, tar and cyanide are some of the harmful chemicals contained in tobacco cigarettes, which cause TB susceptibility and lung cancer. These chemicals, especially nicotine in tobacco cigarettes, are drugs which mainly affect the brain and nerves, and cause addiction. The WHO and the International Union Against Tuberculosis and Lung Disease joint report demonstrated that exposure to tobacco smoke is significantly associated with TB infection and disease. Several studies have noted that the rates of TB infection, disease and mortality were significantly higher among smokers than non-smokers, thus confirming this [70]. For example, a study conducted in Rio de Janeiro, Brazil, observed that TB mortality among smokers was about twice that of non-smokers [25]. Statistically, there are approximately 1.3 billion smokers and more than 5 million deaths per year attributable to tobacco smoking globally. In South Africa, there are approximately 7 million smokers, with a reasonably high prevalence of 20% [115]. Since South Africa has one of the highest burdens of TB, tobacco smoking might be one of the risk factors attributable to TB infection and disease, though HIV is still the major risk factor. Currently, the mortality among smokers in South Africa is approximately twice that of non-smokers. Almost a third of all male deaths in South African adults over the age of 35 years have recently been attributed to tobacco smoking [115]. It has been documented that the group classified as Coloured has the highest smoking prevalence in South Africa. The estimated smoking-related mortality among Coloured individuals is 50% higher than for black or white smokers and ex-smokers [115]. Tobacco smoking is also associated with the world's top five causes of death, which are lung cancer, pneumonia, stroke, ischaemic heart disease and chronic obstructive pulmonary disease (COPD) [25, 43, 70, 115].

Alcohol is yet another factor contributing to TB transmission in households for those who abuse it [54]. In 2004, it was documented that 3.8% of TB deaths globally were associated with alcohol abuse [54, 70]. Furthermore, it has been noted that TB among heavy alcohol drinkers is about 3 to 4 times higher than in non-drinkers or controls. For example, studies conducted in Australia, Canada, Russia, Switzerland and the USA, demonstrate that the prevalence of alcohol abuse among TB cases ranged from 10% to 50% for persons who consume more than

40 g or 50 ml of alcohol per day [54]. The actual causes of TB for alcohol abusers include social mixing with other alcoholics as well as the alcohol itself, which weakens the immune system and influences TB susceptibility, leading to a high risk of TB infection and disease. Furthermore, there is empirical evidence that alcohol is highly correlated with tobacco smoking and sometimes drug abuse, which are undoubtedly associated with TB infection and disease susceptibility for users and people with second hand exposure [30, 43]. Hence, it is plausible to conclude that alcoholics, smokers and drug addicts, are some of the sources contributing to the explosion of TB infection and disease in South African communities. However, there are some groups in the community which are more vulnerable to TB acquisition, such as children and adolescents due to factors discussed in the following section.

1.4 Age distribution, children and adolescents

TB transmission mostly occurs among individuals who spend long periods of time in the same enclosed space or dwelling with a TB infectious individual [68], for instance inmates in prisons and students in schools. Usually, TB infectious individuals will behave in a similar manner to uninfected individuals in the community and thus they cannot be identified easily by physical appearance. Since it is commonly known that people are used to socializing with others of their own age, this implies that the risk of TB infection varies considerably with age and TB prevalence [11]. From findings in recent years, it has been noted that the risk of infection in children and adolescents underestimates the actual risk of infection in the community because public health has not yet concentrated on these age groups [44]. In industrialized countries, the prevalence of TB infection has been observed to be high among the adults, while in other countries such as Latin America, Sub-Saharan Africa and South-East Asia, the prevalence of TB infection is high among young economically productive people of reproductive age. This implies that TB is becoming less of a public health problem in industrialized countries due to rapid decrease in prevalence of TB infection among children and adolescents, while in other parts of the world TB is still a critical problem with high prevalence among children and young adults [12].

The WHO statistics in 2011, demonstrated that every year there are approximately 0.5 million TB cases and $64,000$ deaths among children globally [80]. However, WHO also noted that estimating the burden of TB in children (aged < 15) is difficult and might be underestimated. Some of the reasons for underestimation include: childhood treatment for TB outside of national TB programs (NTPs), lack of routine recording and reporting of childhood TB cases by some NTPs, difficulties with access to health care for TB diagnosis and clinical similarities

with other common childhood diseases. Most of the NTPs focus on reporting the number of adults who have been identified or treated, who have smear-positive TB, and who are mostly considered as a source for TB transmission to children. They keep in mind that even if children are diagnosed, they are often smear-negative, and are not included in reports. But in reality, children are at high risk of acquiring TB infection because their social contacts, interaction and social mixing are extremely high in the community. Social interactions are key to the transmission dynamics of TB in the community [11].

TB control programs demonstrate that adolescence is the period in which TB incidence increases, though there is little investigation into prevalence of TB infection in this age group. TB transmission mostly occurs in crowded areas, such as schools, where students stay in enclosed rooms for a long period of time. This implies that most of the children and adolescents become infected in the school environment and they may develop TB disease while still at school [44, 92]. Thus, children and adolescents are at high risk of TB infection and the probability of infecting others is extremely high due to social contacts, interactions and social mixing in the community [11, 55].

Of all available immunological tests, the tuberculin skin test (TST) has been widely used for TB diagnosis in the community, especially in low TB prevalence settings. A recent study conducted in Cape Town using a cut-off of ≥ 10 mm diameter of induration as epidemiological evidence of latent TB, found that a fifth of children at school entry were already infected [98]. This implies that approximately 50% of adolescents in the community were infected by an average age of 15 years, and about 75% of individuals had epidemiological evidence of latent TB by the age of 25 years, which is when the prevalence of HIV peaks in South Africa [98].

Childhood TB notification declines rapidly after the age of 5 years until the childhood stage between 10 and 14 years, despite the continuation of a high annual TB infection rate. This scenario has been widely recognised in epidemiological studies but it is not well understood, and further research is needed to clarify this, though immunological response might be a major factor [55, 98]. After 10-14 years of age, TB notification rates increase rapidly to a second peak at age $20-24$ years. These two peaks occurred throughout 100 years of TB notification in Cape Town data [108]. The second peak represents the continuation of the TB epidemic as measured by the number of notified cases. It has been documented that most of the children become infected by elders either in their households, schools or public transport as discussed below.

1.5 TB transmission from adults to children

Childhood is one of the age groups in the community which is highly vulnerable to TB infection and disease due to high exposure in social mixing and weak immune response [78]. It is estimated that of 9 million people who develop TB disease annually, 11% are children of < 15 years, and 75% of these childhood TB cases occur in 22 countries of high TB burden, which account for 82% of the world's estimated incidence cases annually.

Most of the children in the community acquire TB infection from adults with active TB disease either in households, public transport, schools or social mixing [97]. Therefore, TB infection risk for children mainly depends on the infectious adults in the community [20]. Children have prolonged contact in poorly ventilated dwellings and share sleeping quarters with adults who are assumed to be a source of TB transmission among children [57]. From a physiological point of view, children breathe heavily, inhaling amounts equivalent to the weight of the body. Since children are highly exposed during social mixing, they inhale a large quantity of rebreathed air from adults that contains airborne infectious particles, and develop active TB 12 months from the period of exposure [49], or even earlier, depending on the immune system. In addition, WHO reported that the probability of children of < 10 years of age progressing to disease after exposure is extremely high, especially in children of $0-4$ years of age, due to an immature immune system [78].

WHO reported that the End TB Strategy that builds on the directly observed treatment short-course strategy (DOTS) has a critical role to play in reducing the burden of TB globally in order to save the lives of children. Quantitative TB infection in children is highly related to the adult TB prevalence in the community. Since infectious adults are a source of TB transmission to children, if TB can be reduced among adults then children might be safer. Children who are at a higher risk of getting TB include those living in the same household with infectious individuals, children less than 5 years old, children with HIV infection and children with severe malnutrition. TB transmission is a big problem that needs to be solved by applying alternative scientific approaches. In the following section we introduce TB transmission mechanisms and properties of airborne infectious particles, which cause airborne infectious diseases.

1.6 TB transmission mechanisms

Droplets produced by TB patients either by talking, coughing, sneezing or singing may contain airborne infectious particles, which cause TB infection in other susceptible individuals

who become exposed [33]. Droplets may evaporate to the size of infectious droplet nuclei by containing either one or more airborne infectious particles which become suspended in a confined space for a long period of time. However, there is a critical diameter of droplet nuclei containing airborne infectious particles which maximizes the probability of inhaling infectious particles and which create the TB infection environment. An experiment conducted by Sonkin, demonstrates that many particles with diameter greater than $5\mu m$ are trapped in the nose, whereas those smaller than $5\mu m$ become suspended in air and can reach the alveoli and cause TB infection [12]. Thus, he drew the conclusion that the critical diameter of the droplet nuclei containing airborne infectious particles with high probability of causing TB infection ranges from $1\mu m$ to $5\mu m$ in order to penetrate and reach the target infection site of the person and cause TB infection. The infectious droplet nuclei which are the critical size for reaching the target infection site are the primary source of *Mycobacterium tuberculosis* transmission. However, even if airborne infectious particles do manage to reach the target infection site, they must overwhelm the immune defenses of the person to commence infection [74]. Hence, when a susceptible individual becomes exposed to airborne infectious particles, that person may be infected or not depending on the threshold level and infectivity strength of the airborne infectious particles to dominate the immune defenses of the person.

The main factors which determine the probability of TB transmission particles include the number of incident infectious individuals, duration of exposure and proximity to infectors or modes of interaction between infectious and susceptible individuals in the community. If the proximity of a susceptible to an infector is ignored, then the probability of an individual to acquire TB infection is primarily dependent on the duration of exposure to the infector [24]. If the concentration of airborne infectious particles in the room is high, the duration of exposure before infection occurs will be short. If airborne infectious particles concentrations are low, the safe exposure duration will be much longer. This is because TB infection depends on the threshold concentration and number of airborne infectious particles required to dominate the immunological state of the host [74].

As discussed earlier, the number of people who might be infected with airborne infectious particles that cause TB, given that there are a number of infectious individuals in the community, will depend on the duration of exposure, number of infectious droplet nuclei that contain airborne infectious particles per air volume and manner of interaction between infectious and susceptible individuals [12, 49]. Duration of exposure is defined as the time individuals spend in a confined space with the probability of being infected if there is an infectious individual. The word exposure can be defined as contact interaction between two or more individuals within confined spaces where the environment of the given space can trigger infection for susceptible

individuals [80]. Extensively high exposure mostly occurs among persons who share the same dwelling or who spend long periods of time in enclosed spaces with an infectious individual.

In overcrowded areas such as townships, prisons and schools, where duration of exposure is long, the number of TB transmission particles is also extremely high, so the number of people who could be exposed to a single infectious individual is high [109]. However, in rural areas the situation is not as critical because the number of people who become exposed to a single infectious individual is smaller than urban areas as rural areas have low population density. In addition, regardless of rural areas or urban areas, TB transmission depends on the population density in the household, nature of the dwelling and interactions which trigger the risk of exposure, provided that there is an infectious individual in the given household. Therefore, population density plays a big role in the transmission of tuberculosis in the community.

Duration of exposure sometimes depends on the weather and climatic conditions, for instance, during winter the duration of exposure is very high because most people prefer indoor activities and stay in confined spaces to maintain body temperature. In some countries, such as northern Europe, which have long, cold winters, outdoor social activities are scarcer than in warm climates [12]. Airborne infectious particles expelled indoors by an infected person in a confined space are retained and evenly distributed anywhere in poorly ventilated spaces, which causes infection over a long period of exposure [12]. Thus, if individuals enter that confined space, they may become infected even if an infectious individual has left, depending on the duration of exposure and their immune system. However, airborne infectious particles disperse rapidly if expelled outdoors and die quickly because they become exposed to high air flow and ultraviolet irradiation from the sun [11]. This implies that TB transmission particles spread more rapidly in cold climates than warm climates because outdoor social activities are reduced due to the cold, and indoor ventilation becomes poor since windows are kept closed for a long period of time. This affects duration of exposure. TB infection and disease progression are discussed in the following section.

1.7 TB infection and progression to disease

There are two major clinical states of TB, latent TB and active TB disease. Latent TB can be categorised into early, late and reinfection latent TB, whilst active TB can be divided into drug susceptible, drug resistant and extensively drug resistant. When a susceptible individual is infected by airborne infectious particles, they usually cause latent TB and if that infected individual does not receive medication, he/she may develop active TB disease. However,

some susceptible individuals become infected and develop active TB very quickly, depending on the virulence of infecting pathogen strains and immunological state of the host. Both clinical states of TB can be treated if medication is taken immediately after TB diagnosis [12]. Additionally, a person with latent TB usually does not feel sick and cannot spread TB to others, while someone who has developed active TB disease is sick and spreads TB to others who are exposed for a prolonged period of time in a confined space.

It is very easy for susceptible individuals with a weak immune system to be infected and develop active TB disease, while those with an effective response and active immune system can be infected but not progress to active TB disease because the immune system will fight off the pathogen. If a person becomes infected and doesn't develop active TB disease then they can remain latently infected whereby TB infectious particles become dormant in the body but rapidly replicative and therefore cannot cause infection to other people as mentioned above. The lifetime probability of a person with latent TB developing TB disease is about $5-10\%$, depending on the host immune system and the virulence of the infecting pathogen strains [33]. However, both latent TB and active TB disease may progress to critical illness or death if preventative medication is not taken.

In addition, a person with latent TB can develop active TB disease if he/she didn't take medication to prevent accumulation of pathogens in the body. A person with active TB is contagious and can cause infection to other people especially in overcrowded locations with low per person ventilation, such as public transport, prisons and schools [44]. However, since TB spreads through air, it can infect any person who lives in proximity to infectious individuals regardless of age, sex or socio-economic status.

TB symptoms may include coughing that may last for a minimum of three weeks, fever, night sweats, haemoptysis, chest pain, weakness, and weight loss. A person with latent TB will be advised to take 1 medication for 6 to 9 months while those with active TB disease should take 3 to 4 medicines for at least 6 months in order to recover and avoid infecting others.

1.8 TB diagnosis

There are numerous TB diagnostic tools which are currently used as tests for TB. Some of these tests can be used to determine if someone has a latent infection, while others are used to identify if an infected person has progressed to active TB. Some TB tests can also determine if someone is infected with drug susceptible or drug resistant TB [14]. These are known as drug susceptibility tests. Though several types of TB tests exist, TB diagnosis is still difficult

even if someone has TB symptoms, as some of the tests are not sensitive or specific, resulting in a delay in obtaining results. These can lead to false positive results, where the test suggests someone has been infected while he/she is not, and false negative results, in which the test indicates that a person is not infected while in reality he/she is.

Latent TB diagnostic tools include the Tuberculin skin test, Interferon Gamma Release Assays, Sputum smear microscopy, Fluorescent microscopy and Culture TB test. The most accurate TB test is the TB culture test. Culturing is a method of studying *Mycobacterium tuberculosis* (MTB) by growing them on media containing nutrients [14]. Culture can provide drug susceptibility and multi-drug resistance testing by indicating which TB drugs are susceptible and which are resistant to observed MTB in a particular TB patient. However, TB diagnosis by using culture can take long time (approximately 2 to 6 weeks) because of the slow growth of TB bacilli [114]. Furthermore, some of these TB diagnostic tools, including TB culture test are complex and expensive with highly advanced technology, which require advanced laboratory tools and well trained operators [14].

The Expert MTB/RIF assay is a new test that seem to bring hope and revolution in TB control by detecting both MTB and drug resistance to rifampin (RIF) simultaneously in a short time (less than 2 hours) [14, 114]. The Xpert MTB/RIF assay is an automated nucleic acid amplification test that uses a disposable cartridge with the GeneXpert instrument system. A sputum sample collected from an infected individual is mixed with the reagent provided with the assay and a cartridge containing this mixture is placed in the GeneXpert machine for detection [114]. The advantage of Expert MTB/RIF assay over other diagnostic tools, such as culture is that it provides results quickly and it requires minimum training to run the test [14, 114]. Since 2010, Xpert MTB/RI assay is the only rapid diagnostic test for detection of TB and rifampicin resistance recommended by WHO, particularly in high TB settings with burdens of HIV and MDR-TB [84, 85].

Active TB can be detected by a chest x-ray, though these are expensive in some countries with limited resources. TB diagnosis has remained a big challenge since there is no 100% specific TB diagnostic tool that can provide significant results, and there is no a specific diagnostic tool that can be used for both latent TB and active TB diagnosis simultaneously [14, 84].

1.9 TB transmission in schools and attributable factors

School is one of the identified settings with high TB transmission in South Africa [44, 92, 97]. It is estimated that 39% of children $(0-15$ years) in South Africa have been infected [97].

A large number of children have been infected and some developed active disease at a young age due to factors correlated with their daily life and a TB transmission environment. Since children and adolescents are at a high risk of acquiring TB infection and disease, TB incidence in South Africa continues to increase annually despite the fact that TB treatment completion improved from $40-74\%$ between 1995 and 2011 [82]. With a TB prevalence of 427 per $100,000$ in schools and the large amount of time they spend indoors, adolescent students are at a high risk of acquiring TB infection and disease [82, 113]. Since students spend 30% of their daytime in schools, exposed to this infectious environment, it means that the likelihood of acquiring infectious disease, such as TB, is remarkably high.

Out of 30% of daytime they spend in schools, students and teachers spend about 97% of the time in confined spaces, with 80.2% of the time indoors used for interaction and social contacts. Since many schools are overcrowded with low per person ventilation and students spend long time periods in confined spaces with a high concentration of polluted air, they are at a high risk of acquiring TB infection in school. Furthermore, since 50% of TB transmission for children and adolescents occurs in schools [113], this implies that the effective contact rate that influences the force of infection is very high in schools.

Apart from school, a large number of students spend 1% of their time each day in public transport, such as minibus taxis, buses and trains to commute between school and home. These students become exposed to indoor air pollution by inhaling rebreathed air from elders, which could contain airborne infectious particles. As discussed earlier, it is estimated that 80% of the population, particularly elders in South Africa, have already been infected, thus, if students share re-breathed air with elders in confined spaces, the probability of acquiring TB infection is very high [90]. Furthermore, students spend 4% of their daytime in other social mixing environments, such as churches, visiting friends in their houses, or work places, where TB transmission probability may be high, depending on social contacts, interaction and environmental exposure [87, 95]. Through all these locations, and interaction with classmates at school, students may get infected by inhaling droplet nuclei, which contains MTB, and develop active disease. Statistically, it shows that a large number of students get TB infection and develop TB disease in the school environment because of high interaction and duration of exposure in confined spaces. Here, we explore some factors correlated with TB transmission in school transport as discussed in the following section.

1.9.1 TB transmission in school transport

School transport seems to be among the problematic areas attributed to TB transmission in schools. Some schools in South Africa, especially private schools, provide transport, such as minibus taxis and buses, which take students from home to school and back again. However, often drivers in these vehicles are randomly employed, provided that they have valid driving licences and experience, they are not required to pass a health test (medical check up), such as tuberculin skin test (TST) or chest radiography screening to examine whether they have latent TB or active disease. If at least one or all school transport drivers is infectious, it means that most of the students can be infected because they become frequently exposed to the infectious individual in a confined space [90, 104]. Hence, TB transmission is assumed to be remarkably high during school transport due to exposure to infectors [90, 104, 113]. For example, in New York, it has been reported that approximately 60% to 80% of students who were exposed to 5 infectious school bus drivers for a period of 6 months had positive TSTs [104]. This implies that school transport drivers are one of the sources of TB transmission in schools because if at least one of the students is infected in the vehicle, it means that other students also become exposed [72, 104].

Since South Africa has one of the highest TB prevalences, a large number of the school transport drivers have probably been infected, so students are at a high risk of acquiring TB infection and disease [90, 113]. TB transmission from school transport drivers to students is estimated to be extremely high, especially during winter, when windows remain closed and concentration of exhaled air that contains airborne infectious particles becomes very high indoors.

1.10 TB transmission in households

TB transmission occurs in different locations in the community, including the household, where members of the family spend up to 68% of their time in the same dwelling after outdoor social activities and during the night. Thus, if there is an infectious individual among the household members, it means that the duration of exposure is extremely high and the probability of being infected for susceptible individuals in the household is high.

Natural ventilation is a problem in most buildings either in urban or rural areas, which leads to creation of an effective TB transmission environment. This is because most of the houses, especially in rural areas are poorly designed and constructed so that natural ventilation is

insufficient [37]. For example, some houses commonly known as shacks in the Western Cape, South Africa rural areas, have been poorly designed and constructed so that air circulation is limited, which fosters indoor air pollution that is associated with the spread of airborne infectious disease [68]. Though ventilation is not one of the most effective interventions for TB control, when air change per hour (ACH) decreases in the room, the probability of being infected becomes significantly high due to accumulation of carbon dioxide, which reflects dispersal of airborne infectious particles [66].

Poverty is another factor that contributes to TB transmission in households, particularly in developing countries. When some members of the household get infected, they cannot always access health care centres due to socio-economic problems, for example, lack of money for TB diagnosis and chemotherapy or transport to reach the hospital [61]. Thus, if one person in the household has been infected and cannot access health care, that person develops TB disease due to lack of treatment and other members of the household become exposed and may get infected. Additionally, poverty is highly associated with malnutrition due to lack of a balanced diet with nutrients that improve and strengthen the immune system to combat pathogens [70]. For persons with malnutrition, the immune system is weak and if they acquire TB infection, they develop active disease in a short period of time.

Overcrowding is also a key contributor to TB transmission in households [58, 61]. For example, it was found that TB transmission in New Zealand was highly associated with overcrowding in households [61]. In this scenario, a large number of people sleep in a single confined room, sharing re-breathed air, where susceptible members of the family become exposed and infected if there is an infectious individual among them. Baker *et al* (2007) [61] suggested that in order to reduce TB transmission in households, TB control programmes should include strategies to reduce crowding in the home. Generally, extensive exposure to infector(s), high population density and low income communities lead to a greater likelihood of TB transmission in households [79]. However, some studies found that people living in the same household do not always have the same infective strain of MTB. For example, in one of the studies it was noted that 55% of those from the same household had different infective strains [72] and another study found that only 19% of TB transmission occurs in households [111]. This implies that TB transmission occurs from both outside and inside households.

1.11 TB transmission in public transport

Public transport, including buses, minibuses and trains, is another problematic system that is associated with TB transmission, especially in countries with high TB prevalence, such as South Africa [90]. For example, Two studies conducted in Lima, Peru, demonstrated that people who commute by public transport have a $4.09 - 4.9$ fold higher risk of acquiring TB infection and disease compared to private forms of transport [35] and concluded that there is a high risk of getting TB when commuting for ≥ 1 hour in public transport. TB transmission in public transport is mainly attributable to social contact, interaction, poor ventilation and proximity to an infector. The number of people and duration of exposure are linearly distributed with the risk of TB transmission by the fact that the concentration of exhaled air becomes higher as the number of occupants and duration of exposure increase in the space [7, 46]. Given the presence of infectious individuals in this polluted environment with high concentration of exhaled breath, high duration of exposure and proximity to infectors, TB transmission risk is high in public transport.

In South Africa, the basic means of transport are minibuses, buses, trains and private forms of transportation. About 43% of South Africans, including adults and children, use public transport as a basic means of transport. However, these modes of public transport tend to become extremely overcrowded [48], particularly in the mornings and evenings when workers and students commute to and from jobs and schools. With the high prevalence of TB in South Africa, there is a high probability of presence of at least one infectious individual on every route for each mode of public transport.

Minibuses accommodate a small number of passengers (about 18), but susceptible individuals are at a very high risk of TB infection given the presence of an infectious individual. This is because the concentration of re-breathed air that may contain airborne infectious particles becomes very high in a small confined space, with insufficient ventilation. Buses have a larger space and carry a larger number of passengers than minibuses, but due to a large number of commuters at certain peak times, the buses often carry as many as twice the recommended number of passengers. Overcrowding, poor ventilation per person, interaction and reasonable proximity to infectious individuals in the buses create a conducive environment for TB transmission.

In South Africa, some areas have neither buses nor minibuses and the community depend only on trains for daily commuting. Furthermore, some people prefer trains to buses or minibuses even if the routes exist, believing that the train is safer and cheaper than any other means of transport. Though trains have many large carriages, overcrowding is a critical problem due to

the large number of people who use this mode of transport in South Africa, especially during peak hours. Long periods of cold weather in South Africa are a challenge, particularly during winter where trains act as enclosed spaces, since all windows are kept closed to conserve the heat. The vehicle acts as an enclosed space if windows are kept closed and the passengers breathe heavily depending on the body mass, respiratory quotient and oxygen consumption, leading to a high accumulation of carbon dioxide [7]. This accelerates TB transmission probability due to high accumulation of re-breathed air, some of which is derived from an infectious source.

Carbon dioxide is among the most diffusible tracer gases that is used to measure the indoor air quality [7, 46]. According to a study conducted in South African cities, particularly in Cape Town in 2011, it was noted that the lowest level of carbon dioxide was $1,000$ ppm in trains, $1,150$ ppm in buses and $1,800$ ppm in minibuses [90]. These values demonstrate that minibuses have the highest risk environment to foster TB transmission due to high accumulation of carbon dioxide. This might be attributed to the small space of the vehicle and large number of routes conducted by the minibuses per day compared to other modes of public transport.

The high prevalence of TB in South Africa increases the already high risk of acquiring TB infection and disease for susceptible individuals who commute twice a day, 5 days a week, due to high exposure, contacts, interactions and social mixing in confined spaces. Drivers and fare-collectors are highly exposed individuals as they commute daily for a long period of time, interacting and mixing with many different infectious individuals [48]. Furthermore, this group is unlikely to go for diagnosis and they only seek care after the disease has progressed, perhaps because they don't have adequate education about infectious diseases, have limited time available, or they can't see the importance of getting tested for TB. This might be one of unidentified sources that led to the eruption of MDR-TB and a high rate of TB transmission in the community.

1.12 TB transmission in health care settings

TB transmission has been noted in different health care sections, including autopsy rooms and hospital wards [4, 58]. Health care workers, including nurses, doctors and pharmacists are at a high risk of acquiring TB infection and disease, because of frequent interaction and contact with infectious individuals during provision of health care services and facilities. Several studies have demonstrated the spread of TB infection and disease among nurses and medical students. For example, a study conducted in 1924 in Oslo, Norway, by Heimbeck, noted

that from 220 tuberculin-negative tests from 420 nursing students on entry into the degree, 210 (95%) became tuberculin-positive by graduation [2, 4]. Furthermore, in his 1946 work, Heimbeck demonstrated that 105 (37%) of 284 nurses who were initially tuberculin-negative became infected and developed TB disease [4]. Based on these findings, he concluded that nurses are at excessively high risk of acquiring TB infection and disease.

Apart from Heimbeck's work, numerous other studies have reported higher rates of TB transmission risk among nurses than the general population, and one of the studies concluded that the risk of developing TB among nurses was 500 times higher than the general population. Another study in 1953, noted that the risk of developing TB for hospital workers in contact with patients, including nurses and technical workers, such as doctors is 8 to 10 times higher than other workers in the same institution without such contact [4]. Numerous studies since then, including empirical evidence demonstrated by Myers *et al* (1930) [2] also show that health care workers, such as nurses and doctors are at a high risk of acquiring TB infection and developing clinical disease in their working environments. The main reservoir and spread of TB strains among health care workers is not clearly understood, however, several factors and conditions are attributable to TB transmission in heath care settings as discussed in the following section.

1.12.1 Factors associated with TB transmission in health care settings

The risk of TB transmission among health care workers is attributable to numerous factors, including interaction with active TB patients seeking treatment, some of whom are multi-drug and extensive-drug resistant TB individuals. Because of a prolonged period of unsuccessful treatment, multi-drug and extensive-drug resistant TB strains are among the key factors accelerating TB infection and disease in health care settings. The source of multi-drug and extensive-drug resistant strains is unknown but an increasing number of drug resistant TB patients in health care settings is attributable to poor diagnostic tools in some centres, late identification of TB cases and insufficient treatment or incomplete doses.

Furthermore, unidentified TB cases and HIV co-infection in TB individuals are additional factors that drive TB transmission in health care settings. In these scenarios, the probability of acquiring TB for health care workers is often higher because excessive precautions are not taken before exposure to infectious individuals. However, even if these cases are identified, some health care centres cannot afford protective devices, so health care workers provide services and interact with TB cases without wearing respiratory protective devices, such as

surgical masks and particulate respirators. Since TB transmission mostly occurs through talking, coughing, sneezing or singing by infectious individuals who expel airborne infectious particles into the air [40, 47], health care workers become exposed and inhale these airborne infectious particles, which can commence with infection. Furthermore, since the concentration of airborne infectious particles increases dramatically in the given space with increasing duration of exposure, health care workers may become infected depending on the proximity of staff offices to TB wards, exposure frequency, interaction with TB patients and strains of airborne infectious particles. TB transmission probability in ambulances during transportation of TB infectious individual is also reasonably high for health care workers [58]. This is exacerbated if engineering controls are not working properly in the ambulance and if personal protective devices used are not effective enough. Therefore, health care workers can have a high risk of TB infection and disease in different locations related to their working environments.

Apart from health care workers, susceptible patients, such as HIV infected individuals and children, are at high risk of acquiring TB infection and disease in the hospitals because of sharing environments and thus expired air with TB patients. Due to either overpopulation or limited ward rooms in some health care settings, particularly in developing countries, HIV infected and TB cases are admitted to the same ward and share exhaled air, some of which is derived from infective sources. This is one of the factors fostering the spread of TB co-infection with HIV in health care settings and the community at large. As mentioned earlier, since they don't receive treatment, unidentified HIV-negative TB patients are an additional threat in health care settings and in the general population [105]. Since they are not yet identified as cases for treatment and interact with people in different locations in the community, this group may also be among unidentified sources of multi-drug and extensive-drug resistant strains in the community [5].

Poor infrastructure is a key factor fostering TB transmission in health care settings, particularly in high TB settings, such as Sub-Saharan Africa and South-East Asia, where health care buildings are of poor quality and can accelerate the transmission of infectious diseases. As mentioned earlier, because of limited income and support for renovation and new building construction, TB cases are not isolated in most of health care settings, especially in developing countries. TB transmission in this sector is highly correlated with high concentration of air pollution, poor air disinfection and high prevalence of TB cases in the region. Although the WHO specified a ventilation of 12 ACH for health care settings, most are constructed with few and small windows, which are insufficient for indoor air circulation and removal of airborne infectious particles. However, though the WHO recommended ventilation is achieved in some health care centres, TB prevalence is still high. The major problem is that the WHO specified

the ventilation but not the number of patients per ward, location or room size. This ventilation is probably insufficient for TB control because ward room size, number of patients per ward, locations and climatic conditions are not the same for all health care settings world wide. Therefore, ventilation cannot be the same in all health care buildings, so it should rather be specified according to the location, climatic condition, room size and approximate number of TB patients to be accommodated.

1.13 TB prevalence in prisons and attributable factors

Though TB control has been successfully implemented in some developed countries such as the United State, TB remains as a public health concern that causes morbidity and mortality in prisons in both developed and developing countries [9]. Among the factors contributing to TB transmission in congregate and confined spaces, such as prisons, are prolonged period of exposure, high TB prevalence, high concentration of infectious particles per air volume, overcrowding, low ventilation per person, proximity to infectors and the virulence of the infecting pathogen strains [9, 15]. Prisons are one of the congregate and confined settings with low per person ventilation rate where TB transmission is noted to be high. Furthermore, prisons are overcrowded due to constant movement of inmates, long waits for trials and a large number of sentenced prisoners. Highly confined, small and contaminated communal cells with a large number of inmates, including infectious individuals lead to a high accumulation and retention of airborne infectious particles per air volume, which can cause infectious disease in susceptible individuals. Some prisons accommodate more than twice the specified number of prisoners. For example, South Africa, has the fourth highest global incarceration rate with $165,000$ prisoners in 237 prisons, with those awaiting trials comprising about one-third of this number [109]. These awaiting trial prisoners are frequently enclosed in communal cells of 40 to 60 prisoners with a small area of about $1.4\ m^2$ per inmate for 23 hours daily [109]. This environmental exposure to indoor air pollution containing airborne infectious particles puts the susceptible individuals at a high risk of acquiring TB infection and disease given the presence of infectious individuals. Thus, due to high TB prevalence, low per person ventilation, long period of exposure to infectors, indoor air pollution and overcrowding, TB transmission in prisons remains a world heath challenge [81].

HIV co-infection associated with TB is an important factor contributing to TB transmission in prisons [15, 81]. Intravenous drug users are at a high risk of acquiring HIV, and individuals with HIV are vulnerable and at a high risk of acquiring TB infection and developing active disease due to low CD4 counts, high viral loads, and a weak immune system. As mentioned

earlier, the risk for an individual with HIV infection to acquire TB is about 7-fold higher than for an HIV-negative individual. HIV co-infection has a great impact on TB diagnosis and treatment, and weakens TB control efforts, as HIV co-infected individuals usually have false negative TSTs and chest radiography results, which delays TB diagnosis, and thus treatment.

Though TB treatment strategies have been implemented globally, as mentioned before, multi-drug resistant TB (MDR-TB) makes the situation more complex and hampers TB control [9, 15, 81]. MDR-TB usually takes a long time to be treated and sometimes results in extensively drug resistant TB (XDR-TB), which is even more difficult to treat than MDR-TB. Due to poor diagnosis strategies, inadequate health care and high population density in prisons, TB cases are often delayed in getting treatment and can become resistant to chemotherapy, hampering TB control in prisons. The WHO postulated that approximately 24% of TB cases in prisons are MDR-TB [81]. Health services in prisons are generally poor, with old facilities, inadequate treatment, incomplete chemotherapy and careless health workers, which together can trigger MDR-TB. Prisons are not usually considered by the governments in terms of renovation and health service improvement. Furthermore, since health services in prisons are not under the Ministry of Health for political reasons, health workers in this sector are not motivated. Reinfection plays a key role in TB transmission probability, especially in high TB burden settings with insufficient TB diagnosis and treatment [34]. Since prisons are overcrowded, with high TB prevalence and inadequate treatment, reinfection might be one of the factors driving the increasing annual TB incidence and MDR-TB [65].

Malnutrition is another factor that accelerates susceptibility to infectious diseases in prisons and in the community at large. Apart from poor health care in prisons, malnutrition there can lead to weak immune systems. Generally, the environmental living conditions and nutrition in prisons are fostering infectious disease susceptibility. As mentioned earlier, tobacco smoking and drug abuse are also key factors contributing to TB infection susceptibility and disease [81]. A large number of prisoners are from populations at a high risk of acquiring TB infection and disease, such as homeless people, alcoholics, intravenous drug users and illegal immigrants [45]. Since a large number of people in these groups are highly susceptible to TB and face malnutrition in prisons, they can acquire TB infection and develop active TB in a short period of time, and then act as a source of TB transmission to other prisoners. In addition, though prisoners are under surveillance in prisons, some of them continue smoking and using drugs, which are associated with TB susceptibility. There is no empirical evidence and it is not well understood how inmates manage to get these substances and use them, perhaps through visitors, prison guards or prison staff.

It is estimated that the world's prisons hold about 8-10 million prisoners on any day, and

because of high entrance and exit rate of inmates, it is estimated that 4 to 6-times this number pass through the prison annually [81]. Furthermore, it is estimated that TB prevalence in prisons is very high, about 5 to 80 times that in the civilian population [15]. In fact, the WHO postulated that the level of TB in prisons is about 100 times higher than that of the civilian population, and these TB cases may account for up to 25% of the country's TB burden [81]. Furthermore, in 2012, WHO reported that TB in prisons in European countries is also remarkably high, like other countries worldwide, and notification rates of new TB cases in prisons in all reporting countries were multiple times higher than in civilian populations [82]. Due to high TB prevalence in prisons, a large number of susceptible inmates are at a high risk of acquiring TB infection and developing active TB. Some prisoners are released while they are still on treatment and interact direct with the civilian community, which is another challenge. Furthermore, since visitors, prison staff and former prison inmates who have already developed active TB interact directly with the community, they transmit TB to susceptible individuals and the fuel of TB infection and disease continues. Hence, since TB is not hampered by the prison walls, prisons act directly as a reservoir for TB transmission in the civilian community. Thus, while prisons are reserved for criminal punishment, the civilian community is punished indirectly in terms of disease transmission.

1.14 Project motivation and outline

Tuberculosis (TB) is a disease of endemic proportions, particularly in the Western Cape, South Africa which has one of the highest TB incidences in the world. The progression and severity of disease depend on a number of different factors, including the state of the host immune system, host genetics, and the virulence of the infecting strain of *Mycobacterium tuberculosis* (MTB). Transmission of TB occurs through sneezing, talking or coughing out of small droplets into the air which contain MTB. The efficiency of transmission is dependent on a number of factors, including proximity to infected people, length of contact, ventilation in the area, etc., and with enough information, can be modelled.

The Desmond Tutu HIV Centre (DTHC) is investigating the transmission of TB, particularly in crowded communities, such as in prisons and townships. They have the capacity to measure carbon dioxide levels in enclosed spaces in order to measure how much air we *"rebreathe"*, as an indication of the level of potential exposure in different places. DTHC clinicians are identifying TB cases in the study community and will investigate the clinical and radiological factors associated with infected aerosol production. Newly diagnosed TB cases are assessed for infectiousness by direct sputum smear status, quantitative culture, and direct measurement

of aerosols during coughing and normal activity. In addition, they have collected social mixing data, in particular for children from a school in Cape Town. This data includes movements of children from home to school, and interaction with others at school and in transit. Carbon dioxide levels are being monitored in these different locations. The advantage of this group is that the children are of similar ages and their movements have been tracked over time.

The aim of this project is to develop models of TB transmission in crowded locations including schools, households, public transport, prisons and health care settings. These models will use the movement, carbon dioxide as a marker of exhaled air and other data, together with the Wells-Riley equation, to determine the risk of TB infection over time. However, since it is somewhat difficult to monitor indoor air conditions due to climatic changes, we shall modify the Wells-Riley equation so that it can be applied to determine the risk probability of TB transmission in all conditions regardless of steady-state ventilation. Though Rudnick and Milton modified the Wells-Riley model under non-steady state conditions, they applied the same concept of quanta and well mixed airspace as postulated by Wells (1995). Infectious quantum hides many significant parameters, such as particle size, deposition fraction, bacteria mortality and survival, which have previously been difficult to quantify, but they may be amenable to modern technological measurement. Thus, the Rudnick and Milton equation can be further modified. Additionally, we aim to develop a specific mathematical model that determines TB transmission probability in a group of people contributing rebreathed air (carbon dioxide) equally in a confined space. Moreover, we aim to develop a general mathematical model that determines infection risk probability of TB transmission in all manners of interaction in the community in general mixing environments associated with TB transmission. We shall quantify the quantity of exhaled air that can be inhaled in the buildings with high probability of inducing infection. We shall explore factors attributable to TB transmission in each of these five locations and demonstrate measures for TB prevention and control. Furthermore, we shall explore the impact of effective contact rate on TB epidemiology using a compartmental model. Using an age-structured mathematical model we shall discuss the impact of the vaccines on TB control.

Modelling TB transmission is an important tool that provides new knowledge about the dynamics of TB burden and can suggest alternative methods for TB infection and disease control. Chapter two in this study, describes our model for the transmission of TB. Here, we modified the Wells-Riley and Rudnick-Milton models to obtain a new mathematical model, which predicts the risk of airborne infectious diseases in all conditions without the limitation of one quanta of contagion and assumptions of well mixed airspace. By numerical simulation, we applied the mathematical model to different real life conditions to predict the risk of TB

transmission probability under all conditions by monitoring exhaled air by infectors in confined spaces. Furthermore, this chapter demonstrates the quantity of rebreathed air required to induce infection in the buildings.

Chapter three describes reanalysis of previous *in vivo* studies by applying the mathematical model developed in this study to guinea pig experimental data. Since it is not clear what number of infective organisms are required to induce TB infection, this chapter aimed to explore the probability of exposed guinea pigs acquiring infection using *in vivo* experimental data, while varying airborne infectious particles and deposition fraction. We demonstrated the number of surviving airborne infectious particles required to attain the threshold level to induce infection for exposed guinea pigs. Here, we dispute that TB is transmitted by a single infective organism as reported by prior studies.

Chapter four explores TB transmission in congregate settings, including schools, households, public transport, health care settings and prisons using mathematical modelling approach. We demonstrate the contribution of biological, socio-economic and environmental factors to TB prevalence in these locations, and investigate TB transmission in these locations using mathematical models developed in this study. Additionally, this chapter describes preventive measures for TB control in these crucial locations.

Chapter five demonstrates TB transmission using a compartmental model, where we explored the impact of effective contact rate on TB epidemiology. Here, we used a next generation method to explore the basic reproduction number and computed eigenvalues to predict the stability of the disease free equilibrium. Furthermore, we simulated the model by introducing an infectious individual with varying effective contact rate and observed the number of primary infection, reinfected and active TB individuals, with increasing effective contact rate.

Chapter six describes the impact of vaccines on TB control using an age-structured mathematical model. This chapter demonstrates conditions under which TB vaccines can be used to have greater impacts on TB control. Furthermore it shows active disease progression in different age groups and attributable factors. Finally, chapter seven provides the conclusions of the study.

Chapter 2

Mathematical models for TB transmission

Abstract

In this study we develop a flexible mathematical model that predicts the risk of airborne infectious diseases, such as tuberculosis (TB) under steady state and non-steady state conditions by monitoring exhaled air by infectious individuals in a confined space. In the development of the model, we use rebreathed air accumulation rate concept to directly quantify the average volume fraction of exhaled air in a given space. From a biological point of view, exhaled air by infectious individuals contains airborne infectious particles viable with potential for TB infection. Since not all infectious particles can reach the alveolar, we take into consideration that the infectious particles that establish the infection are determined by alveolar deposition fraction, which is the probability of each infectious particle reaching the target infection site of the respiratory tracts and causing infection. Furthermore, we compute the quantity of carbon dioxide as a marker of exhaled air, which can be inhaled in the space with high probability of causing airborne infectious disease given the presence of infectious individual(s). We demonstrated mathematically and schematically the correlation between TB transmission probability and airborne infectious particle generation rate, ventilation rate, average volume fraction of exhaled air, TB prevalence and duration of exposure to infectious individuals in confined spaces.

2.1 Introduction

Mathematical modelling is one of the computational tools that can be used to investigate or predict tuberculosis (TB) transmission and identify measures for infection and disease control. Mathematical model development in epidemiological studies usually involves equations which helps understand how the phenomena under investigation evolves over time. Additionally, in developing the model, we make assumptions about the numerous factors that influence the evolution of the time dependent process that we are dealing with. We obtain the model by analysing these assumptions in terms of mathematics, and use mathematical techniques to analyse the model. If the model takes the form of an equation, we apply mathematical tools to solve this equation. Finally, we assess the outcome of our mathematical analysis and translate this back into the real world situation to find out how closely the predictions from our model agree with actual observations. Mathematical models will usually only be an approximation of what is actually happening in the community in real life.

In this study we modified the Wells-Riley and Rudnick-Milton equations to develop another, more flexible equation to study the transmission of infectious diseases, such as TB. In the development of the model, we use rebreathed air accumulation rate concept to directly quantify the average volume fraction of exhaled air in a given space. From a biological point of view, exhaled air by infectious individuals contains airborne infectious particles, which cause airborne infectious diseases [66, 92, 100, 113]. Since not all infectious particles can reach the alveolar, we take into consideration that the infectious particles that reach the alveolar to establish the infection are determined by alveolar deposition fraction, which is the probability of each infectious particle reaching the target infection site of the respiratory tracts and causing infection [66]. Furthermore, we compute the quantity of rebreathed air required to induce airborne infectious diseases in confined spaces with the presence of infectious individuals, as discussed in the following sections.

2.2 The Wells-Riley model

The Wells-Riley equation has been extensively used to model infectious diseases, such as TB risk probability for susceptible individuals to be infected if they are exposed to an infectious individual in a confined space [24]. Additionally, this equation has been widely used to illustrate how ventilation is associated with airborne infection risks in the context of the clinical environment. For example, it has been used to demonstrate the outbreaks of measles and TB in the USA, and it has also been used to assess the risk of contracting TB infection during

commercial aircraft flights [24].

The Wells-Riley equation was developed by Riley and co-workers in an epidemiological study to demonstrate the outbreak of measles in an elementary school [74]. The equation is focused on the quanta, which is the number of droplet nuclei required to cause infection for 63.2% of susceptible individuals in a confined space as demonstrated by Wells (1955) and this is known as the Wells-Riley model. In the derivation of this equation, Riley *et al* (1978) made two assumptions: first, that airborne infectious particles (viable particles with potential for TB infection) are spread under steady-state conditions, implying that quanta concentration and the rate of outdoor air supply do not vary with time, and second, that the airspace is well mixed, which implies that infectious particles are evenly distributed in the airspace of the room regardless of the source proximity and duration of generation [73]. Based on these assumptions, this equation is useful in a confined space where air flow is almost constant, since it works under steady-state conditions. The Wells-Riley equation was developed from the concept of quanta generation rate and the average number of quanta as described below.

The average number of quanta $(\bar{\mu})$ inhaled by a susceptible individual in a confined space, is given by the following equation:

$$\bar{\mu} = pt\bar{N} \tag{2.2.1}$$

where p is the breathing rate of the susceptible individual (L/s), t is the time spent in a confined space, and $\bar{N}$ is the average quantum concentration (quanta/m^3).

Quanta accumulation rate in an enclosed space of volume, V (m^3), is equal to quanta generation rate minus the rate of quanta removed by ventilation:

$$V\frac{dN}{dt} = Iq - NQ \tag{2.2.2}$$

where q denotes quanta generation rate (quanta/s), Q is the indoor ventilation rate $(\mathrm{L/s})$, I is the number of infectious individuals and N is the number of quanta in the space.

Assuming that the infectious individual stays in the confined space in a given time interval and there is no occurrence of new infectious individuals, the steady-state condition was assumed, implying that $\frac{dN}{dt} = 0$. Hence, the average quantum concentration $(\bar{N})$ from Equation (2.2.2) can be expressed as

$$\bar{N} = \frac{Iq}{Q} \tag{2.2.3}$$

Substituting $\bar{N}$ from Equation (2.2.3) into Equation (2.2.1), the average number of quanta

($\bar{\mu}$) inhaled by susceptible individuals was obtained as

$$\bar{\mu} = \frac{Iqpt}{Q} \tag{2.2.4}$$

Wells (1955) postulated that the number of susceptible individuals infected in a confined space bears a Poisson distribution to the number of tubercle bacilli, which they breathe [3], such that

$$P = 1 - e^{-\bar{\mu}} \tag{2.2.5}$$

Thus, the Wells-Riley equation, which predicts the risk of TB transmission probability for susceptible individuals is written as

$$P(T \leq t|I, q, Q, p) = 1 - e^{-\frac{Iqpt}{Q}} \tag{2.2.6}$$

where $P(T \leq t|I, q, Q, p)$ denotes the risk of TB transmission probability for susceptible individuals and $T \leq t$ is the random variable representing infection risk for susceptible individuals up to the time spent in the confined space.

In his book entitled "Airborne contagion and air hygiene", Wells (1955) postulated the concept of the quantum of infection, and defined a quanta as being the number of infectious droplet nuclei required to infect 63.2% of susceptible individuals in a confined space [3]. He demonstrated that the number of susceptible individuals who become infected follows a Poisson distribution to the number of infectious particles which they breathe, implying that 63.2% $(1 - e^{-1})$ of a population becomes infected when, on the average, each susceptible individual inhales one quanta of contagion [3].

However, in contrast to Wells' (1995) postulate, the overall infectivity of any airborne infectious particle mostly depends on the immunological state of the susceptible individuals as well as the virulence of the infecting pathogen strains. We can't directly measure and determine the exact number of airborne infectious particles present in any infectious disease outbreak, however, it is possible to indirectly determine airborne infectious particles associated with an outbreak, if the numerous physical parameters associated with the outbreak are known [24]. When a host organism is exposed to the airborne infectious particles, whether the organism will be infected or not depends on the infectivity of the infectious particles and the immune response of the host organism [74]. Different regions of the respiratory tract may have different immune mechanisms, implying that airborne infectious particles generally have different infectivity in these different regions. The threshold level is the minimum amount of infectious particles required to induce infection. When the intake dose reaches or exceeds the threshold level, the

probability of infection cannot be zero. These facts clarify that for a susceptible individual to be infected, the number of infectious particles inhaled should attain the threshold level to dominate the immunological state of the host to commence the infection.

In contrast to Wells' postulate, it is not plausible that one infective organism is likely to cause infection from each exposure. For example, Wells agreed with and emphasised Chapin's postulate that "the room air is not very dangerous to breathe in a short time even if airborne infectious particles can be found in the settled dust" [59]. This postulate suggests that Wells was wrong in his observation, and shows that airborne infectious diseases, such as TB are not directly caused by a single infective organism, otherwise it would be very dangerous to breathe contaminated air in a short period of exposure. The probability of inhaling a single infective organism is very high in any period of exposure in a contaminated space.

In reality, TB infection is a somewhat complex scenario that incorporates the immune response of the host and the threshold level of airborne infectious particles, which is determined by respiratory deposition fraction, duration of exposure, strains of airborne infectious particles and proximity to infectious individual(s). Different airborne infectious particles may have different strains with different threshold levels and it is not obvious that every infected human or organism is infectious [5]. For example in Wells' experiment it was noted that there were 5 different strains among 22 cultures, 12 cultures were the same strain, 7 had another strain and different strains were detected in the remaining 3 of 22 cultures [59].

Airborne infectious particles are randomly distributed in air and any estimated exposure level or intake dose would be an expected value rather than an exact one. Respiratory deposition fraction of airborne infectious particles is also an expected value rather than an exact one. This implies that when the respiratory deposition fraction of airborne infectious particles with a particular size is θ, each infectious particle with this size would have a probability of successful deposition equal to θ. When airborne infectious particles are inhaled by the susceptible individual, not all, but a fraction of the inhaled infectious particles may successfully reach the target infection site in the respiratory tract depending on the deposition fraction. In addition, because of the dynamics of airborne infectious particles, the respiratory deposition of these airborne infectious particles is dependent on the particle dynamic size. Because of the difference in respiratory deposition of airborne infectious particles with different sizes, the airborne infectious particles have different deposition fractions on different regions of the respiratory tract [74]. For example, airborne infectious particles with sizes $> 5\mu m$ are trapped dramatically on the upper respiratory tract [86], and those with sizes $> 10\mu m$ generally do not reach the alveolar region. However, airborne infectious particles with critical size range $1\mu m$ to $5\mu m$ have a high probability of reaching and depositing on the alveolar region [12]. This implies that

not all inhaled airborne infectious particles can reach or be retained in the target infection site. Infectectivity of airborne infectious particles increases dramatically with increasing deposition fraction, thus, when assessing the risk of airborne infectious disease, the respiratory deposition fraction of infectious particles has to be taken into consideration as demonstrated in Section 2.4 below.

Since the Wells-Riley equation seems to have several limitations as discussed above, including assumptions and an equilibrium condition, which cannot be achieved consistently as the climate changes, it should therefore be modified to one which can operate under all situations. Rudnick and Milton (2003), modified the Wells-Riley equation by monitoring carbon dioxide, though there are some similarities, including assumptions and concepts such as well mixed air and quanta, which are still not well understood in epidemiological studies and the community, as discussed below.

2.3 Rudnick and Milton approach

Rudnick and Milton (2003), modified the Wells-Riley equation using exhaled air (carbon dioxide) volume fraction to estimate the number of quanta inhaled by susceptible individuals. In their approach, they used the same assumptions as those used in the Wells-Riley equation, for example, airspace should be well mixed. Biologically, this assumption is not plausible since in reality the room cannot contain uniformly mixed air. This is because the concentration of airborne infectious particles is higher close to the infector (source) than other parts of the room and is why when considering TB transmission, we should take into consideration the duration of exposure and proximity to the infector. Despite the fact that, since Wells (1955) first used the word quanta, it has caused some confusion in understanding TB transmission, Rudnick and Milton still used the same approach to modify the Wells-Riley equation. The derivation of the Rudnick and Milton equation started by considering carbon dioxide volume fraction (f) as follows:

$$f = \frac{C - C_o}{C_a} \tag{2.3.1}$$

where C is the indoor carbon dioxide volume fraction, C_o is the outdoor carbon dioxide volume fraction and C_a is the volume fraction of carbon dioxide in exhaled air.

The quantum concentration (N), given by the product of quanta concentration in exhaled air and the volume fraction of exhaled air by infectors in the space was introduced as follows:

$$N = \frac{fIq}{np} \tag{2.3.2}$$

where q is the quantum generation rate by infectors (quanta/s) and n is the total number of people in the space.

Rudnick and Milton postulated that the average volume fraction $(\bar{f})$ of exhaled air was computed by integrating f in Equation (2.3.1) over time divided by elapsed time, though it was not clearly shown. Hence, the average quantum concentration $(\bar{N})$ was obtained by using the following equation

$$\bar{N} = \frac{\bar{f}Iq}{np} \tag{2.3.3}$$

The average number of quanta inhaled by susceptible individuals was given by

$$\bar{\mu} = pt\bar{N} \tag{2.3.4}$$

Substituting $\bar{N}$ from Equation (2.3.3) into Equation (2.3.4), the average number of quanta inhaled by susceptibles was obtained:

$$\bar{\mu} = \frac{Iq\bar{f}t}{n} \tag{2.3.5}$$

As stated earlier, Wells (1955), postulated that the number of susceptible individuals infected in a confined space bears a poisson distribution to the number of TB bacilli they breathe, such that

$$p = 1 - e^{-\mu} \tag{2.3.6}$$

Hence, the probability of infected individuals was expressed as:

$$P(T \leq t|I,q,n,\bar{f}) = 1 - e^{-\frac{Iq\bar{f}t}{n}} \tag{2.3.7}$$

Equation (2.3.7) is known as the Rudnick and Milton equation, and determines the risk of TB transmission under all conditions. However, in this equation, $\bar{f}$ was not directly determined from the volume fraction of carbon dioxide, instead the quantum concentration $(\bar{N})$ was introduced indirectly by using the same equation as that used in the Wells-Riley equation as follows:

$$V\frac{dN}{dt} = Iq - NQ \tag{2.3.8}$$

This equation is exactly the same as Equation (2.2.2), which is used in the Wells-Riley equation to determine the quantum concentration under steady state conditions, and it has no

relationship with monitored carbon dioxide as a marker of rebreathed air in the space. Rudnick and Milton used this equation to determine the average quantum concentration under non-steady-state conditions as follows:

$$\int_0^N \frac{dN}{Iq - NQ} = \int_0^T \frac{1}{V} dt \tag{2.3.9}$$

Integrating Equation (2.3.9) by applying a substitution method and rearranging it, we obtain:

$$\ln(Iq - NQ) - \ln(Iq) = -\frac{QT}{V} \tag{2.3.10}$$

Applying logarithmic rules, Equation (2.3.10) can be written as:

$$\ln\left[\frac{Iq - NQ}{Iq}\right] = -\frac{QT}{V} \tag{2.3.11}$$

Hence, quantum concentration under non-steady-state conditions from Equation (2.3.11) is:

$$N = \frac{Iq}{Q}\left[1 - e^{-\frac{QT}{V}}\right] \tag{2.3.12}$$

where T is the random variable representing infection risk for susceptible individuals up to the time spent in the confined space.

The average quanta concentration was obtained by integrating Equation (2.3.12) per elapsed time:

$$\begin{aligned} \bar{N} &= \frac{1}{T}\int_0^T \frac{Iq}{Q}\left[1 - e^{-\frac{QT}{V}}\right] dT \\ &= \frac{Iq}{Q}\left[1 - \frac{V}{QT}\left(1 - e^{-\frac{QT}{V}}\right)\right] \end{aligned} \tag{2.3.13}$$

$\bar{N}$ from Equation (2.3.13) was substituted into Equation (2.3.4) to obtain the average number of quanta ($\bar{\mu}$) inhaled by susceptible individuals:

$$\bar{\mu} = \frac{Iqpt}{Q}\left[1 - \frac{V}{QT}\left(1 - e^{-\frac{QT}{V}}\right)\right] \tag{2.3.14}$$

Finally, $\bar{\mu}$ from Equation (2.3.14) was substituted into Equation (2.3.6) to obtain the modified Wells-Riley equation as:

$$P(T \leq t|I,q,Q,p) = 1 - e^{-\frac{Iqpt}{Q}\left[1-\frac{V}{QT}\left(1-e^{-\frac{QT}{V}}\right)\right]} \tag{2.3.15}$$

Equation (2.3.15) is the modified Wells-Riley equation, by Rudnick and Milton (2003), under non-steady state conditions. However, derivation of this equation carries the same concept as the Wells-Riley equation under steady-state conditions since both used the same equations (Equations 2.2.2 and 2.3.8) and idea of quanta. Furthermore, this equation has no link with monitored carbon dioxide since it only applies the concept of quanta under non-steady-state conditions. As discussed earlier, the average volume fraction ($\bar{f}$) was not directly determined from monitored carbon dioxide as a marker of rebreathed air as expected. Hence, this demonstrates that the average volume fraction of exhaled air was not directly applied in the modification of the Wells-Riley equation, instead the concept of quantum concentration ($\bar{N}$) was considered and extended. This implies that both the Wells-Riley and Rudnick-Milton equations have limitations, which impact the prediction of infectious disease risks. In this study, we modified the Wells-Riley and the Rudnick-Milton equations by monitoring carbon dioxide as a marker of rebreathed air and used it to determine the average volume fraction of exhaled air, $\bar{f}$, directly from the volume fraction of exhaled air as discussed below.

2.4 Modification of the Wells-Riley and Rudnick-Milton equations

As discussed earlier, both the Wells-Riley and Rudnick-Milton equations assume completely mixed airspace, implying that the airborne infectious agents are evenly distributed throughout a room. In reality and from a biological point of view, this is not true, the room air can never be completely mixed [24, 74]. This is because regions of high and low contaminant concentrations will exist simultaneously within the same airspace, with the highest concentrations usually occurring close to the contaminant source. Furthermore, in the derivation of these equations, the quanta generation rate concept, which is not well understood, was considered, as demonstrated in Equations (2.2.2) and (2.3.8). Infectious quantum hides very important parameters such as particle size, deposition fraction, bacterial mortality and survival, which have previously been difficult to quantify. Now, however, they may be amenable to modern technological measurement. Though it has been applied in different respiratory infectious disease scenarios, the Wells-Riley equation should therefore be modified to develop a new equation which is flexible and holds for all infectious disease transmission environments. Additionally,

since the Rudnick-Milton equation seems to follow the same concepts and assumptions as the Wells-Riley equation, it should also be modified.

The quantity of air rebreathed from others has been estimated in a variety of indoor congregate settings including households, schools and transport by use of a portable carbon dioxide monitor with geo-positioning capacity. Rebreathed air volumes vary considerably between individuals and locations and have been proposed as a novel metric, which can identify social and environmental factors associated with potential airborne transmission risk [100, 113]. We use carbon dioxide concentrations in confined spaces as a marker of rebreathed air to directly compute the fraction of inhaled air that has been exhaled previously by individuals in the space, called the average volume fraction of exhaled air. Furthermore, we determine the average number and concentration of airborne infectious particles inhaled by susceptible individuals to induce infection. Carbon dioxide is a very diffusible natural tracer gas, which can be easily measured within an enclosed environment [90, 100, 113]. We assume that all occupants of the room contribute equally to the elevated indoor carbon dioxide level as a maker of exhaled air, and susceptible individuals become infected if they inhale rebreathed air from infectors, which contains airborne infectious particles.

Respiratory activities such as talking, coughing, sneezing and singing could contribute to respiratory particle production [40, 47]. Since not all infectious particles can reach the target infection site, we took into account that the infectious particles that commence the infection are determined by respiratory deposition fraction, which is the probability of each infectious particle reaching the target infection site of the respiratory tracts and causing infection. Hence, in contrast to quanta, we use airborne infectious particles in exhaled air from infectors to modify the Wells-Riley and Rudnick-Milton equations. For a susceptible individual to be infected, the number and concentration of airborne infectious particles inhaled should attain the threshold level to dominate the immunological state of the host [66]. Using the average volume fraction of exhaled air, respiratory deposition fraction, breathing rate, ventilation rate, generation, mortality and survival rates of airborne infectious particles by infectors, we modify both the Wells-Riley and Rudnick-Milton equations and obtain a flexible mathematical model that predicts the risk of airborne infectious diseases under non-steady state and steady state conditions. This approach will enhance our understanding of TB transmission scenarios in the community and improve preventive measures for TB control.

In the modification of these equations, we made three assumptions. First, ventilation rate should not necessarily be the same for all susceptible individuals in a confined space, second, accumulated exhaled air by infectors contains airborne infectious particles in a confined space and third, the probability of infection for each susceptible individual in the space is independent.

This is because for a susceptible person to be infected, the average number and concentration of infectious particles inhaled by each susceptible individual should reach the threshold level, which is the minimum number and concentration of infectious particles required to reach the target infection site of the host to cause infection [74]. Additionally, since the concentration of airborne infectious particles is higher near the source (infector) than other parts of the room, airspace cannot be uniform as assumed in the Wells-Riley model and subsequent modified Wells-Riley models [66].

As stated earlier, exhaled air from infectors is the carrier of airborne infectious particles that cause airborne infectious diseases, such as TB. Since we have the ability to monitor carbon dioxide concentration as a marker of rebreathed air in a room [100, 113], we use the exhaled air generation rate concept to modify the Wells-Riley and Rudnick-Milton equations as follows: Let us consider the concentration of exhaled air in a confined space of volume V (m^3), which contains n persons and let carbon dioxide fraction contained in breathed air be C_a, while the ventilation rate is Q (L/s), and indoor carbon dioxide concentration is C (ppm). Airborne infectious particles are generated in the accumulated exhaled air in confined spaces. Hence, exhaled air accumulation rate in the space is equal to indoor exhaled air generation rate minus the rate of exhaled air removed by ventilation as demonstrated in the following differential equation:

$$V\frac{dC}{dt} = npC_a - QC,\ n \geq 2 \tag{2.4.1}$$

where n is the total number of persons in the space and p is the breathing rate (L/s).

From this exhaled air basic equation (Equation (2.4.1)), we can determine the average volume fraction of exhaled air in an enclosed space at either non-steady state or steady-state conditions. Therefore, we can develop an equation that predicts the risk of infectious disease transmission under all conditions by monitoring carbon dioxide as a marker of rebreathed air in the given space.

Arranging Equation (2.4.1) and assuming that exhaled air started to rise from 0 to $C_{(T)}$ when persons entered the space, and time spent is counted from 0 to T, we obtain sampled exhaled air in the space at non-steady-state conditions as demonstrated in the following equation:

$$\int_0^{C_{(T)}} \frac{dC}{npC_a - QC} = \frac{1}{V}\int_0^T dt \tag{2.4.2}$$

After integrating Equation (2.4.2) by application of a substitution method and simplifying it, we obtain:

$$\ln(npC_a - QC_{(T)}) - \ln(npC_a) = -\frac{QT}{V} \tag{2.4.3}$$

If we further simplify Equation (2.4.3) by applying logarithmic rules we obtain:

$$\ln\left[\frac{npC_a - QC_{(T)}}{npC_a}\right] = -\frac{QT}{V} \tag{2.4.4}$$

Simplifying Equation (2.4.4) further, by applying logarithmic and exponential rules, we obtain sampled exhaled air concentration $(C_{(T)})$ in the given space, which is the difference between indoor exhaled air concentration and outdoor exhaled air concentration (rebreathed air removed by ventilation) divided by the rate of ventilation:

$$C_{(T)} = \frac{npC_a}{Q}\left[1 - e^{-\frac{QT}{V}}\right] \tag{2.4.5}$$

where $\frac{Q}{V}$ is the rate of air change outdoors and T is the elapsed time in the given space.

Taking into account the volume fraction of exhaled air, (f) which is given by the sampled exhaled air concentration $(C_{(T)})$ in the space divided by carbon dioxide concentration in breathed air $(C_a \approx 0.04)$ we get:

$$\begin{aligned} f &= \frac{npC_a}{QC_a}\left[1 - e^{-\frac{QT}{V}}\right] \\ &= \frac{np}{Q}\left[1 - e^{-\frac{QT}{V}}\right] \end{aligned} \tag{2.4.6}$$

Hence, we obtain the average volume fraction of exhaled air $(\bar{f})$ per elapsed time by integrating Equation (2.4.6) with respect to time from 0 to T:

$$\bar{f} = \frac{1}{T}\int_0^T \frac{np}{Q}\left[1 - e^{-\frac{QT}{V}}\right] dT \tag{2.4.7}$$

$$= \frac{1}{T}\left[\frac{npT}{Q} + \frac{npV}{Q^2}e^{-\frac{QT}{V}}\right]_0^T \tag{2.4.8}$$

Thus,

$$\bar{f} = \frac{1}{T}\left[\frac{npT}{Q} + \frac{npV}{Q^2}e^{-\frac{QT}{V}} - \frac{npV}{Q^2}\right] \tag{2.4.9}$$

If we further simplify Equation (2.4.9), we obtain the average volume fraction of exhaled air for non-steady-state conditions, and if we apply the same procedure in the exhaled air basic equation (Equation (2.4.1)) while $\frac{dC}{dt} = 0$, we obtain the average volume fraction under steady state conditions, or if $\frac{QT}{V} \to \infty$, Equation (2.4.9) adopts steady-state conditions:

$$\bar{f} = \begin{cases} \frac{np}{Q}\left[1 - \frac{V}{QT}\left(1 - e^{-\frac{QT}{V}}\right)\right] & \text{if non} - \text{steady} - \text{state} \\ \frac{np}{Q} & \text{if steady} - \text{state} \end{cases} \tag{2.4.10}$$

Therefore, Equation (2.4.10) denotes the average volume fraction of exhaled air, $\bar{f}$ $(0 < \bar{f} < 1)$ under non-steady-state and steady-state conditions, where each part can be derived from Equation (2.4.1) depending on the condition used to solve the problem.

As discussed earlier, the likelihood of airborne infectious particles released by infectors causing infection in susceptible individuals is extremely high if they reach the target infection site of the host at a threshold level. However, some airborne infectious particles can be trapped in the upper respiratory tract or be reflected to other parts of the body, where the probability of causing infection is almost negligible. Let β be the total airborne infectious particle generation rate (particles/s) released by an infector and μ be the mortality rate of generated airborne infectious particles (particles/s) that do not reach the alveolar. Hence, airborne infectious particles released by infectors that reach the target infection site of the susceptible individual to cause infection, are generated with the rate $\beta - \mu$ (particles/s) as demonstrated in Figure 2.1.

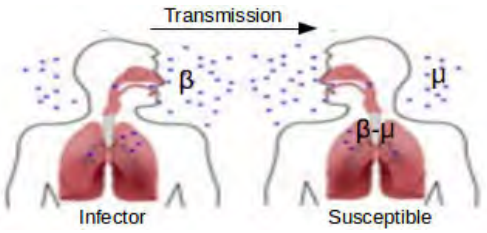

Figure 2.1: Movement of airborne infectious particles

Thus, the average concentration of airborne infectious particles $(\bar{\mathscr{N}})$, is equal to the average volume fraction of rebreathed air by infectors $(\frac{I\bar{f}}{n})$ multiplied by the average concentration of airborne infectious particles released by infectors in the space $(\frac{\beta-\mu}{p})$ that reach the target infection site of the respiratory tract:

$$\bar{\mathscr{N}} = \frac{I\bar{f}(\beta - \mu)}{np},\ I \geq 1 \text{ and } (\beta - \mu) \geq 1 \tag{2.4.11}$$

where $\bar{\mathscr{N}}$ is the average concentration of airborne infectious particles (particles/m^3), $(\beta - \mu)$ is the survival rate of infectious particles (particles/s) that deposit in the alveolar, n is the total number of individuals in the space and $\bar{f}$ is the average volume fraction of exhaled air that is obtained by integrating the volume fraction of exhaled air per time spent in the given

space as discussed above.

Substituting $\bar{f}$ from Equation (2.4.10) into Equation (2.4.11) gives:

$$\bar{\mathscr{N}} = \begin{cases} \frac{I(\beta-\mu)}{Q}\left[1-\frac{V}{QT}\left(1-e^{-\frac{QT}{V}}\right)\right] & \text{if non}-\text{steady}-\text{state} \\ \frac{I(\beta-\mu)}{Q} & \text{if steady}-\text{state} \end{cases} \tag{2.4.12}$$

which is the average concentration of airborne infectious particles that cause TB infection when a threshold level is attained.

Since not all infectious particles can reach and deposit in the alveolar, let θ be a respiratory deposition fraction of infectious particles that reach the target infection site of the host. Hence, the average number of infectious particles $(\bar{\lambda})$ breathed by a susceptible individual that causes infection, is equal to the product of the volume of breathed air by susceptibles (pt), respiratory deposition fraction of infectious particles, θ $(0<\theta<1)$ and the average concentration of infectious particles $(\bar{\mathscr{N}})$:

$$\bar{\lambda} = pt\theta\bar{\mathscr{N}},\ t>0 \tag{2.4.13}$$

Substituting $\bar{\mathscr{N}}$ from Equation (2.4.12) into Equation (2.4.13), we obtain the average number of airborne infectious particles that reach the target infection site of the host to commence the infection:

$$\bar{\lambda} = \begin{cases} \frac{I(\beta-\mu)\theta pt}{Q}\left[1-\frac{V}{QT}\left(1-e^{-\frac{QT}{V}}\right)\right] & \text{if non}-\text{steady}-\text{state} \\ \frac{I(\beta-\mu)\theta pt}{Q} & \text{if steady}-\text{state} \end{cases} \tag{2.4.14}$$

Therefore, Equation (2.4.14) denotes the average number of infectious particles inhaled by a susceptible individual that reach the target infection site of the host to cause TB infection under non-steady-state and stead-state conditions.

Computing an expected average number of airborne infectious particles in Equation (2.4.14), the percentage of airborne infectious particles, γ, that cause airborne infectious diseases in exhaled air can be estimated as:

$$\gamma = \frac{\bar{\lambda}}{C_T}\times 100 \tag{2.4.15}$$

where C_T is the sampled exhaled air in the given space (refer to Equation (4.3.1)).

Applying Wells' (1995) assumption that the infected number of susceptible individuals in a

confined space follows a Poisson distribution, the modified equation should be written as:

$$P(T \leq t|I,\beta,\theta,\mu,Q,p) = 1 - e^{-\bar{\lambda}} \tag{2.4.16}$$

Where $P(T \leq t|I,\beta,\theta,\mu,Q,p)$ is the probability of TB infection risk for susceptible individuals under non-steady-state and steady-state conditions.

Substituting $\bar{\lambda}$ from Equation (2.4.14) into Equation (2.4.16), we obtain an equation that predicts the risk of TB transmission probability at non-steady-state and steady state conditions:

$$P(T \leq t|I,\beta,\theta,\mu,Q,p) = \begin{cases} 1 - e^{\left(-\frac{I(\beta-\mu)\theta pt}{Q}\left[1-\frac{V}{QT}\left(1-e^{-\frac{QT}{V}}\right)\right]\right)} & \text{if non} - \text{steady} - \text{state} \\ 1 - e^{-\frac{I(\beta-\mu)\theta pt}{Q}} & \text{if steady} - \text{state} \end{cases} \tag{2.4.17}$$

Thus, Equation (4.4.1) demonstrates that both the Wells-Riley and Rudnick-Milton equations can be modified to model the risk of infectious disease transmission under all conditions by applying a carbon dioxide accumulation rate concept as a marker of exhaled air. In our approach in the modification of these equations, we monitored carbon dioxide in the room as a marker of rebreathed air by means of portable carbon dioxide monitors [100] and used it to determine the average volume fraction of exhaled air $(\bar{f})$. This is because carbon dioxide as a marker of exhaled air is one of the most diffusible gases, which reflect the dispersal of airborne infectious particles that cause airborne infectious diseases in a confined space. From a biological point of view, a susceptible individual can be infected by one or more infectious particles depending on the virulence of the infecting pathogen strain and the threshold level of the number and concentration of infectious particles which successfully reach the target infection site to dominate the immunological state of the host [66]. However, we can't directly measure and determine the exact number of infectious particles that dominate the immune system of the host and cause infectious disease, as postulated by Wells (1955). As stated earlier, this is because the average number and deposition fraction of airborne infectious particles are expected values rather than exact ones.

Taking Equation (2.4.10) into consideration and dividing by n on both sides, we obtain:

$$\frac{\bar{f}}{n} = \begin{cases} \frac{p}{Q}\left[1 - \frac{V}{QT}\left(1 - e^{-\frac{QT}{V}}\right)\right] & \text{if non} - \text{steady} - \text{state} \\ \frac{p}{Q} & \text{if steady} - \text{state} \end{cases} \tag{2.4.18}$$

Hence, if we make a substitution of $\frac{\bar{f}}{n}$ into Equation $(4.4.1)$, we obtain the modified equation

of the Wells-Riley and Rudnick-Milton equations that predicts the risk of TB transmission under all conditions in terms of the average volume fraction of exhaled air:

$$P(T \leq t|I,\beta,\theta,\mu,n,\bar{f}) = 1 - e^{-\frac{I(\beta-\mu)\theta\bar{f}t}{n}} \tag{2.4.19}$$

Where $P(T \leq t|I,\beta,\theta,\mu,n,\bar{f})$ is the probability of TB transmission risk for susceptible individuals under any condition given the presence of infectious individuals in a confined space.

As mentioned earlier, in our approach we monitored the carbon dioxide concentration in the room as a marker of rebreathed air and used the exhaled air accumulation rate concept to directly compute the average volume fraction of exhaled air. An exponential term of this equation is equal to the average number of airborne infectious particles inhaled by each susceptible individual to induce infection, and not quanta. This approach provides more information for understanding the transmission of airborne infectious diseases.

2.4.1 New TB cases

From Equation (4.4.2), prevalence (Λ) is the ratio of infectious (I) and total number of individuals (n) in a given population, as

$$\Lambda = \frac{I}{n} \tag{2.4.20}$$

The general modified equation in terms of prevalence, can be written as:

$$P(T \leq t|\beta,\theta,\mu,\Lambda,\bar{f}) = 1 - e^{-(\beta-\mu)\theta\bar{f}t\Lambda} \tag{2.4.21}$$

TB prevalence is the product of TB incidence rate (M) and infectiousness period $(\triangle)$. Thus, in terms of incidence, Equation (2.4.21) can be written as

$$P(T \leq t|\beta,\theta,\mu,\Lambda,\bar{f}) = 1 - e^{-(\beta-\mu)\theta\bar{f}tM\triangle} \tag{2.4.22}$$

Hence, Equation (2.4.21) is a general equation to determine the risk probability for TB transmission in terms of TB prevalence that holds under all conditions by monitoring carbon dioxide in the room as a marker of rebreathed air. Furthermore, in terms of incidence, Equation (2.4.22) can be used to determine the risk probability for TB transmission under all conditions.

With this equation that predicts the risk of TB transmission under all conditions, we can determine the number of new TB cases (D) in terms of prevalence, which is the product of

the probability in Equation (2.4.21) and the number of susceptible individuals:

$$D = S\left[1 - e^{-(\beta-\mu)\theta\bar{f}t\Lambda}\right] \tag{2.4.23}$$

where S is the number of susceptible individuals.

In contrast to quanta, the exact number of inhaled airborne infectious particles required to cause an infectious disease outbreak is unknown, but a susceptible individual becomes infected if surviving airborne infectious particles in exhaled air by infectors attain a threshold level to dominate the host immunological state [66]. Additionally, the respiratory deposition fraction of airborne infectious particles on the host alveolar is an expected value and not an exact one. Thus, the modified mathematical model in this study is unique and better reflects real life in the community by matching both individuals and environment without limitations of well mixed air and equilibrium conditions.

The mathematical model developed in this study by modifying the Wells-Riley and Rudnick-Milton equations introduces both viable particles and successful deposition fraction into the Wells-Riley and the prior modified Wells-Riley models. We modified these models because they have limitations, which impact on the prediction of infectious disease risks, including uniformly mixed air in the room and the theoretical construct of infectious quantum. The concept of infectious quantum originated from animal infection experiments where it was noted that the variable particle size of bacillary containing droplets resulted in differential infection rates. The concept of infectious quantum was then expanded to quantify transmission of TB from humans to guinea pigs (Wells and Riley) and has subsequently been used as a back calculated measure of infectivity in TB outbreak investigation. However, infectious quantum includes many significant parameters as discussed above and it's not well understood in the context of epidemiological studies.

Note that TB exposure is not the same as TB infection, which is subject to both host and bacterial factors. In our model, bacterial survival is considered within the parameter $(\beta - \mu)$ and the host factors by the successful deposition fraction (θ), which defines the infectious dose. In this model, we do not address the probability of progression from infection to disease, which is impacted by many other factors including age, gender, comorbidities etc. Rather, we have the ordinate to reflect TB transmission probability. Model applications (numerical simulations) with different factors and conditions correlated to TB transmission risks are demonstrated in the following subsection.

2.4.2 Simulation results

Figure 2.2a is a numerical simulation of Equation (4.4.2). In this figure, the horizontal dotted line denotes the absence of infectors $(I = 0)$ and the other lines denote the presence of infectors (I = 1, I = 2 and I = 4) in the given space. This figure shows that TB transmission probability becomes high in the given space as the number of airborne infectious particles generated by infectors increases with increasing number of infectors, and no infection occurrence if there is no infectious individual(s) in the given space. Furthermore, a numerical simulation of Equation (4.4.1) is illustrated in Figure 2.2b, with increasing duration of exposure from $t = 0$ to $t = 100$ hours for different ventilation air changes per hour (ACH) of 1 ACH, 3 ACH, 8 ACH and 12 ACH. From this figure, we note that when ventilation rate decreases in the given space, and duration of exposure increases, the probability of acquiring TB infection becomes extremely high given the presence of an infectious individual. The numerical simulation of Equation (2.4.10) is demonstrated in Figure 2.2c, which shows that the average volume fraction of exhaled air increases with increasing number of occupants(n), and decreases with increasing ventilation rate in the given space. Figure 2.2d, a numerical simulation of Equation (4.4.1) under non-steady state conditions, shows that as the room volume and ventilation rate increases, TB transmission probability decreases. This implies that if ventilation can be improved in buildings, the accumulation rate of airborne infectious particles can be reduced in the community and airborne infectious diseases, such as TB can also be reduced [41, 117]. On the other hand, the concentration of airborne infectious particles released by infectors in the room increases with decreasing room volume and ventilation rate. The graphical illustration of Equation (4.4.2) in Figure 2.2e shows that TB transmission probability increases in the given space as the average volume fraction of exhaled air increases with increasing number of occupants. Furthermore, Equation (2.4.21) is demonstrated graphically in Figure 2.2f, showing that when TB prevalence becomes high in the community, TB transmission probability that is attributed to the increasing number of airborne infectious particles becomes extremely high. In reality, TB transmission is directly correlated to TB prevalence, which accelerates the high concentration of airborne infectious particles in the community.

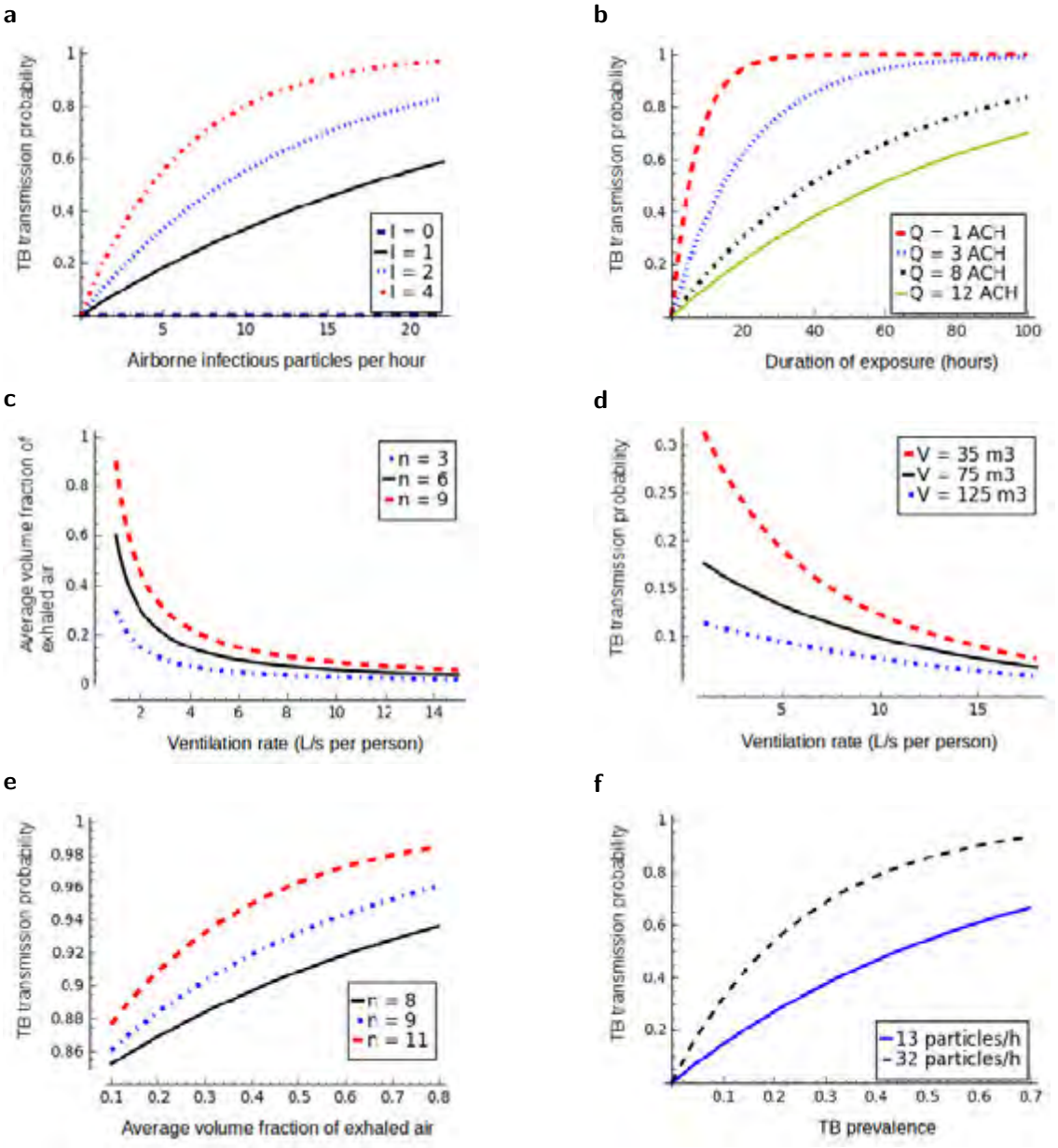

Figure 2.2: Model simulation, showing TB transmission probability and attributable factors. (a) TB transmission probability attributed to the increasing number of airborne infectious particles and number of infectors in the space (Equation (4.4.2) simulation). (b) TB transmission probability increases with increasing duration of exposure and decreasing ventilation air change per hour (Equation (4.4.1) simulation). (c) Average volume fraction of exhaled air increases with increasing number of occupants and decreases with increasing per person ventilation rate (Equation (2.4.10) simulation). (d) TB transmission probability decreases with increasing room volume and ventilation rate per person (non-steady-state condition of Equation (4.4.1)). (e) TB transmission probability attributed to the increasing average volume fraction of exhaled air and number of occupants (Equation (4.4.2) simulation). (f) TB transmission probability increases with increasing TB prevalence and production rate of airborne infectious particles (Equation (2.4.21) simulation).

2.5 Quantity of rebreathed air required to induce infection

Airborne infectious diseases, such as TB are transmitted in multiple congregate locations in the presence of infectious individuals and with a low per person ventilation rate [3, 58, 73, 90, 113]. Carbon dioxide has been used as a measure of indoor air quality based on the concept that people emit carbon dioxide at a rate dependent on body mass and physical activity and that indoor carbon dioxide levels are determined by fresh air clearance [7, 46]. When the concentration of exhaled air increases in the room with infectors present, the probability of susceptible individuals acquiring airborne infectious diseases also increases [113].

Generally, high indoor carbon dioxide concentration is considered to be harmful [7, 46, 100]. This is because exhaled air from infectious individuals usually contains airborne infectious particles within droplet nuclei that may remain airborne for prolonged periods and when inhaled may result in new infection of a susceptible individual [3]. The progression from infection to TB disease depends on a number of different factors, including the state of the host immune system, host genetics, and the virulence of the infecting pathogen strain [3, 11, 12]. We make an assumption that the building, such as a class room of volume, V, starts the day with environmental carbon dioxide concentration (C_E), which is about 400 ppm and it becomes occupied by a number of people (n). This implies that the level of exhaled air concentration that might contain airborne infectious particles will start to increase in the room given the presence of an infector, and depending on the ventilation rate (Q), room volume and number of people in the room [7, 46, 68]. This is because people in the room contribute to the increase in rebreathed air depending on their oxygen consumption, respiratory quotient and physical activities [7, 46]. People in the room will contribute equally to the generation of carbon dioxide as a marker of exhaled air and susceptible individuals may acquire airborne infectious disease if they inhale rebreathed air from infectious individual(s) [66]. The fundamental equation for exhaled air accumulation rate in the room with environmental carbon dioxide, which then becomes occupied, is equal to the rate of exhaled air generated by occupants plus environmental carbon dioxide rate, minus exhaled air removed by ventilation rate:

$$V\frac{dC}{dt} = npC_a + QC_E - QC \tag{2.5.1}$$

where C is the indoor exhaled air concentration (ppm), p is the breathing rate for each person in the room (L/s) and C_a is the carbon dioxide fraction contained in breathed air (ppm).

To determine the quantity of exhaled air accumulated in the room with respect to elapsed

time, we arrange Equation (2.5.1) and integrate from C_E (which is the environmental carbon dioxide in the room) to $C_{(t)}$ (which is the total exhaled air in the room) and elapsed time from 0 to t as follows:

$$\int_{C_E}^{C_{(t)}} \frac{dC}{npC_a + QC_E - QC} = \frac{1}{V}\int_0^t dt \tag{2.5.2}$$

After integrating Equation (2.5.2) by application of integration rules (substitution method), we obtain the following equation

$$\ln(npC_a + QC_E - QC_{(t)}) - \ln(npC_a) = -\frac{Qt}{V}, \tag{2.5.3}$$

which can be written as

$$\ln\left[\frac{npC_a + QC_E - QC_{(t)}}{npC_a}\right] = -\frac{Qt}{V} \tag{2.5.4}$$

Simplifying Equation (2.5.4) further by applying logarithmic and exponential rules, we obtain the mathematical model for exhaled air accumulated $(C_{(t)})$ in a room that started with environmental carbon dioxide, and then became occupied by a number of people:

$$C_{(t)} = C_E + \frac{npC_a}{Q}\left[1 - e^{-\frac{Qt}{V}}\right] \tag{2.5.5}$$

where t is the time spent in the room.

Equation (2.5.5) is demonstrated in Figure 2.3, which shows that when the room becomes occupied the level of exhaled air increases as time elapses in the space. An experiment was conducted in a room of 75 m^3 while regulating ventilation from 3 L/s to 4 L/s and measuring the quantity of carbon dioxide as a marker of rebreathed air. We noted that when the ventilation rate decreases, the concentration of exhaled air increases depending on the number of occupants and room ventilation rate.

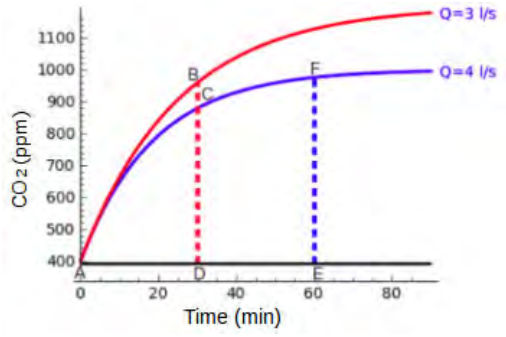

Figure 2.3: The level of exhaled air in a room, which started a day with environmental carbon dioxide, then became occupied by a number of people.

We compute the total amount of exhaled air in the room, demonstrated in Figure 2.3, as follows: Let $Q_{ABCDA} = Q_1$ and $Q_{CDEFC} = Q_2$. The horizontal line indicates environmental carbon dioxide ($C_E = 400$ ppm), which was assumed to be in the room before the entrance of occupants. If we take the summation integral of $ABCDA$ and $CDEFC$, we obtain the total quantity of exhaled air that was rebreathed by each person present in the room for one hour when ventilation rates were $Q_1 = 3$ L/s and $Q_2 = 4$ L/s, respectively. If T denotes elapsed time, the quantity of carbon dioxide as a marker of rebreathed air $(C_{(T)})$, which is generated in the room can be computed by taking the summation integral from T_A to T_D and T_D to T_E (refer to Figure 2.3) as follows:

$$C_{(T)} = \int_{T_A}^{T_D} \left(C_E + \frac{npC_a}{Q_1}(1 - e^{-\frac{Q_1 t}{V}})\right)dt + \int_{T_D}^{T_E} \left(C_E + \frac{npC_a}{Q_2}(1 - e^{-\frac{Q_2 t}{V}})\right)dt \tag{2.5.6}$$

$$= C_E(T_D - T_A) + \frac{npC_a(T_D - T_A)}{Q_1} + \frac{npC_aV}{Q_1^2}e^{-\frac{Q_1 T_D}{V}} - \frac{npC_aV}{Q_1^2}e^{-\frac{Q_1 T_A}{V}}$$

$$+ C_E(T_E - T_D) + \frac{npC_a(T_E - T_D)}{Q_2} + \frac{npC_aV}{Q_2^2}e^{-\frac{Q_2 T_E}{V}} - \frac{npC_aV}{Q_2^2}e^{-\frac{Q_2 T_D}{V}} \tag{2.5.7}$$

Simplifying Equation (2.5.7) further, given that $T_A = 0$, we obtain an equation for exhaled air accumulated in the room that started with environmental carbon dioxide then became occupied:

$$C(T) = T_D C_E \left[1 + \frac{npC_a}{Q_1}\left(1 - \frac{V}{Q_1 T_D}\left(1 - e^{-\frac{Q_1 T_D}{V}}\right)\right)\right]$$

$$+ (T_E - T_D)C_E \left[1 + \frac{npC_a}{Q_2}\left(1 - \frac{V}{Q_2(T_E - T_D)}\left(e^{-\frac{Q_2 T_D}{V}} - e^{-\frac{Q_2 T_E}{V}}\right)\right)\right] \tag{2.5.8}$$

where $T_D = 30$ min and $T_E = 60$ min as shown in Figure 2.3.

In our experiment we used $C_E = 400$ ppm, $p = 0.12$ L/s, $n = 50$, $C_a = 0.04$, and $V = 75\ m^3$. By substituting these values into Equation (2.5.8), we obtain the quantity of exhaled air that is inhaled by each person in the room as $C_{(T)} = 50,211$ ppm.

However, when the room starts with zero environmental carbon dioxide and becomes occupied, Equation (2.5.5) becomes:

$$C(t) = \frac{npC_a}{Q}\left[1 - e^{-\frac{Qt}{V}}\right] \tag{2.5.9}$$

We can obtain the quantity of exhaled air in the room with given ventilation by making a schematic plot of this equation. Plotting Equation (2.5.9), produces the diagram in Figure 2.4.

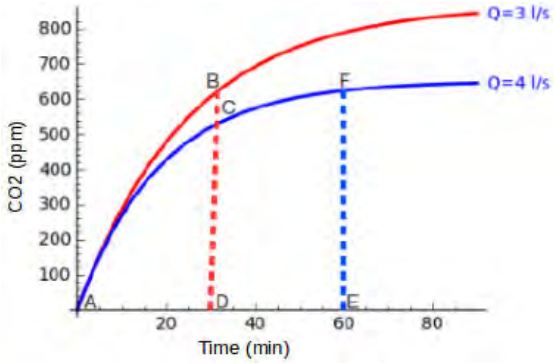

Figure 2.4: The level of exhaled air in a room, which started a day with no environmental carbon dioxide then became occupied by a number of people.

In Figure 2.4, if we take the summation integral of $ABCDA$ with time from T_A to T_D and $CDEFC$ with time from T_D to T_E, we obtain exhaled air accumulation in the room, which started a day with no environmental carbon dioxide, and then became occupied as follows:

$$C(T) = \int_{T_A}^{T_D} \frac{npC_a}{Q_1}\left(1 - e^{-\frac{Q_1 t}{V}}\right)dt + \int_{T_D}^{T_E} \frac{npC_a}{Q_2}\left(1 - e^{-\frac{Q_2 t}{V}}\right)dt \tag{2.5.10}$$

$$= \frac{npC_a(T_D - T_A)}{Q_1} + \frac{npC_aV}{Q_1^2}e^{-\frac{Q_1 T_D}{V}} - \frac{npC_aV}{Q_1^2}e^{-\frac{Q_1 T_A}{V}}$$

$$+ \frac{npC_a(T_E - T_D)}{Q_2} + \frac{npC_aV}{Q_2^2}e^{-\frac{Q_2 T_E}{V}} - \frac{npC_aV}{Q_2^2}e^{-\frac{Q_2 T_D}{V}} \tag{2.5.11}$$

Arranging Equation (2.5.11), and simplifying it further when $T_A = 0$, we obtain an equation of exhaled air generated in the room:

$$C_{(T)} = \frac{npC_aT_D}{Q_1}\left[1 - \frac{V}{Q_1T_D}\left(1 - e^{-\frac{Q_1 T_D}{V}}\right)\right]$$

$$+ \frac{npC_a(T_E - T_D)}{Q_2}\left[1 - \frac{V}{Q_2(T_E - T_D)}\left(e^{-\frac{Q_2 T_D}{V}} - e^{-\frac{Q_2 T_E}{V}}\right)\right] \tag{2.5.12}$$

where $T_D = 30$ min and $T_E = 60$ min as shown in Figure 2.4.

Substituting the same values used in Equation (2.5.8) into Equation (2.5.12), we obtain the quantity of exhaled air, which accumulated in the room as $C_{(T)} = 26,211$ ppm. If susceptible individuals become exposed in an enclosed room with a high volume of exhaled air, as demonstrated in this experiment, they get infected, given the presence of infectors. Infection for human and animals has been documented at a minimum level of carbon dioxide as a marker of exhaled air of about $10,000$ ppm [7, 46]. This implies that carbon dioxide or exhaled air is

harmful, especially in confined spaces with low per person ventilation rates.

Note that Equations (2.5.5) and (2.5.9) hold only under non-steady-state conditions. However, as time, t approaches infinity, the concentration, $C_{(t)}$ approaches the steady-state value and the time required to reach steady-state depends on the value of outdoor air change rate $(\frac{Q}{V})$, implying that the higher the value, the less the time required to reach the steady-state. However, for constant carbon dioxide generation rate, constant ventilation rate and constant outdoor concentration, the indoor concentration will attain steady-state conditions and these equations will be expressed as follows:

$$C(s) = \begin{cases} C_E + \frac{npC_a}{Q} & \text{if with environmental } CO_2 \\ \frac{npC_a}{Q} & \text{if with no environmental } CO_2 \end{cases} \tag{2.5.13}$$

where $C(s)$ is the concentration of carbon dioxide in the room under steady state conditions.

Equation (2.5.13) demonstrates that when the ventilation rate decreases in the buildings, the concentration of exhaled air increases and vice versa. This implies that the accumulation and concentration of airborne infectious particles from infectious individuals increases in the given space with decreasing per person ventilation rate [41].

The increase in carbon dioxide as a marker of exhaled air in an indoor setting in the absence of any other significant source of carbon dioxide reflects the quantity of exhaled breath, which is available for inhalation. We assume that all occupants, including TB infectious and non-infectious individuals, contribute to this exhaled air. Elevated carbon dioxide in inhaled air therefore consists of exhaled air from (a) active TB cases and (b) uninfected individuals. The proportion of that inhaled air derived from infectious cases $(a/a+b)$ is determined by the number of infectious cases and prevalence of active TB in the population being studied. When the number of individuals in a space (room) is small then the Poisson distribution probability of the presence of an infectious individual is used. Note that raised carbon dioxide as a marker of exhaled air without the presence of an infectious source is only a measure of air exchange between non-infectious individuals. The proportion of this air exchange, which is potentially infectious, is therefore determined by the number of infectious individuals and prevalence of active TB cases in the population under study.

2.6 Discussion

Mathematical modelling is one of the most powerful tools in the context of epidemiological studies that is used to investigate, predict and demonstrate the transmission risks of infectious diseases and highlight preventive measures for infection and disease control. The Rudnick-Milton model is a non-steady state version of the Wells-Riley model that has been extensively used to demonstrate the risk probability of acquiring airborne infectious diseases in confined spaces. However, in the derivation of their equation, Rudnick and Milton used the same approach and assumptions as the Wells-Riley model under steady state conditions, for example, completely mixed air in the room and quanta of contagion as postulated by Wells (1955). This causes limitations in understanding TB transmission scenarios by hiding useful parameters, including particle size, deposition fraction, bacterial mortality and survival rates.

In this study, we used respiratory deposition fraction and airborne infectious particles in contrast to quanta to modify both the Wells-Riley and Rudnick-Milton models and obtained a flexible mathematical model that predicts the transmission risks of airborne infectious diseases in multiple environments without limitations of well mixed airspace and equilibrium conditions (Section 2.4). In the modification of these equations, θ is used as the respiratory deposition fraction that determine infectious particle threshold level, β is a measure of all airborne infectious particles irrespective of the respiratory mechanism of production, μ denotes infectious particle mortality rate and $(\beta - \mu)$ is the survival rate of airborne infectious particles with high likelihood of inducing airborne infectious disease at a threshold level. We believe that this is the first study to date to incorporate both respiratory deposition fraction and airborne infectious particles in contrast to quanta to modify the Wells-Riley and prior modified Wells-Riley equations under all conditions by monitoring carbon dioxide as a marker of exhaled air without assuming well mixed airspace. Furthermore, we explored the application of the developed model schematically considering different factors and conditions attributed to TB transmission (Figure 2.2). The non-steady-state condition seems to be more practical than steady-state since it demonstrates the real world schematically and mathematically as discussed in Section 2.4. This means that the transmission of airborne infectious disease mostly occurs under non-steady-state conditions. Furthermore, we noted that, in all conditions (steady-state and non-steady-state), ventilation plays a key role in TB control by diluting the concentration of polluted air, which accelerates the transmission of airborne infectious diseases in the room.

Hence, there are significant differences between our model and existing model approaches. Firstly, our model addresses both steady state and non-steady state conditions and ventilation is not required to be uniform. Second, the model introduces important parameters such as

particle production, mortality, survival rates and successful deposition at the site of infection, which determines infectious dose at a threshold level. Furthermore, the flexibility of inhaled carbon dioxide allows summation of risk acquisition in multiple endemic environments. However, the current model does assume that successfully deposited viable bacteria in terminal airways result in TB infection in susceptible individuals. Additionally, the model does not capture the stochasticity associated with TB transmission.

Figures 2.3 and 2.4 and their corresponding calculated values of carbon dioxide as a marker of exhaled air indicate that, when persons enter a confined space with the presence of an infectious individual(s) and contribute equally to rebreathed air, then each person inhales a large quantity of exhaled air, which might contain airborne infectious particles [66]. When the concentration of exhaled air becomes very high in the room, the probability of acquiring airborne infectious diseases such as TB also becomes high. When infectious particles are inhaled by susceptible individuals and successfully reach a threshold level at the target infection site of the hosts, they can cause TB infection. According to an experiment demonstrated in Figures 2.3 and 2.4, it was noted that when ventilation rate was 4 L/s, exhaled air declined in the room though it was not diminished, but when the ventilation rate became 3 L/s, the level of exhaled air started to rise implying that the generation rate of infectious particles also increased provided the presence of infectious individual(s) in the room [66]. This implies that when ventilation rate is very low, for example 1 L/s, the community becomes at high risk of acquiring airborne infectious disease due to high social contact and indoor air pollution.

To our knowledge, there is no empirical evidence that demonstrate differences in carbon dioxide levels in exhaled air between airborne infectious disease transmitting and non-transmitting individuals. Carbon dioxide excretion as a surrogate for exhaled air is directly related to the oxygen consumption required for metabolic activity. The ratio of exhaled carbon dioxide to the oxygen consumption is defined by the respiratory quotient, which is somewhat diet dependent but relatively constant at a value of 0.83. Our analysis assumes similar contribution of carbon dioxide as a marker of exhaled air from all individuals (infectious and non-infectious individuals) in the indoor space. However, infectious particles have been measured in TB patients, which are capable of transmitting TB via the airborne rate to animal models.

Chapter 3

Seminal *Mycobacterium tuberculosis in vivo* transmission studies: Reanalysis using probabilistic modelling

Abstract

Much of our current knowledge of *Mycobacterium tuberculosis* (MTB) transmission originates from seminal human-to-guinea pig *in vivo* studies, carried out in the 1950's. Similar methodology has been used to investigate human immunodeficiency virus (HIV) co-infection and multidrug resistant TB. However, all these studies have had to reconcile the need to use high facility ventilation rates in order to decrease risks of human-to-human infection while demonstrating human-to-guinea pig transmission. While these studies demonstrate tuberculosis (TB) contagion can be airborne, they also estimated extremely low infectivity of TB cases. However, calculated infectivity was based on a theoretical concept of quantal infection and assumed that the guinea pig model was 100% sensitive for the remote detection of viable TB organisms in highly diluted air exhausted from the facility. High facility ventilation markedly decreases the probability of a successful guinea pig infection by both dilution of the exhaled breathe and decreasing the proportion of air sampled by guinea pigs. In this study, we used a new mathematical model based on Poisson distribution and previous guinea pig experimental data to quantify more realistic estimates of the number of infective organisms required to produce a successful infection for exposed guinea pigs in the *in vivo* studies. Furthermore, we explored the probability of exposed guinea pigs acquiring infection in these studies. We found that the *in vivo* studies to date were underestimated to demonstrate transmission derived from

any but the most productive infectious cases. All four *in vivo* studies have remarkably low probability of infection of exposed guinea pigs due to either high ventilation rates or insensitive mathematical model used in these studies. Therefore, our analysis would suggest that the production of infective organisms by TB cases might have been markedly underestimated. This reassessment of the infectivity of guinea pigs is compatible with recent findings of very high numbers of TB genomes present in health care environments and the very diverse distribution of TB strains present in highly endemic settings which indicates a multiplicity of infective sources.

3.1 Introduction

Our current knowledge of the nature of *Mycobacterium tuberculosis* (MTB) transmission owes much to the *in vivo* guinea pig model of infection. In 1882 Koch, identified the causative agent responsible for consumption and demonstrated tuberculosis (TB) transmission to guinea pigs exposed to dried sputum from infected patients. Consequently, emphasis was placed on avoidance of desiccated secretions in dust and fomites, which was then considered the principal mode of transmission [5].

In the $1930's$ Wells, expanding on the earlier work of Flugge *et at* (1897) [1], proposed that TB transmission was the result of inhalation of infected droplet nuclei exhaled or coughed by a TB case [38]. In the $1950's$, Riley and colleagues performed seminal experiments, which confirmed airborne transmission from TB cases to guinea pigs, supporting Well's theory [59]. Riley observed that guinea pig infections in his model occurred only as rare singleton lesions. He postulated that guinea pig TB infection was quantal, lesions followed a Poisson distribution $(1 - e^{-\lambda})$ and that TB case quanta production was as low as $1 - 2$ per day. A Poisson distribution following a quantum exposure (expected value $\lambda = 1$) would result in 36.8% with no lesions and 63.2% with lesions (36.8% with a single lesion and 26.4% with multiple lesions). However, the Poisson distribution of lesions remained theoretical, as multiple lesions were not observed.

Riley *et al* (1962) [60], Escombe *et al* (2008) [93] and Dharmadhikari *et al* (2011) [106] subsequently used similar guinea pig methodology to investigate differing infectiousness of human clinical populations. High facility ventilation makes the back calculation of TB case infectious quanta production very sensitive to sampling efficiency. However, quanta concentrations calculated from individual guinea pigs exposed to as little as $2 - 3$ milliliters of patient-derived air per hour were used for cross-study quanta production comparisons [93, 106].

All four guinea pig studies A [59], B [60], C [93] and D [106] identified only a minority of efficient transmitters or "super-spreaders". While "super-spreaders" may be responsible for explosive outbreaks of TB in low prevalence settings [39], in endemic settings, molecular epidemiology indicates more generalized TB transmission [56]. Additionally, variable human [89] and guinea pig [106] immunological responses to TB infection that are predictive of subsequent reversion and TB progression risk may be more compatible with quantitative rather than quantal exposure. Recent advances in molecular technologies have enabled direct measurement of airborne TB patient derived particles that are several orders of magnitude greater than those estimated from guinea pig experiments [59, 76, 88]. However, protagonists of the *in vivo* guinea pig model have questioned the clinical relevance of these large numbers of airborne TB genomes [10] and newer viability assays are awaited.

In this study we hypothesized that the guinea pig sampling system may lack sensitivity to identify any but the highest levels of infectivity. In order to re-explore the quantitative findings from these *in vivo* transmission studies, we developed a steady state mathematical model to estimate the likely source-patient airborne infectious particle (viable particles with potential for TB infection) production. The model incorporated relevant parameters that likely decrease guinea pig sampling efficiency including ventilation, sampling fraction and alveolar deposition proportion.

3.2 *In vivo* study methodology

The data derived from four *in vivo* studies A [59], B [60], C [93] and D [106] is shown in Table 3.1. Patients (range $6-8$) with untreated, treated, drug resistant TB disease or complications of treated TB disease were housed in facilities with closed circuit ventilation systems which were supplied with disease free ventilation at a rate Q (range 8.7×10^6 L/day to 57.6×10^6 L/day). Patient facilities were either communal wards, two bedded or single roomed facilities with all exhausted air piped to a guinea pig exposure chamber. Within each exposure chamber S number of guinea pigs (range $120-362$) were housed in communal cages through which the exhaled air from the patient facility was passed. The guinea pig cages were designed such that excreta fell through the floors in order to minimize chances of cross infection between animals by means of contaminated bedding. The temperature and relative humidity of the guinea pig cage environments were closely controlled. Each guinea pig was estimated to breathe approximately $p=10$ L/h. Regular tuberculosis skin testing identified G infections (range $63-213$) in the guinea pigs during time t (range $112-730$ days) with TB diagnosis confirmed by histology and or culture at subsequent autopsy. Uninfected substitute guinea pigs

constantly replaced infected or euthanized animals in order to maintain an average number S of susceptible animals. Most newly infected animals had evidence of only one infectious focus in their lungs, supporting the study hypothesis that TB entered the body through a single invasive site in the respiratory system and the assumption that the number of infections reflected the number of airborne infectious particles inhaled.

Two studies A [59] and B [60] used proportionality to estimate the concentration of airborne infectious particles in the exhausted ward air from the number of infected guinea pigs G divided by the total air volume V (range 3.8×10^6 L to 27.3×10^6 L) breathed by all susceptible guinea pigs during the period of t days of the study. The total airborne infectious particles produced by I TB patients were calculated from the total facility ventilation Q divided by calculated volume per infected guinea pig V/G containing a single airborne infectious particle. The calculated number of airborne infectious particles causing infection was considered to be identical to the number of airborne infectious particles inhaled by the guinea pigs and the concentration of such particles in the patient ward was identical to that of the inhaled guinea pig air.

One study, C [93], incorporated calculation of airborne infectious particles using a Poisson probability, but similar to studies A and B, assumed that the inhaled number of airborne infectious particles by guinea pigs was identical to the number of airborne infectious particles causing infection, and that there were no losses between exhalation from patients and inhalation by guinea pigs. The fourth study, D [106], focused predominantly on a new finding that some guinea pigs were observed to revert their tuberculin reactions after infection with drug resistant TB. This observation led to a proposal that drug resistant strains were less virulent than the drug sensitive strains reported in the prior studies A [59], B [60] and C [93]. However, the number of susceptible guinea pigs (S) exposed and the number infected or dying of tuberculosis (G) after exposure to TB cases (I) was reported. Facility ventilation was reported only as 12 air changes per hour, which, in conjunction with published facility dimensions [77], allowed facility ventilation (Q) to be calculated.

For each of the studies A to D we estimated the probability of finding the published infection rates using the Poisson distribution approach with sensitivity analysis of TB infectious doses of between 10 to 50 colony forming units as reported in a review of the guinea pig as an infectious model [52]. We then went on to estimate the mean patient production rate of airborne infectious particles necessary to reproduce the reported guinea pig infection rates of each study as discussed in Section 3.3. Note: Study $A =$ Wells-Riley et al (1959), study $B =$ Riley *et al* (1962), study $C =$ Escombe *et al* (2008), study $D =$ Dharmadhikari *et al* (2011).

Table 3.1: Guinea pig experimental data in studies A, B, C and D.

Study	Time $=t$, days	Patient $=I$ (total)	Ventilation $=Q$, m^3/day	Susceptible guinea pigs $=S$	Guinea pig infected $=G$	Guinea pig inhaled vol$=p$, m^3/day	Air proportion sampled $=p/Q$
A [59]	730	$6(88^{*})$	$8,685$	156	71	35.3	0.0041
B [60]	730	$6(130^{**})$	$9,379$	120	63	27.2	0.0029
C [93]	505	$8(97^{\dagger})$	$39,675$	292	129	66.1	0.0017
D [106]	112	$6(26^{\ddagger})$	$57,600^{\dagger\dagger}$	362	213	82.0	0.0014

I = maximum patient occupancy at any time, total = total number of patients in each study. Patient characteristics: * treatment-naïve and treatment failures, ** untreated, treatment-naïve and drug resistant, † All HIV-infected, suspected tuberculosis, treatment-naïve, and with treatment complication, ‡ multi-drug resistant tuberculosis and $^{\dagger\dagger}12$ ACH estimated volume rate.

3.3 Mathematical modelling and simulation results

Using guinea pig experimental data in the four *in vivo* studies A [59], B [60], C [93] and D [106] (Table 3.1), we explore the probability of exposed guinea pigs acquiring infection in these studies by application of the mathematical model developed in Issarow *et al* (2015) [66] under steady state conditions. Furthermore, we quantify the number of surviving airborne infectious particles (infective organisms) required to reach the alveolar to induce infection for exposed guinea pigs in these *in vivo* studies. The mathematical model used in this study for the *in vivo* studies reanalysis is demonstrated as:

$$P(\psi|I,\mathscr{F},\theta,p,Q,t) = 1 - e^{-\frac{I\mathscr{F}\theta pt}{Q}} \tag{3.3.1}$$

where $P(\psi|I,\mathscr{F},\theta,p,Q,t)$ denotes the probability of infection of exposed guinea pigs, ψ is whether or not infection occurred given that TB infection conditions are fulfilled, Q is the ventilation rate (L/h), p is the guinea pig breathing rate (L/h), I is the number of infectious individuals in the space, θ is the alveolar deposition fraction, t is the duration of exposure (h) and $\mathscr{F}$ $(\beta_{total} - \mu_{loss})$ is the number of surviving airborne infectious particles per unit time (particles/h) that reach the alveolar to establish infection. β_{total} is the total airborne infectious particle production rate and μ_{loss} is the mortality rate of airborne infectious particles before reaching the host infection site.

This mathematical model (Equation (3.3.1)) was preferred over others as it incorporates all

significant parameters in the prediction of airborne infectious disease risks, without assumption of well mixed airspace and equilibrium conditions [66, 67] (see Chapter 2, Section 2.4). The *in vivo* studies claimed that they used a Poisson distribution approach (Wells-Riley model) to predict the number of infective organisms required to induce infection and the probability of exposed guinea pigs acquiring infection. However, they didn't demonstrate mathematically or schematically how they used the Wells-Riley model in their studies to estimate the number of infective organisms and the probability of exposed guinea pigs acquiring infection. Using Equation (3.3.1), in this study, we estimate the number of surviving airborne infectious particles required to reach the alveolar to induce infection and the probability of exposed guinea pigs acquiring TB infection in the four *in vivo* studies. Since the *in vivo* studies used a steady state mathematical model (Wells-Riley model), Equation (3.3.1) should provide a more accurate prediction of the probability of exposed guinea pigs acquiring infection in these studies. Furthermore, this equation should estimate a more accurate number of surviving airborne infectious particles required to reach the alveolar to induce infection in exposed guinea pigs.

In the application of Equation (3.3.1) to guinea pig experimental data, we made the following assumptions: first, there is no immune control of infection i.e. a single or more than one airborne infectious particle arriving at the alveolus will result in a guinea pig infection if the probability of exposed guinea pigs acquiring infection is attained; second, the experimental conditions were such that there was no cross infection between guinea pigs; and third, the infective TB dose required to establish infection in guinea pigs varies between 10 and 50 colony forming units resulting in alveolar deposition fractions between 0.02 and 0.1 [52].

Here, we explore the probability of infection of exposed guinea pigs by applying *in vivo* experimental data in studies A [59], B [60], C [93] and D [106] (Tables 3.1 for I, t, Q, p and 3.2 for $\mathscr{F}$) to Equation (3.3.1), while varying alveolar deposition fraction ($\theta = 0.02, 0.1$). We use $0.9(0.8-1)$ as the probability of exposed guinea pigs acquiring infection, with the probability of 1 being the saturation point (threshold level) where infection will occur. Simulating Equation (3.3.1) numerically, we found that the maximum probability of exposed guinea pigs acquiring infection in the four *in vivo* studies A [59], B [60], C [93] and D [106] was 0.054, 0.074, 0.08 and 0.00062, respectively, with deposition fraction of 0.02. Furthermore, with deposition fraction of 0.1, the maximum probability of exposed guinea pigs to acquire infection in these studies was 0.24, 0.32, 0.35 and 0.0031, respectively (Figures 3.1a, 3.1b, 3.1c and 3.1d). All four *in vivo* studies A [59], B [60], C [93] and D [106] seem to have remarkably low probability of infection of exposed guinea pigs due to high ventilation rates in their studies, which dilute the concentration of airborne infectious particles. It shows that of all four *in vivo* studies, study D [106] (Figure 3.1d) had the lowest infection probability of exposed guinea

pigs, perhaps because of shorter duration of exposure and higher ventilation rate than the other studies (Table 3.1). The findings in this study show that the expected probability of exposed guinea pigs to acquire infection was not attained in all four *in vivo* studies, implying that their observations may be inaccurate or underestimated [67].

The four *in vivo* studies seem to have several issues, including high ventilation rates, which led to remarkably low probability of exposed guinea pigs to acquire infection. Alveolar deposition fraction and surviving airborne infectious particles also seem to have a significant impact on the prediction of exposed guinea pigs acquiring TB infection. Here, we quantify and demonstrate the number of surviving airborne infectious particles required to attain the threshold level to establish infection for exposed guinea pigs in the four *in vivo* studies by simulating Equation (3.3.1) numerically using *in vivo* experimental data (Table 3.1), varying airborne infectious particles ($\mathscr{F} = 10, 100, 1000$ particles/h) and alveolar deposition fraction ($\theta = 0.02, 0.1$). We chose these values of airborne infectious particles because the number of surviving particles that reach the host infection site to induce infection is an expected value and not an exact one [66]. By simulating Equation (3.3.1) numerically using *in vivo* experimental data, varying airborne infectious particles and alveolar deposition fraction, we determined the threshold level of surviving airborne infectious particles ($\mathscr{F}$) required for exposed guinea pigs to acquire TB infection in each *in vivo* study as follows: For study A, the threshold level of surviving airborne infectious particles was reached when $\mathscr{F} \geq 69$ particles/h with deposition fraction of 0.02 and $\mathscr{F} \geq 14$ particles/h with deposition fraction of 0.1 (Figures 3.2a and 3.2b); for study B, the threshold level was attained when $\mathscr{F} \geq 75$ particles/h with deposition fraction of 0.02 and $\mathscr{F} \geq 15$ particles/h with deposition fraction of 0.1 (Figures 3.2c and 3.2d); for study C, the threshold level was reached when $\mathscr{F} \geq 341$ particles/h with deposition fraction of 0.02 and $\mathscr{F} \geq 69$ with deposition fraction of 0.1 (Figures 3.3a and 3.3b); and for study D, the threshold level was reached when $\mathscr{F} > 1000$ particles/h with deposition fraction of 0.02 and $\mathscr{F} \geq 596$ particles/h with deposition fraction of $= 0.1$ (Figures 3.3c and 3.3d). It shows that none of the four *in vivo* studies reached the threshold level for exposed guinea pigs to acquire TB infection when $\mathscr{F} \leq 10$ particles/h with deposition fraction of $0.02 \leq 0.1$. Unfortunately, all four *in vivo* studies estimated that exposed guinea pigs were infected with less than 10 particles/h [59, 60, 93, 106] and concluded that TB infection is induced by a single organism [59]. This implies that their observations may be inaccurate and they lacked sensitivity in their experimental studies, perhaps due to using a mathematical model with implausible assumptions and some limitations [67].

Because of shorter duration of exposure and higher ventilation rate than other *in vivo* studies, study D failed to reach the threshold level at the maximum number of airborne infectious

particles (1000 particles/h) with deposition fraction of 0.02 (Figure 3.3c). Furthermore, we noted that studies C and D (Figure 3.3) seem to require larger numbers of airborne infectious particles to reach the threshold level for exposed guinea pigs to acquire infection than studies A and B (Figure 3.2), perhaps because of high ventilation rates and short durations of exposure in the former studies (Table 3.1). Studies A and B are very similar schematically (Figure 3.2), probably because of the same number of infectious individuals and duration of exposure in the two *in vivo* experiments (Table 3.1). However, due to higher ventilation rate in study B than that of study A, we show that study B requires a larger number of airborne infectious particles to attain the threshold level than study A. It shows that high ventilation rates in these studies is one the key factors which led to remarkably low probability of exposed guinea pigs to acquire infection. Since ventilation dilutes the concentration of airborne infectious particles, duration of exposure needs to be higher with high ventilation rate to attain the threshold level for exposed guinea pigs to acquire infection. As mentioned earlier, due to high ventilation rates in all four *in vivo* studies, our findings suggest that the minimum number of airborne infectious particles required to reach the threshold level for infection in each study was greater than 11 particles/h per person with deposition fraction of 0.02 and greater than 2 particles/h per person with deposition fraction of 0.1 (Table 3.2). However, none of the four *in vivo* studies quantified these values, implying that their observation may be highly underestimated or false-negative. It shows that the likelihood of TB infection is directly correlated with alveolar deposition fraction, which determines the number of surviving airborne infectious particles that reach the alveolar to establish infection (Figures 3.2 and 3.3). Table 3.2 compares the number of surviving airborne infectious particles/h per person, which are required to reach the target infection site of the host to induce infection in the four *in vivo* studies and our study.

Table 3.2: Comparison of the number of airborne infectious particles per hour per person in our study and the *in vivo* studies that required to reach the alveolar to establish infection.

Study	Airborne infectious particles/person in the *in vivo* studies	Airborne infectious particles/person in our study.	
		Alveola deposition fraction of 0.02	Alveolar deposition fraction of 0.1
A [59]	0.167^{*}	11.5	2.333
B [60]	0.25^{*}	12.5	2.5
C [93]	1.025^{*}	42.625	8.625
D [106]	0.083^{**}	> 166.667	99.333

* Airborne infectious particles per person from *in vivo* studies, ** Calculated airborne infectious particles per person from *in vivo* study experimental data.

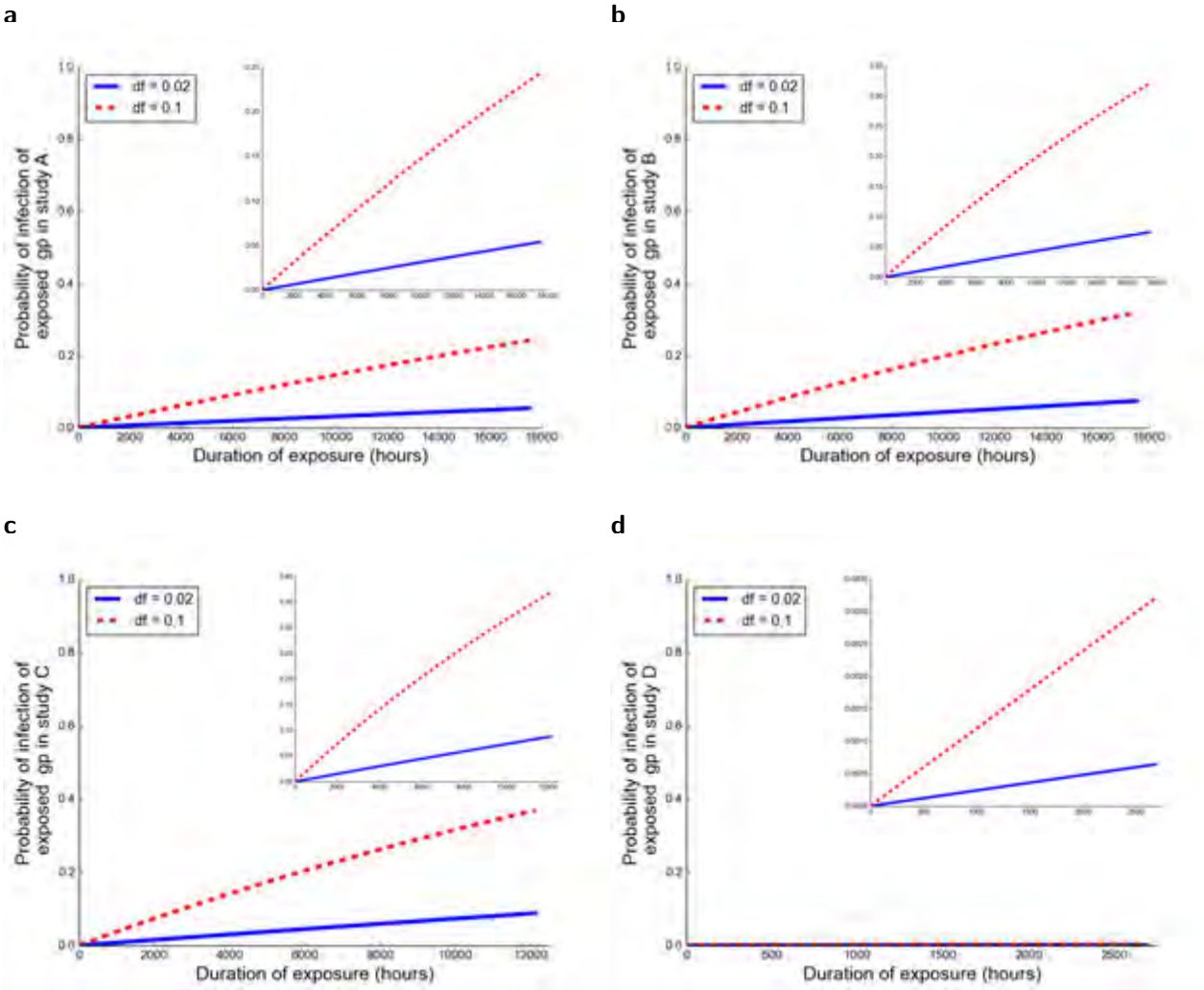

Figure 3.1: Exploration of the probability of exposed guinea pigs to acquire TB infection in studies A, B, C and D using *in vivo* experimental data (Tables 3.1 and 3.2) and varying deposition fraction in Equation (3.3.1) (numerical simulation) in each study.
(a) Probability of infection of exposed guinea pigs in study A with deposition fraction of 0.02 and 0.1. (b) Probability of infection of exposed guinea pigs in study B with deposition fraction of 0.02 and 0.1. (c) Probability of infection of exposed guinea pigs in study C with deposition fraction of 0.02 and 0.1. (d) Probability of infection of exposed guinea pigs in study D with deposition fraction of 0.02 and 0.1. Note: gp $=$ guinea pig, df $= \theta =$ alveolar deposition fraction.

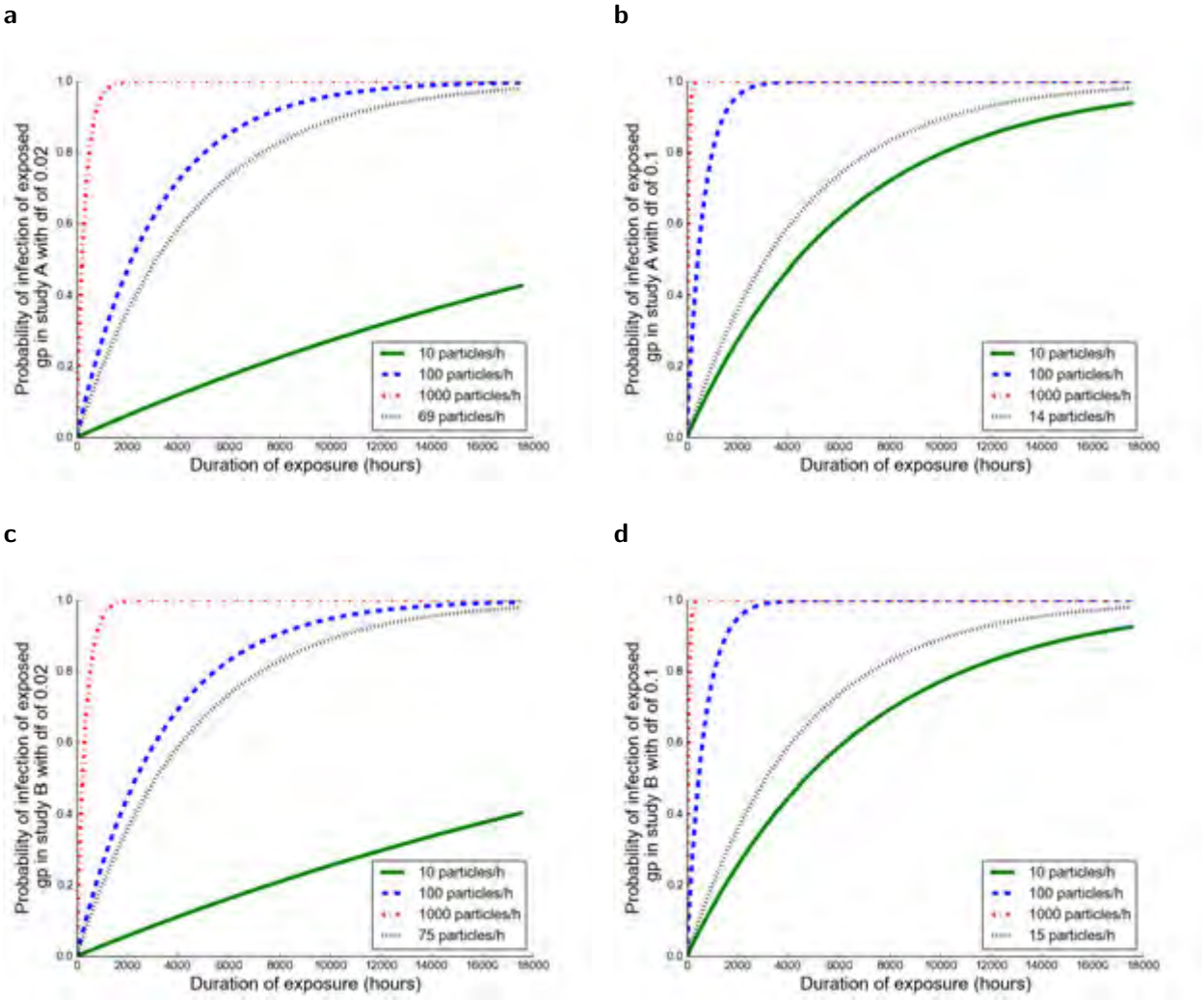

Figure 3.2: Numerical simulation of Equation (3.3.1) using *in vivo* experimental data in studies A and B (Table 3.1) with varying alveolar deposition fraction to quantify the number of surviving airborne infectious particles required to reach the threshold level for exposed guinea pigs to acquire TB infection. Note: gp = guinea pig, df = θ = alveolar deposition fraction. (a) The number of surviving particles required to reach the alveolar to induce infection in exposed guinea pigs in study A with deposition fraction of 0.02. (b) The number of surviving particles required to reach the alveolar to induce infection in exposed guinea pigs in study A with deposition fraction of 0.1. (c) The number of surviving particles required to reach the alveolar to induce infection in exposed guinea pigs in study B with deposition fraction of 0.02. (d) The number of surviving particles required to reach the alveolar to induce infection in exposed guinea pigs in study B with deposition fraction of 0.1.

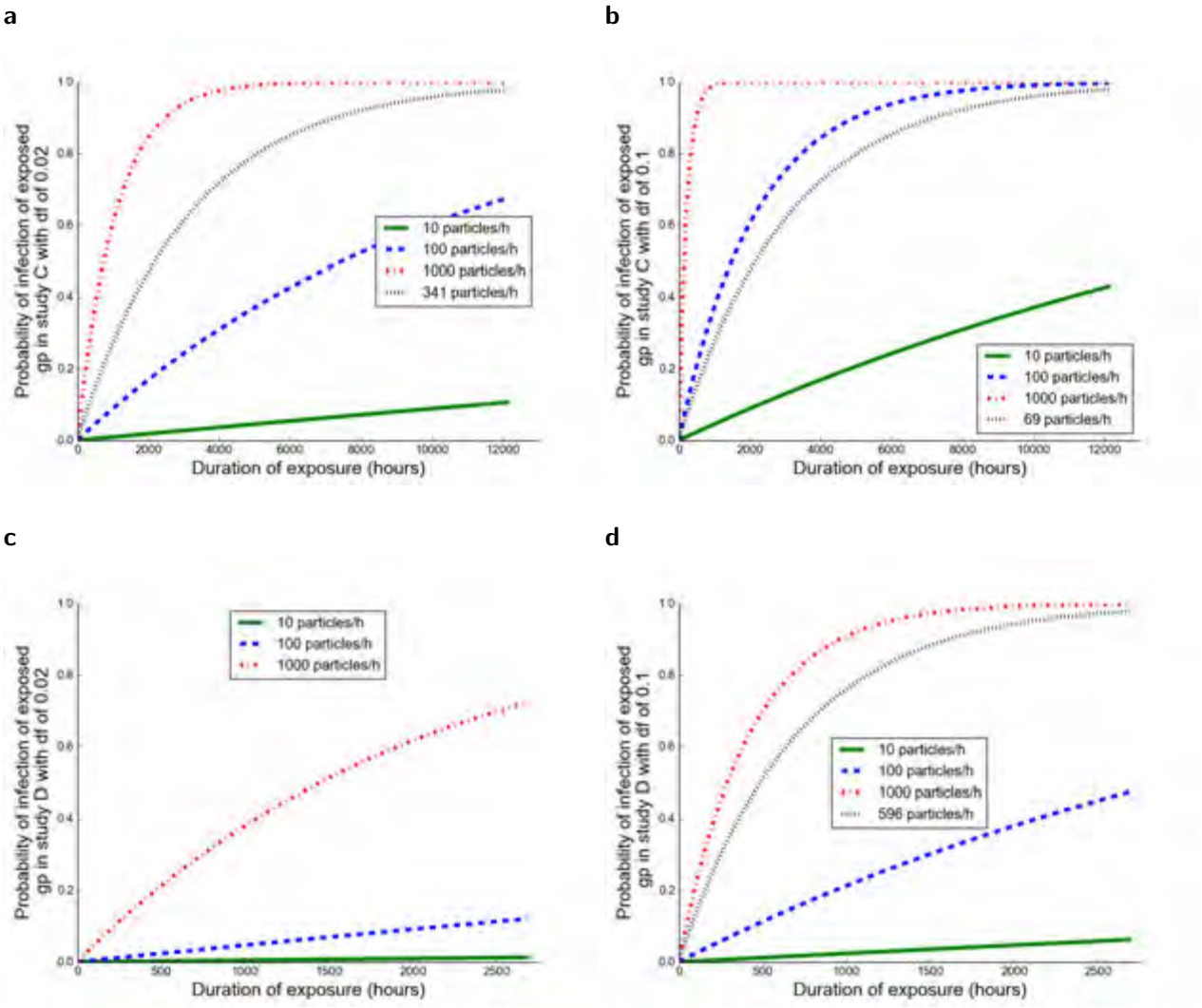

Figure 3.3: Numerical simulation of Equation (3.3.1) using *in vivo* experimental data in studies C and D (Table 3.1) with varying alveolar deposition fraction to quantify the number of surviving airborne infectious particles required to reach the threshold level for exposed guinea pigs to acquire TB infection. Note: gp = guinea pig, df = θ = alveolar deposition fraction. (a) The number of surviving particles required to reach the alveolar to induce infection for exposed guinea pigs in study C with deposition fraction of 0.02. (b) The number of surviving particles required to reach the alveolar to induce infection for exposed guinea pigs in study C with deposition fraction of 0.1. (c) The number of surviving particles required to reach the alveolar to induce infection for exposed guinea pigs in study D with deposition fraction of 0.02. (d) The number of surviving particles required to reach the alveolar to induce infection for exposed guinea pigs in study D with deposition fraction of 0.1.

3.4 Discussion

Guinea pig is a suitable model of human TB because of its susceptibility to the infection, similar symptoms and pathophysiology. Our reanalysis of *in vivo* experiments of human to guinea pig MTB transmission shows that they lacked sensitivity and suggests that the production of infectious particles by TB cases reported in these studies may have been greatly underestimated. The guinea pig facilities used in each study lack sensitivity due to the fundamental conflict between the need for enhancing transmission from human to animals while being constrained by the need to reduce human to human cross infection. The ventilation of the patient wards increased with each successive study, such that patient exhaled air was diluted by 125-fold, 135-fold, 530-fold and 833-fold in studies A [59], B [60], C [93] and D [106], respectively.

Concurrently, with the increasing dilution of the ward vented air, the sampling proportion determined by the number of guinea pigs used in each study decreased progressively from 0.0041, 0.0029, 0017 and 0.0014 in studies A [59], B [60], C [93] and D [106], respectively. Furthermore, we have questioned the assumption that because only a single bacterium was the source of a single granuloma at the site of infection within a guinea pig that the infective dose for a guinea pig is a single airborne infectious particle. The respiratory anatomy of mammals has evolved to filter environmental threats in order to limit access to the vulnerable alveolar bed. The infective TB dose required to establish infection in guinea pigs varies between 10 and 50 colony forming units, resulting in deposition fractions between 0.02 and 0.1 [52]. The deposition of inhaled particles in the lung is determined by breathing patterns and lung geometry in conjunction with attributes of particles affecting physical processes, such as inertial impaction, gravitational sedimentation and Brownian diffusion [23]. The proportion of small-respired particles in the 1-2 microns range capable of transporting one or more MTB organisms capable of deposition in the human alveolar has been estimated at around 10% [16].

There are some important consequences of our findings. Cross study comparisons of the relative infectivity of different types of TB infected individuals may lead to false conclusions because the sensitivity of each study differed markedly, as did the methodology for calculation of airborne infectious particle production. For example, the conclusion that HIV infected patients in study C were more infectious than non HIV-infected patients in studies A and B should be viewed in light of the above limitations [93]. The use of calculated airborne infectious particle production from *in vivo* animal studies may also be inaccurate for mathematical modelling of human-to-human transmission [21, 42, 51, 96]. If TB airborne infectious particles are much more frequent than previously estimated there should be a greater emphasis on environmental searching for airborne TB.

Chapter 4

Modelling TB transmission in congregate settings

Abstract

Tuberculosis (TB) transmission in congregate settings, such as schools, households, public transport, health care settings and prisons has been noted to be remarkably high due to numerous factors. In this study, we explore the contribution of biological, socio-economic and environmental factors attributable to TB prevalence in these locations using mathematical modelling approach. Furthermore, we describe preventive measures for TB control in these crucial locations. We noted that high interaction and duration of exposure to infectious individuals are among the factors accelerating TB transmission in congregate settings. Furthermore, the study shows that increasing number of infectious individuals, overcrowding and insufficient ventilation are another key contributing factors to the increasing TB incidence in congregate settings. Identification and treatment of TB cases may have a greater impact on TB control in these locations.

4.1 Introduction

Tuberculosis (TB) transmission in congregate settings, such as schools, households, public transport, health care settings and prisons is estimated to be high. Increasing TB incidence in these locations is contributed by several factors, including interaction, contacts, social mixing and duration of exposure to infectious individuals [11]. Undoubtedly, exhaled air is the carrier

of airborne infectious particles viable with potential for TB infection in confined spaces with the presence of infectious individuals [46, 113, 117]. Overcrowding and insufficient ventilation are some of the factors, which accelerate accumulation of exhaled air in confined spaces, and susceptible individuals become infected given the presence of infectious individual(s) [24, 113].

As mentioned earlier (Chapter 1), in most of the schools, households and public transport in South Africa, are highly overcrowded with high interaction and social contacts between infectious and susceptible individuals, which create reasonable proximity for TB transmission. Furthermore, insufficient ventilation, increasing number of infectious individuals and high duration of exposure to infectious individuals in health care settings and prisons are assumed to be among the factors contributing to the increasing TB incidence in these locations.

In this study, we demonstrate social and environmental factors attributable to TB transmission in congregate settings using mathematical modelling approach. Furthermore, we describe preventive measures for TB control in these locations.

4.2 Integrated model for TB transmission in transport, schools and households

4.2.1 Group interaction model

If we want to determine the risk probability for TB transmission among students who enter the classroom or passengers who enter the vehicle at the same time and sit as a group, we need to develop a specific mathematical model for people who contribute re-breathed air equally, such that susceptible individuals can easily be infected. In this study we developed a mathematical model that predicts the risk of TB transmission probability when people are in a group (group interaction model), such as students in the classroom or passengers in the vehicle.

Let us consider an enclosed space (classroom or vehicle) of n susceptible individuals (students or passengers) and the probability that at least one individual might be smear-positive is r. The number of infectious individuals (i) in the given space can be expressed as $i = nr$. Thus, for the probability of having new infected individuals in the space, we should consider a binomial distribution as follows:

$$P(I = i) = \binom{n}{i} r^i (1-r)^{n-i} \tag{4.2.1}$$

where $P(I = i)$ denotes the probability of having new infected individuals in the space, for i $=$

0, 1,..., n.

In order to determine the probability of infection risk outbreak and spread for susceptible individuals (n) in a group in a given period of exposure t, we should take the product of Equations (2.4.19) and (4.2.1), such that:

$$P(g) = \sum_{i=0}^{n} P(I = i)P(n|I = i) \tag{4.2.2}$$

Where

$$P(n|I = i) = 1 - e^{-\frac{i(\beta-\mu)\theta\bar{f}t}{n}},$$

which is the probability of acquiring infection for n susceptible individuals given the presence of infectious individuals. Where $I = i$ is the number of infectious individuals, $(\beta - \mu)$ is the surviving airborne infection particles that reach the alveolar (particle/s), θ is the respiratory deposition fraction, $\hat{f}$ is the average volume fraction and t is the duration of exposure.

$$P(g) = \sum_{i=0}^{n} \binom{n}{i} r^i (1-r)^{n-i} \left(1 - e^{-\frac{i(\beta-\mu)\theta\bar{f}t}{n}}\right) \tag{4.2.3}$$

$$P(g) = 1 - \sum_{i=0}^{n} \binom{n}{i} \left(re^{-\frac{(\beta-\mu)\theta\bar{f}t}{n}}\right)^i (1-r)^{n-i} \tag{4.2.4}$$

If we further simplify Equation (4.2.4), we obtain the probability, $P(g)$, of TB transmission risk occurring in a group in a given time, t as

$$P(g) = 1 - \left[(1-r) + re^{-\frac{(\beta-\mu)\theta\bar{f}t}{n}}\right]^n \tag{4.2.5}$$

Equation (4.2.5), implies that when n persons enter the room at the same time, they contribute equally to the re-breathed air, such that susceptible individuals can easily be infected, given the probability of having at least one smear-positive individual (r) in the room. This equation is valid for a group of people, for instance, when students enter the classroom and sit as a group or when passengers enter an enclosed vehicle and share re-breathed air for a long period of time, but it does not account for random entrance and exit of students in the classroom or passengers exiting the vehicle randomly because the time spent by the smear-positive individual in the space is the same as the duration of exposure for susceptible individuals. Therefore, we need to develop a general equation which can hold for all manners of interactions in the community either in groups or with random interactions, where duration of exposure should not necessarily be the same as the time spent by the smear-positive in the given space as

discussed below.

4.2.2 Random interaction model

Here, we develop a general mathematical model that determines the risk probability of TB transmission in all manners of interaction in the community (random interaction model). The difference between random and group interaction models, is the manner of interaction between smear-positive and susceptible individuals. This means that the random interaction model holds under all conditions of the TB transmission environment regardless of group formation since duration of exposure for susceptible individuals is not necessarily the same as the time spent by the smear-positive individual in the given space as discussed below.

Let us consider a classroom or vehicle of n individuals who enter the space and leave randomly such that i individuals might be smear-positive with the probability r. Thus, the number of susceptible individuals is $n-i$. For new infections (x) to occur, the time spent by susceptible individuals in the space should be greater than or equal to the time spent by a smear-positive individual, and the time spent by the smear-positive should be less than or equal to the time taken for infection to occur:

$$k = \sum_{j=0}^{n-i} x_j \tag{4.2.6}$$

where k is the total number of new infected individuals and x_j is the new infection for a person j.

$$x_j = \begin{cases} 1 & if \quad \tau \leqslant t_j, \tau \leqslant t \\ 0 & \text{otherwise} \end{cases}$$

$x_j = 1$ denotes an occurrence of a new TB infection and $x_j = 0$ if there is no occurrence of new infection, where t_j is the time for a person j to be infected, τ is the time spent by the smear-positive individual, and t is the time spent by susceptibles in the space.

The probability of having k new infected individuals in the space is binomially distributed, such that

$$P(k_{random}) = \binom{n-i}{k} r^k [1-r]^{(n-i)-k} \tag{4.2.7}$$

where $P(k_{random})$ is the probability of having k new infected individuals in the space with random interaction, $k = 0, 1, ..., (n-i)$.

Thus, infection risk probability, $P(m)$ that susceptible students or passengers will be randomly infected given that there are i smear-positives in the space, is equal to the probability of infec-

tion spreading given that there are i infectious individuals in the space, $P(n|I=i)$ multiplied by the probability of having k new infected individuals in the space with random interaction, $P(k_{random})$:

$$P(m) = \sum_{k=0}^{n-i} P(k_{random}) P(n|I=i) \tag{4.2.8}$$

Where

$$P(n|I=i) = 1 - e^{-\frac{i(\beta-\mu)\theta\bar{f}t}{n}}$$

Thus

$$P(m) = \sum_{k=0}^{n-i} \binom{n-i}{k} r^k [1-r]^{(n-i)-k} \left(1 - e^{-\frac{i(\beta-\mu)\theta\bar{f}t}{n}}\right) \tag{4.2.9}$$

If we simplify Equation (4.2.9) further by applying probability rules and rearrange it, we obtain:

$$P(m) = 1 - \sum_{k=0}^{n-i} \binom{n-i}{k} r^k [1-r]^{(n-i)-k} \left(e^{-\frac{i(\beta-\mu)\theta\bar{f}t}{n}}\right) \tag{4.2.10}$$

where $P(m)$ is the probability of TB infection risk occurrence in enclosed spaces in random interaction.

Note that the difference between group and random models is that duration of exposure for susceptible individuals for a group model is the same as the time spent by a smear-positive individual in a confined space, while for a random model, duration of exposure may be greater than or equal to the time spent there by the smear-positive. In the random model, the number of susceptible individuals is more flexible since the model adopts a random condition compared to the group model.

Equation (4.2.10) implies that students can enter the classroom and leave randomly but the total time spent in the room is still t as the duration of exposure. According to this equation it means that students who were previously in the classroom and left before entrance of the smear-positive should not be infected, while those who entered together with or after the smear-positive could be infected. Moreover, even students who remained in the classroom after exit of the smear-positive could be infected since this equation is valid for random movement at any time of exposure which is counted as duration of exposure. In addition, this equation is applicable to passengers who enter and exit the vehicle provided that the environment is conducive to TB transmission and given the presence of a smear-positive individual in that environment.

Therefore, Equation (4.2.10) is regarded as a random interaction model that can be applied for modelling TB transmission in confined spaces in a given population, as a sample in a

large community, in all manners of interaction under all conditions. This implies that people can either enter or leave individually or in a group such that students can enter or exit the classroom in any way but if there is at least one infectious individual, then susceptible students can also be infected. Furthermore, in public transport where commuters (elders and students) enter and exit randomly, while all windows are fully or half closed, susceptible individuals can easily be infected as demonstrated by this random interaction model. In the case of the annual risk of TB infection, we should consider a Poisson distribution as it is applicable in rare events as discussed below.

4.2.3 Measures for TB control in schools, households and transport

Factors contributing to TB transmission in schools, households and public transport are closely related [92]. For example, interactions, social contacts and environmental exposure in these locations are similar and are highly correlated with TB transmission. Due to random interaction and social contacts between infectious and susceptible individuals in confined spaces, TB prevalence in one location may act as a reservoir for TB transmission in another [92]. For example, TB prevalence in schools is highly dependent on public transport and the households. Furthermore, TB transmission in the households is dependent on that in public transport and schools, and the TB burden in public transport is linked to TB prevalence in schools and households. Of all three congregate locations discussed in this section, public transport has the highest TB prevalence followed by schools because of high interactions and duration of exposure in confined spaces, especially during winter. TB transmission can be reduced in these locations if interactions, social contacts and duration of exposure can be reduced between infectious and susceptible individuals [11, 92].

Controlling the spread of airborne infectious particles in the air is one of the more efficient interventions for TB control in schools, households and public transport. For example, if airborne infectious particles can be reduced then $(\beta - \mu)$ in Equations (4.2.5) and (4.2.10) approaches or becomes zero, implying that TB transmission probability becomes approximately zero. Furthermore, reducing duration of exposure, TB transmission probability in these equations also approaches zero. Therefore, early diagnosis and case detection is one of the most important interventions for TB control in the community [79]. The big challenge is that some TB cases are not yet identified in the community due to either lack of health care or poor diagnostic tools, which provide false-negative results.

4.3 Modelling TB transmission in health care settings

Since carbon dioxide is one of the most diffusible tracer gas, it is usually used to measure the quality of airspace [66, 99]. We therefore monitor carbon dioxide as a surrogate for exhaled re-breathed air to demonstrate the risk of airborne infectious diseases. Let us consider a hospital with a TB ward as illustrated in Figure 4.1 and use carbon dioxide as a surrogate for exhaled air to demonstrate TB transmission and control in health care settings by monitoring exhaled air by infectious individuals in the TB ward as follows:

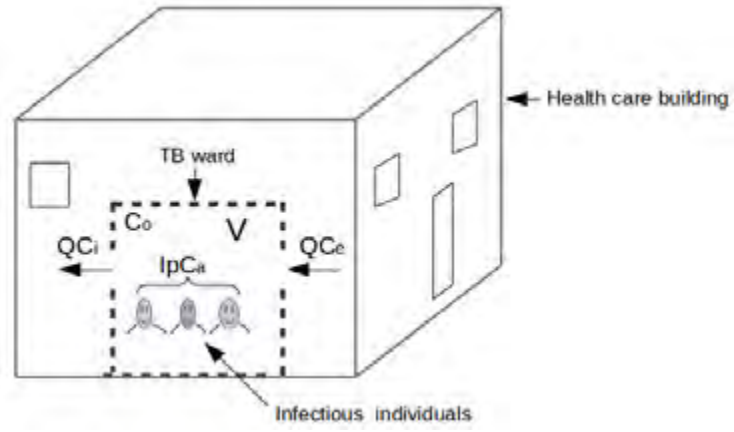

Figure 4.1: TB transmission in hospitals, a schematic of a ward.

Mathematically, accumulated exhaled air in the TB ward of volume V, is equal to the rate of exhaled air generated by TB patients (IpC_a) plus ambient air in the room (QC_e) minus indoor air removed by ventilation (QC_i) [99] as demonstrated in the following differential equation:

$$V\frac{dC_i}{dt} = IpC_a + Q(C_e - C_i), I \geq 1 \tag{4.3.1}$$

where C_i denotes indoor carbon dioxide concentration (ppm), Q is the ventilation rate (L/s), C_e is the outdoor carbon dioxide concentration (ppm), p is the breathing rate of the patients in the TB ward (L/s), C_a is the carbon dioxide fraction contained in breathed air and I is a number of TB patients in the TB ward.

Arranging Equation (4.3.1) and integrating with respect to time for $CO_2 = C_o$ when time, $t = 0$ to $CO_2 = C_T$ when time, $t = T$, we obtain the concentration of the sampled exhaled air in the TB ward as follows:

$$\int_{C_o}^{C_T} \frac{dC_i}{IpC_a + Q(C_e - C_i)} = \int_0^T \frac{dt}{V} \tag{4.3.2}$$

Integrating Equation (4.3.2) by applying a substitution method, we obtain:

$$\ln\left[IpC_a + Q(C_e - C_i)\right]_{C_o}^{C_T} = -\frac{Q}{V}\left[t\right]_o^T \tag{4.3.3}$$

Simplifying Equation (4.3.3) further, gives:

$$\ln\left[IpC_a + Q(C_e - C_T)\right] - \ln\left[IpC_a + Q(C_e - C_o)\right] = -\frac{QT}{V}, \tag{4.3.4}$$

which can be written as

$$\ln\left[\frac{IpC_a + Q(C_e - C_T)}{IpC_a + Q(C_e - C_o)}\right] = -\frac{QT}{V} \tag{4.3.5}$$

Applying logarithmic and exponential rules in Equation (4.3.5) and simplifying it further by making C_T the subject, we obtain an expression that describes the sampled exhaled air concentration-time curves:

$$C_{(T)} = C_e + \frac{IpC_a}{Q}\left[1 - e^{-\frac{QT}{V}}\right] + (C_o - C_e)\left[e^{-\frac{QT}{V}}\right] \tag{4.3.6}$$

where C_o is the indoor carbon dioxide at time, $t = 0$, which is greater than C_e.

Simulation of Equation (4.3.6) in Figures 4.2a and 4.2b demonstrate factors associated with TB transmission in health care settings.

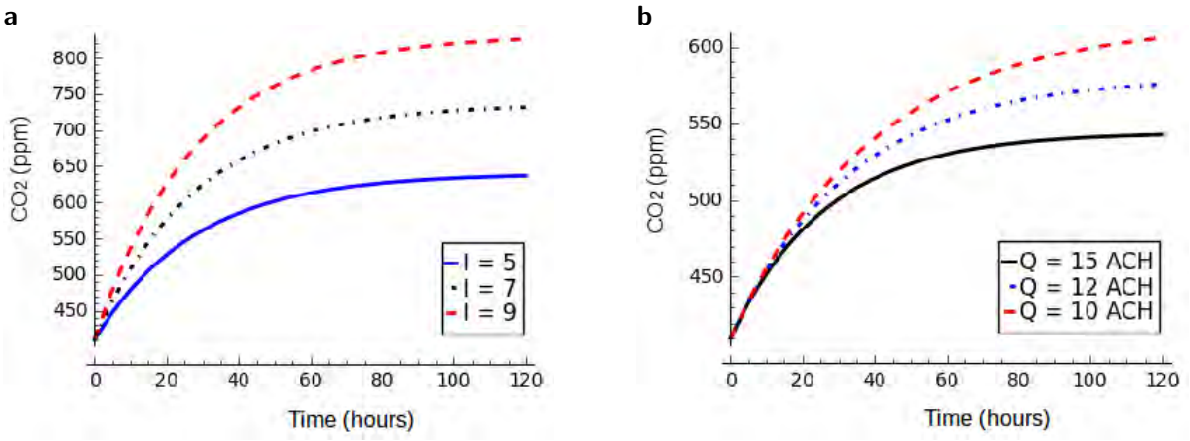

Figure 4.2: Risk factors correlated with tuberculosis transmission in health care settings. (a) Concentration of exhaled air increases in the ward with increasing number of infectors and duration of exposure. (b) Exhaled air from infectors increases in the ward with decreasing ventilation rate and increasing duration of exposure.

Figures 4.2a and 4.2b (simulation of Equation (4.3.6)) show risk factors correlated with TB transmission in health care settings with increasing duration of exposure. Results show that the concentration of exhaled air increases in the space with increasing number of infectious

individuals and duration of exposure (Figure 4.2a)). Figure 4.2b shows that the concentration of carbon dioxide as a surrogate of exhaled air increases in space with decreasing ventilation rate and increasing duration of exposure.

Equation (4.3.6) that is illustrated in Figure 4.2a, shows that when the number of TB patients increases in the TB ward, the concentration of exhaled air that may contain airborne infectious particles becomes high and a large number of exposed susceptible individuals may be infected. However, if the number of TB patients in the TB ward can be treated with effective chemotherapy and cured then $IpC_a \to 0$ and Equation (4.3.6) becomes:

$$C_{(T)} = C_e + (C_o - C_e)\left[e^{-\frac{QT}{V}}\right], \tag{4.3.7}$$

which describes the decay exponential curve [99] as demonstrated in Figure 4.3.

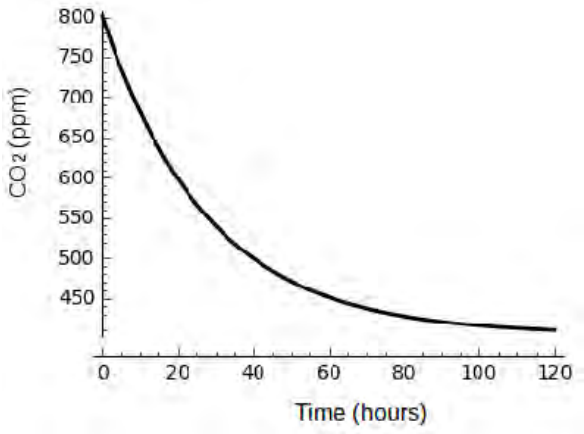

Figure 4.3: Exhaled air from infectors decreases in the TB ward with decreasing number of TB patients per given period of time.

Figure 4.3 shows that if the number of TB cases can be reduced/cured, a TB control strategy in health care settings is likely to be achieved. We further discuss TB control interventions in health care settings in the following section.

4.3.1 TB control interventions in health care settings

As mentioned earlier, although it is not the most effective intervention for TB control, natural or mechanical ventilation plays a key role in TB control by reducing (diluting) the concentration of airborne infectious particles expelled by infectors. The WHO recommend a ventilation rate of 12 ACH for health care settings, which includes TB isolation wards. However, in exceptionally hazardous areas, such as autopsy rooms, airflow rates should be increased to $15-25$ ACH [58].

Mechanical air disinfections, such as negative pressure ionisation and ultraviolet germicidal irradiation in hospital wards can act as TB control interventions and may replace ventilation if installed properly [58, 94]. Negative pressure ionisation removes polluted air from the room and replaces it with fresh air, such that airborne infectious particles are not able to settle in the given space to induce infection. It has been noted that large-scale negative ionizers reduce airborne infectious particles by up to approximately 99% [94]. However, installation and maintenance of mechanical air disinfectors is very expensive for some health care centres to afford and requires experts to provide this service, though ultraviolet germicidal irradiation is still cheaper than mechanical ventilation [94].

High efficiency particulate air (HEPA) filters have been demonstrated to provide a minimum efficiency of 99.97% by trapping small particles with diameter $\geq 0.3\ \mu m$ [58]. Although they may have aerodynamic diameter of less than $1\ \mu m$, airborne infectious particles viable with potential for TB infection have a critical diameter of approximately $1-5\ \mu m$ [58], implying that if HEPA filters can be implemented and used properly, they should be one of the most effective interventions for TB control among health care workers. Furthermore, if multi-drug resistant and extensive-drug resistant patients can be supplied with and encouraged to wear HEPA filters, the concentration of airborne infectious particles expelled by TB patients can be reduced in the atmosphere and TB transmission probability in health care settings may be reduced.

Surgical masks have been demonstrated to reduce the transmission of multi-drug resistant TB by 56% if worn by multi-drug resistant TB patients [105]. The efficacy of surgical masks seems to be lower than that of HEPA, implying that its face-seal leakage is high and a large number of susceptible individuals may be infected despite the use of this device. For an effective respiratory protective device against airborne infectious disease, its face-seal leakage should not exceed 10% [58]. Thus, though they have been used in different health care settings, perhaps because of their affordable price, surgical masks are not recommended for TB control. Although the efficacy and face-seal leakage of mist/dust respirators are not clearly specified, they have been demonstrated to be cheap, and provide comfort and protection against airborne infectious diseases [6]. However, since none of the air disinfection devices provide 100% protection against airborne infectious disease, rather than depending on one disinfection device, they should be combined. For example, HEPA filters should be used together with ultraviolet germicidal irradiation to provide high protection against airborne infectious diseases [58].

4.4 Modelling TB transmission in prisons

Many studies apply the Wells-Riley model, which assumes steady-state ventilation conditions and well mixed airspace to estimate the probabilities of TB transmission in confined spaces [113]. Since airborne infectious diseases, such as TB, mostly occur in congregate locations with low per person ventilation either under non-steady-state or steady-state conditions, here, we apply a mathematical model developed in this project (Chapter 2, Section 2.4) by monitoring carbon dioxide as a marker of exhaled air to demonstrate factors attributable to TB transmission in prisons as follows:

$$P(T \leq t|I,\beta,\theta,\mu,Q,p) = \begin{cases} 1 - e^{\left(-\frac{I(\beta-\mu)\theta pt}{Q}\left[1-\frac{V}{QT}\left(1-e^{-\frac{QT}{V}}\right)\right]\right)} & \text{if non} - \text{steady} - \text{state} \\ 1 - e^{-\frac{I(\beta-\mu)\theta pt}{Q}} & \text{if steady} - \text{state} \end{cases} \tag{4.4.1}$$

combined, the two equations give

$$P(T \leq t|I,\beta,\theta,\mu,\bar{f},n) = 1 - e^{-\frac{I(\beta-\mu)\theta \bar{f} t}{n}} \tag{4.4.2}$$

Where $P(T \leq t|I,\beta,\theta,\mu,\bar{f},n)$ is the probability of TB transmission risk for susceptible individuals under non-steady-state and steady-state conditions, $T \leq t$ denotes duration of exposure up to the point of infection (s). I is the number of infectious individuals, $(\beta - \mu)$ is the surviving airborne infection particles that reach the alveolar (particle/s), θ is the respiratory deposition fraction, Q is the ventilation rate (L/s), V is the room volume (m^3), $\bar{f}$ is the average volume fraction and n is the total number of individuals in the given space.

Through application of these equations, we explored TB transmission in prisons by considering numerous factors and conditions attributable to TB transmission probability in this congregate location as illustrated in Figure 4.4. Graphically, Equation (4.4.1) (under non-steady-state conditions), is illustrated in Figure 4.4a, which shows that TB transmission probability increases with increasing number of infectious individuals and decreases as the room volume increases. This implies that small area per person communal cells with the presence of infectious individuals in prisons accelerates the risk of acquiring infectious diseases. Application of Equation (4.4.2) is demonstrated in Figure 4.4b. From this figure we note that as the number of inmates increases in prisons with increasing number of infectious individuals, TB transmission probability becomes extremely high, implying that TB transmission probability in prisons is highly correlated with overcrowding and increasing number of infectious individuals. By application

of Equation (4.4.1), we explored the impact of ventilation air change per hour (ACH) under non-steady state and steady state conditions from the minimum (Q = 3 ACH), intermediate (Q = 8 ACH) to the maximum (Q = 12 ACH), which is recommended by the WHO for health care settings. It was noted that the probability of acquiring TB infection increases as ventilation rate decreases and the number of infectious individuals increases in the given space (refer to Figure 4.4c). This implies that low per person ventilation rate in prisons is one of the factors attributed to TB transmission. Figure 4.4d (generalized numerical simulation of Equations (4.4.1) and (4.4.2)), shows that increasing number of infectious individuals and duration of exposure are among the factors which accelerate TB transmission probability in prisons. The fact that a large number of inmates stay in prisons for a long time, some of whom have already been infected, leads to the increasing risk of TB transmission probability in prisons and the community at large.

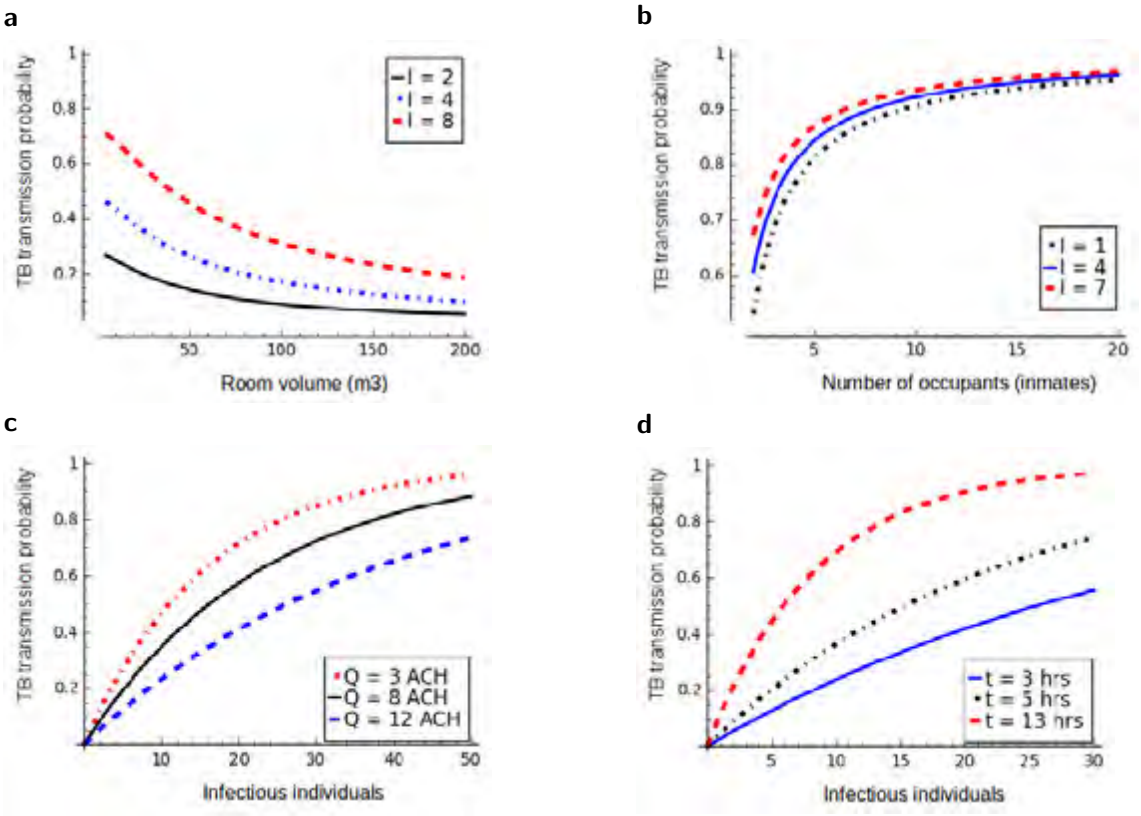

Figure 4.4: Mathematical model simulation, showing TB transmission probability in prisons. (a) TB transmission probability decreases with increasing room volumes and increases with increasing number of infectious individuals. (b) TB transmission probability increases with increasing number of inmates some of whom are infectious individuals. (c) TB transmission probability increases with increasing number of infectious individuals and decreasing room ventilation. (d) TB transmission probability increases with increasing number of infectious individuals and duration of exposure.

4.4.1 Strategies for TB control in prisons

Identification and isolation of infected from non-infected individuals might be among the best strategies of reducing TB transmission in prisons. Infected individuals should be identified and be given a specific living area while undergoing TB treatment. As mentioned earlier, proximity to infectors and high concentration of airborne infectious particles per air volume are among the factors attributable to TB transmission. If isolation can be implemented and maintained in prisons, it can play a vital role in TB control.

Though the value of air change per hour is not well specified for prison environments, natural ventilation is one of the cheapest effective TB control interventions if implemented properly. The accumulation and retention of airborne infectious particles in communal cells can be reduced if natural ventilation can be improved in prisons. Communal cells are highly confined with a small area per inmate, which is one of the best environments for transmission of airborne infectious disease, due to high concentration of airborne infectious particles per air volume and reasonable proximity to infectors. If communal cells can be expanded with large secured windows, which allow air circulation it can have a greater impact on TB control in prisons. It has been noted that if communal cells can be expanded to a minimum floor space of about $5.4\ m^2$ per inmate (International recommendation), TB transmission in prisons can be reduced by over 50%, and if they can be expanded to a minimum floor space of $3.34\ m^2$ per inmate (South African recommendation), TB transmission can be reduced by 30% [109]. However, since most of the world's prisons are still highly confined with a high concentration of polluted air and high rates of transmission of airborne infectious diseases, it means that these recommendations can not be implemented practically.

As mentioned earlier, overcrowding is one of the problematic factors that leads to high TB prevalence in prisons. The key question is, what can be done to reduce overcrowding in prisons? Though it is convincing that prisons are reserved for punishing and reshaping the criminals, overcrowding and explosion of infectious diseases are threatening the lives of the inmates. Furthermore, prisoners are acting as a source of TB transmission in the civilian community after their release, implying that TB burden in prisons affects the civilian community indirectly. Generally, prison environmental conditions are not conducive to a healthy life, which is why the prevalence and incidence of airborne infectious diseases are remarkably high. Reducing overcrowding in prisons can play an important role in TB control, and can be implemented if the period of those either awaiting sentencing or awaiting trials can be reduced in prisons. Furthermore, the time spent in confined communal cells for 23 hours per day should be reduced to either 8 hours or 12 hours per day [109]. This can reduce the prolonged period of exposure

to infectors and contribute to TB control in prisons.

4.5 Discussion

Using mathematical modelling approach, we demonstrated factors attributable to TB transmission in congregate settings, including schools, households, public transport, health care settings and prisons. The study suggests that identification, isolation and successful treatment of TB cases in congregate settings is one of the most effective interventions for TB control in these crucial locations [58]. If identified TB cases can be treated with effective chemotherapy, it will significantly impact TB control strategies by reducing the number of airborne infectious particles viable with potential for TB infection.

Insufficient ventilation plays an important role in the transmission of airborne infectious diseases and if ventilation can be improved, this might be an important intervention for TB control in congregate settings. However, though ventilation plays a key role in reducing TB transmission, it does not ensure 100% air disinfection [21, 58], it dilutes the concentration of airborne infectious particles or moves them from one space of high concentration to another, and it does not destroy them. Destruction of airborne infectious particles in exhaled air from infectors should be the most effective intervention for TB control and other airborne diseases.

Ultraviolet germicidal irradiation damages the DNA of airborne pathogens, destroys their replication ability and makes them non-infectious [21, 58]. Furthermore, ultraviolet germicidal irradiation has the ability to kill airborne infectious particles in the given space [21, 47, 58]. If ultraviolet germicidal irradiation can be applied with precautions in different congregate locations with high likelihood of airborne infectious disease transmission, such as schools, health care settings and prisons it may have a greater impact on disease prevention and control. Furtheemore, all modes of public transport should be sterilised after a given number of routes using ultraviolet germicidal irradiation. Substantial research show that if general ventilation can be considered together with application of ultraviolet germicidal irradiation, a disinfection rate of 45 ACH can be achieved if properly installed [58], which may have a greater impact on TB control. However, the correlation between ventilation and ultraviolet germicidal irradiation is not clearly understood, but high rates of ventilation hamper the killing of airborne infectious particles [58], perhaps because of high dilution. We suggest that both ventilation and ultraviolet germicidal irradiation should be applied in congregate locations for airborne infectious disease prevention and control.

Chapter 5

Impact of effective contact rate and post treatment immune status on population TB infection and disease states using a mathematical model

Abstract

Tuberculosis (TB) is transmitted by *Mycobacterium tuberculosis* (MTB) in an environment allowing interaction between infectious and susceptible individuals, usually in indoors. Progression from TB infection to disease depends on the interaction between the immunological state of the host and the virulence of the pathogen strain. Recent studies of TB vaccines are investigating high risk individuals who have had active TB and successfully completed a full course of combination TB chemotherapy. In this study, we explore the population impact of effective contact rate (β) and post-treatment immune status on TB epidemiology using a mathematical model we developed that consists of five states of susceptible, newly infected, reinfected, active TB and treated individuals. The study explores the population impact of effective contact rate on TB epidemiology by comparing the number of newly infected and reinfected individuals at stability point of a TB epidemic with increasing effective contact rate (ranging from 5 to $30\ yr^{-1}$). Furthermore, we examine the impact of post-treatment immune status by comparing the number of active TB cases when all treated individuals move to either a susceptible, newly infected or reinfected state at stability point of a TB epidemic. This is an important study population as the incidence of TB can be higher in people recently cured of

the disease. We found that the number of newly infected cases increases when $\beta = 5$ to $\beta = 10$ yr^{-1} then decreases with increasing effective contact rate, while that of reinfected individuals increases in all values of effective contact rate, implying that TB prevalence might be driven by reinfection, especially in high burden settings. Furthermore, we noted that the number of active TB becomes higher when all treated individuals move to a susceptible state than when they move to either a newly infected or reinfected state, probably because of immunological factors. Results show that post-treatment immunological memory reduces the risk of active disease by $7 - 16\%$ compared to susceptible individuals.

5.1 Introduction

Tuberculosis (TB) is caused and thus transmitted by *Mycobacterium tuberculosis* (MTB) in an infective environment with the presence of infectious and susceptible individuals. Effective contact rate is assumed to be one of the factors correlated with the force of infection, which fosters TB transmission in a community. For example, TB transmission in congregate settings, such as households, public transport, schools, and work places is associated with high effective contact rate between infectious and susceptible individuals [92, 100]. The effective contact rate between infectious and susceptible individuals varies in different locations depending on the interactions and environmental exposure. Progression from TB infection to disease depends on the interaction between the immunological state of the host and the virulence of the pathogen strain [36]. TB disease may arise either early or late following a new infection and also from reinfection of previously infected cases. Empirical evidence suggests that reinfection is among the factors hampering successful TB control [34, 64, 112]. It is unclear what leads to a remarkably high number of reinfected individuals in the community, but since effective contact rate is directly correlated with the force of infection, it might be the main driving factor.

Recent studies of TB vaccines are investigating high risk individuals who have had active TB and successfully completed a full course of combination TB chemotherapy [19, 91]. This chapter describes a mathematical model we developed that incorporates susceptible, newly infected, reinfected, active TB and treated individuals to study the population impact of effective contact rate and post-treatment immune status on TB epidemiology. An infectious individual with varying effective contact rate (ranging from 5 to 30 yr^{-1}) was introduced among $100,000$ fully susceptible individuals and we observed the number of individuals in all five states at stability point of a TB epidemic. This range of effective contact rate was selected because $\beta = 5 - 10$ yr^{-1} is related to TB transmission in the United Kingdom in $1900 - 1950$ [34], $\beta = 15$ yr^{-1} is related to TB transmission in schools in South Africa [100],

and $\beta = 30\ yr^{-1}$ is related to TB transmission in prisons in South Africa [109]. Here, we explore the population impact of effective contact rate by comparing the number of newly infected and that of reinfected individuals at stability point of a TB epidemic, with increasing effective contact rate. Furthermore, we examine the population impact of post-treatment immune status by comparing the number of active TB cases when all treated individuals move to either a susceptible, newly infected or reinfected state with increasing effective contact rate. This is an important study population as the incidence of TB can be higher in people recently cured of the disease. The study was divided into three parts and simulated the model numerically when all treated individuals move to: (i) susceptible (ii) newly infected or (iii) reinfected state, and we observed the number of individuals in all five states. We compute the basic reproduction number and eigenvalues from the model when treated individuals move to all three states of susceptible, newly infected and reinfected to examine the stability of the disease free equilibrium.

5.2 Methods

5.2.1 Model design and development

The model consists of five states of susceptible individuals (S) who are not yet infected but at a high risk of acquiring TB infection or disease if become exposed to infectious individual(s), newly infected individuals (L_1) who have been infected once in lifetime with MTB and they can move to either reinfected or active TB state if become exposed, reinfected individuals (L_2) who have been infected multiple times with MTB and remain latently infected or move to active TB state through endogenous reactivation, active TB individuals (I) who are infectious and they can transmit TB, and treated individuals (T) who were previously infectious and become cured by chemotherapy and some are still on treatment. Note that the difference between newly infected and reinfected individuals is that newly infected individuals are latently infected individuals who have been infected once with MTB and they can develop active disease through either exogenous reinfection or endogenous reactivation depending on the virulence of the pathogen strain and immune response of the host, while reinfected individuals are repeatedly exposed latent TB individuals who can only develop active disease through endogenous reactivation.

The design and development of the model was based on an actual population in Cape Town, South Africa, where many already infected individuals are repeatedly exposed to different infectious sources and become reinfected, and start treatment after acquiring TB disease.

Furthermore, since natural MTB infection and chemotherapy induce an immune response that reduces TB susceptibility [65], we take into consideration the fact that treated individuals move to either a newly infected or reinfected state if they maintain immunological memory after successful treatment, and if they become susceptible due to waning of the immune response, they move to a susceptible state. This is because the average duration for the waning of induced immune response by MTB and chemotherapy is not well understood. However, if treatment fails or is not completed, they can move back to active disease and become infectious. As it has been reported that TB disease incidence in TB treated individuals is several-fold higher than in latently infected [110], we explored post-treatment cases returning to either the susceptible, newly infected or reinfected immunological state. This approach makes our model more unique and different from the prior studies, which apply infection force for treated individuals moving to latent TB states without considering immunological memory of the host. In order to explore the population impact of effective contact rate and post-treatment immune status on TB epidemiology, the model does not incorporate the following states: (i) multi-drug resistance TB (MDR-TB) (ii) vaccination (iii) human immunodeficiency virus (HIV) infection or (iv) age stratification.

5.2.2 Model description and assumptions

In the development of the model, we assume that the population consists of fully susceptible individuals, hence, the number of births or recruitment individuals become susceptibles at a rate $\pi\ yr^{-1}$. When susceptible individuals become infected with MTB, a proportion p in this group develop active TB very fast and it's complement proportion $1-p$, which constitute the majority become latently infected and move to a newly infected state depending on the virulence of the pathogen strain and host immunological factors. Newly infected individuals are at a high risk of developing active disease through either endogenous reactivation or exogenous reinfection. Here, we take into consideration that one group of newly infected individuals develop active TB slowly through endogenous reactivation at a rate $c\ yr^{-1}$, and a fraction q of the second group of newly infected individuals develop active TB very fast after infection through exogenous reinfection, while a remaining fraction 1-q of this group move to a reinfected state. Reinfected individuals develop active TB through endogenous reactivation either fast or slowly at a rate $y\ yr^{-1}$, depending on the immunological state of the host and the virulence of the pathogen strain. Individuals with active TB receive medical treatment and move to a treated state at a rate k, while some die of active TB at a rate $\mu_t\ yr^{-1}$. Treated and successfully cured individuals may become susceptible and move to a susceptible state at a rate r or retain immunological memory and move to either a newly

infected at a rate g or a reinfected state at a rate $z\ yr^{-1}$, without exposure to the force of infection. This is because latently infected and treated individuals acquire an immune response that reduces TB susceptibility though it may wane and individuals become susceptible. As mentioned earlier, we only implement treatment for active TB cases because in the real world, many TB patients only start treatment after active disease development. However, if TB cases are not well treated, treatment fails or chemotherapy is incomplete, they incubate the infection and relapse back to active TB at a rate $\alpha\ yr^{-1}$. As stated earlier. it has been noted that latently infected individuals acquire immunity that reduces TB susceptibility [64, 86], though they can be (re)infected and develop active disease if they become frequently exposed to infectious individuals in confined spaces. Thus, $\omega(0 < \omega < 1)$ is the preventive factor due to prior natural MTB infection, which partially prevents latently infected individuals from TB susceptibility [64]. In each of the five states, there is a natural mortality rate $\mu\ yr^{-1}$ as demonstrated in Figure 5.1.

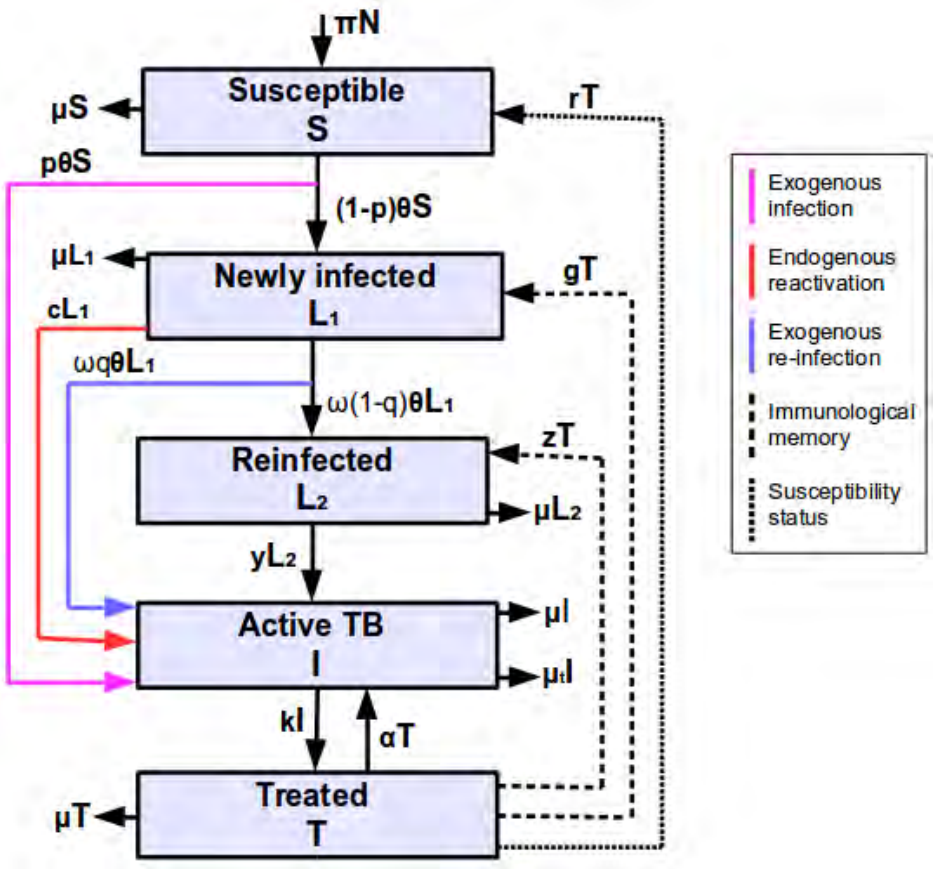

Figure 5.1: TB transmission model to study the impact of effective contact rate and post-treatment immune status on TB epidemiology. Parameters are described in Table 5.1.

From the model (Figure 5.1), we developed a mathematical model as follows:

$$\left.\begin{aligned}
\dot{S} &= \pi N - (\theta + \mu)S + rT \\
\dot{L}_1 &= (1-p)\theta S - (c + \omega\theta + \mu)L_1 + gT \\
\dot{L}_2 &= \omega(1-q)\theta L_1 - (y + \mu)L_2 + zT \\
\dot{I} &= p\theta S + (c + \omega q\theta)L_1 + yL_2 - (k + \mu + \mu_t)I + \alpha T \\
\dot{T} &= kI - (r + g + z + \alpha + \mu)T
\end{aligned}\right\} \tag{5.2.1}$$

where $\theta = \beta\frac{I}{N}$, which is the force of infection, β is the effective contact rate, $\frac{I}{N}$ is the prevalence, I is the number of infectious individuals and N is the total number of individuals in the population. Other parameters are described in Table 5.1.

Table 5.1: Description of parameters used in Figure 5.1. The values of parameters used in this study were estimated from published literature and computed others by matching infection and incidence data in South Africa.

Parameters	Description	Values	Reference
β	Effective contact rate	$5-30\ \text{yr}^{-1}$	estimated
p	Probability of fast progression from susceptible to active TB after infection	0.05	[22, 62]
c	Rate of progression from newly infected to active TB through endogenous reactivation	$0.0053\ \text{yr}^{-1}$	[22, 62]
q	Probability of moving from newly infected to active TB through exogenous reinfection	0.03	[112]
y	Rate of endogenous reactivation from reinfected to active TB	$0.0026\ \text{yr}^{-1}$	[22, 62]
r	Rate of moving from treated to susceptible state	Variable	Depends on the immunological status
π	Birth or recruitment rate	$0.02\ \text{yr}^{-1}$	[17]
g	Rate of moving from treated to a newly infected state	Variable	Depends on the immunological status
ω	Preventive factor that reduces TB susceptibility due to prior natural MTB infection	0.21	[91]
z	Rate of moving from treated to a reinfected state	Variable	Depends on the immunological status
k	Case detection rate from active TB to treated state	$0.68\ \text{yr}^{-1}$	[84]
α	Rate of treatment failure and move to active TB	$0.01\ \text{yr}^{-1}$	[62]
μ	Natural mortality rate	$0.02\ \text{yr}^{-1}$	[112]
μ_t	Active TB mortality rate	$0.075\ \text{yr}^{-1}$	[84]

Computed values: In the design of the model, we take into consideration that treated and successfully cured individuals may become either susceptible or immune due to immunological memory. Thus, successful treatment = 1 - relapse (α), such that $Q = 1-\alpha$. Where $Q = r, g$ or z. Or $r = g = z = 0$, depending on immunological status.

Disease free equilibrium is defined as the point at which there is no existence of the disease in the population. By computing S, L_1, L_2, I and T at disease free equilibrium (i.e.,

$L_1 = L_2 = I = T = 0$) and assuming that birth rate is equal to death rate, we obtain disease free equilibrium point as $(S^o, L_1^o, L_2^o, I^o, T^o) = (N, 0, 0, 0, 0)$. This implies that at disease free equilibrium, the total number of population is equal to that of susceptible individuals, such that $N = S$. However, during epidemic active disease at any time, t, we have $N_{(t)} = S_{(t)} + L_{1(t)} + L_{2(t)} + I_{(t)} + T_{(t)}$, implying that the population is comprised of all five states and disease free equilibrium might be unstable. The model is epidemiologically balanced. From the mathematical model (Equation 5.2.1), we compute the basic reproduction number to determine the stability of the disease free equilibrium as discussed below.

5.2.3 Basic reproduction number

Basic reproduction number (R_o) is the average number of secondary cases generated by a single case connected with the fully susceptible population [31, 62, 75]. We use the next generation method to determine the basic reproduction number, which is an important figure in the epidemiology of infectious diseases. It is among the most frequently estimated quantities to predict the outbreak of infectious diseases, and its value provides information for designing control interventions for the infectious disease burden [62, 75]. R_o thus plays an important role in the analysis of infectious disease models, such as TB [22]. If $R_o < 1$, the disease free equilibrium is asymptotically stable, and it is unstable if $R_o > 1$ [31, 62, 75].

The next generation method is used extensively to compute the basic reproduction number, though numerous other methods are discussed in the literature [75]. It generates a next generation matrix, and the basic reproduction number is the spectral radius of this matrix. The next generation matrix is defined as a matrix that relates the numbers of newly infected individuals in the various states in consecutive generations [75]. The dominant eigenvalue in a next generation matrix is referred to as the basic reproduction number. The next generation matrix (M) is defined mathematically as

$$M = F(S^o, L_1^o, L_2^o, I^o, T^o)V^{-1}(S^o, L_1^o, L_2^o, I^o, T^o),$$

and the basic reproduction number is the dominant eigenvalue of M. Where $F(S^o, L_1^o, L_2^o, I^o, T^o)$ and $V(S^o, L_1^o, L_2^o, I^o, T^o)$ are the transmission and transition matrices ($n \times n$ matrix) at disease free equilibrium, respectively. These are defined mathematically as

$$F(S^o, L_1^o, L_2^o, I^o, T^o) = \left[\frac{\partial f_i(x_0)}{x_j}\right] \text{ and } V(S^o, L_1^o, L_2^o, I^o, T^o) = \left[\frac{\partial v_i(x_0)}{x_j}\right] \text{ for } i, j = 1, \cdots, n$$

where x_o is the disease free equilibrium, f_i is the rate of appearance of the new infection in

classes, v_i is the transfer of the infection from one class to another and n is the number of infective classes.

However, prior to the formation of the next generation matrix, we generate the transmission (f) and transition (v) subsystems from Equation (5.2.1). We then linearise subsystems f and v by applying the Jacobian (J_c) and obtain matrices $F(S,L_1,L_2,I,T)$ and $V(S,L_1,L_2,I,T)$, which are $n \times n$ transmission and transition matrices, respectively. The transmission subsystem is an infected subsystem that describes the production of newly infected individuals and changes in the states of existing infected individuals. The transition subsystem is the transfer of the infection from one class to another. On the other hand, the transmission matrix describes the production of new infections, and the transition matrix describes changes of infected states, such as the immunity acquisition or removal by death [75]. Considering Equation (5.2.1), the Jacobian method that is used to linearise subsystems f and v is described mathematically as

$$J_c = \begin{pmatrix} \frac{\partial \dot{S}}{\partial S} & \frac{\partial \dot{S}}{\partial L_1} & \frac{\partial \dot{S}}{\partial L_2} & \frac{\partial \dot{S}}{\partial I} & \frac{\partial \dot{S}}{\partial T} \\ \frac{\partial \dot{L_1}}{\partial S} & \frac{\partial \dot{L_1}}{\partial L_1} & \frac{\partial \dot{L_1}}{\partial L_2} & \frac{\partial \dot{L_1}}{\partial I} & \frac{\partial \dot{L_1}}{\partial T} \\ \frac{\partial \dot{L_2}}{\partial S} & \frac{\partial \dot{L_2}}{\partial L_1} & \frac{\partial \dot{L_2}}{\partial L_2} & \frac{\partial \dot{L_2}}{\partial I} & \frac{\partial \dot{L_2}}{\partial T} \\ \frac{\partial \dot{I}}{\partial S} & \frac{\partial \dot{I}}{\partial L_1} & \frac{\partial \dot{I}}{\partial L_2} & \frac{\partial \dot{I}}{\partial I} & \frac{\partial \dot{I}}{\partial T} \\ \frac{\partial \dot{T}}{\partial S} & \frac{\partial \dot{T}}{\partial L_1} & \frac{\partial \dot{T}}{\partial L_2} & \frac{\partial \dot{T}}{\partial I} & \frac{\partial \dot{T}}{\partial T} \end{pmatrix} \tag{5.2.2}$$

Hence, from Equation (5.2.1), we form the transmission, f and transition, v subsystems as

$$f = \begin{pmatrix} 0 \\ (1-p)\beta\frac{I}{N}S \\ \omega(1-q)\beta\frac{I}{N}L_1 \\ p\beta\frac{I}{N}S + \omega q\beta\frac{I}{N}L_1 \\ 0 \end{pmatrix} \text{ and } v = \begin{pmatrix} -\pi N + (\beta\frac{I}{N} + \mu)S - rT \\ (c + \omega\beta\frac{I}{N} + \mu)L_1 - gT \\ (y+\mu)L_2 - zT \\ -cL_1 - yL_2 + (k+\mu+\mu_t)I - \alpha T \\ -kI + (r+z+g+\alpha+\mu)T \end{pmatrix}$$

In Figure 5.1, there are three infected states, which are L_1, L_2 and I, giving a 3×3 matrix. Hence, we form the transmission matrix, $F(S,L_1,L_2,I,T)$, by applying Jacobian (see Equation (5.2.2)) in f with respect to L_1, L_2 and I as

$$F(S,L_1,L_2,I,T) = \begin{pmatrix} 0 & 0 & (1-p)\beta\frac{S}{N} \\ \omega(1-q)\beta\frac{I}{N} & 0 & \omega(1-q)\beta\frac{L_1}{N} \\ \omega q\beta\frac{I}{N} & 0 & p\beta\frac{S}{N} + \omega q\beta\frac{L_1}{N} \end{pmatrix} \tag{5.2.3}$$

Substituting S, L_1, L_2, I and T at disease free equilibrium point $(S^o, L_1^o, L_2^o, I^o, T^o) = (N, 0, 0, 0, 0)$ into Equation (5.2.3), we obtain the transmission matrix at disease free equilibrium, $F(S^o, L_1^o, L_2^o, I^o, T^o)$, as

$$F(S^o, L_1^o, L_2^o, I^o, T^o) = \begin{pmatrix} 0 & 0 & (1-p)\beta \\ 0 & 0 & 0 \\ 0 & 0 & p\beta \end{pmatrix} \tag{5.2.4}$$

By applying the Jacobian with respect to L_1, L_2 and I in v above, we obtain the transition matrix, $V(S, L_1, L_2, I, T)$, as

$$V(S, L_1, L_2, I, T) = \begin{pmatrix} c + \omega\beta\frac{I}{N} + \mu & 0 & \omega\beta\frac{L_1}{N} \\ 0 & y + \mu & 0 \\ -c & -y & k + \mu + \mu_t \end{pmatrix} \tag{5.2.5}$$

Substituting disease free equilibrium point into Equation (5.2.5), we obtain the transition matrix at disease free equilibrium, $V(S^o, L_1^o, L_2^o, I^o, T^o)$, as

$$V(S^o, L_1^o, L_2^o, I^o, T^o) = \begin{pmatrix} c + \mu & 0 & 0 \\ 0 & y + \mu & 0 \\ -c & -y & k + \mu + \mu_t \end{pmatrix} \tag{5.2.6}$$

Since the transition matrix consists of many variables, to be consistent we used a computational tool (Sage) to compute the inverse. Hence the inverse of Equation (5.2.6), $V^{-1}(S^o, L_1^o, L_2^o, I^o, T^o)$, is demonstrated as

$$V^{-1}(S^o, L_1^o, L_2^o, I^o, T^o) = \begin{pmatrix} \frac{1}{c+\mu} & 0 & 0 \\ 0 & \frac{1}{y+\mu} & 0 \\ \frac{c}{(c+\mu)(k+\mu+\mu_t)} & \frac{y}{(y+\mu)(k+\mu+\mu_t)} & \frac{1}{k+\mu+\mu_t} \end{pmatrix} \tag{5.2.7}$$

We obtain the next generation matrix, which is the product of $F(S^o, L_1^o, L_2^o, I^o, T^o)$ and $V^{-1}(S^o, L_1^o, L_2^o, I^o, T^o)$ as

$$F(S^o, L_1^o, L_2^o, I^o, T^o)V^{-1}(S^o, L_1^o, L_2^o, I^o, T^o) = \begin{pmatrix} \frac{(1-p)\beta c}{(c+\mu)(k+\mu+\mu_t)} & \frac{(1-p)\beta y}{(y+\mu)(k+\mu+\mu_t)} & \frac{(1-p)\beta}{k+\mu+\mu_t} \\ 0 & 0 & 0 \\ \frac{p\beta c}{(c+\mu)(k+\mu+\mu_t)} & \frac{p\beta y}{(y+\mu)(k+\mu+\mu_t)} & \frac{p\beta}{k+\mu+\mu_t} \end{pmatrix} \tag{5.2.8}$$

As mentioned earlier, the basic reproduction number is a spectral radius of the next generation matrix. Thus, the basic reproduction number, which is also defined as the dominant eigenvalue in the next generation matrix, was obtained from Equation (5.2.8) as

$$R_o = \frac{\beta(\mu p + c)}{(k+\mu+\mu_t)(\mu+c)}$$

The computed basic reproduction number has a positive real part, implying that it might be greater than 1. As mentioned earlier, if $R_o < 1$ it means that the risk of TB transmission is decreasing and it might be controlled by chemotherapy, and if $R_o = 1$, the risk of TB transmission is endemic. If $R_o > 1$, the TB burden is increasing and it cannot be controlled by the implementation of chemotherapy only, particularly in high TB burden settings, such as South Africa. We further examined the stability of the disease free equilibrium by computing eigenvalues as discussed below.

5.2.4 Stability analysis of the disease free equilibrium

Since the basic reproduction number computed in this study has a positive real part, it is likely to be greater than 1, implying that TB transmission is increasing, regardless of the implementation of medical treatment. Here, we explore the stability of the disease free equilibrium by computing eigenvalues in Equation (5.2.1). Disease free equilibrium is stable if all eigenvalues have negative real parts, and unstable if any of the eigenvalues is positive [31]. Hence, applying the Jacobian in Equation (5.2.1), gives

$$J = \begin{pmatrix} -(\beta\frac{I}{N}+\mu) & 0 & 0 & -\beta\frac{S}{N} & r \\ (1-p)\beta\frac{I}{N} & -(c+\omega\beta\frac{I}{N}+\mu) & 0 & (1-p)\beta\frac{S}{N}-\omega\beta\frac{L_1}{N} & g \\ 0 & \omega(1-q)\beta\frac{I}{N} & -(y+\mu) & \omega(1-q)\beta\frac{L_1}{N} & z \\ p\beta\frac{I}{N} & c+\omega\beta\frac{I}{N} & y & H & \alpha \\ 0 & 0 & 0 & k & Q \end{pmatrix} \tag{5.2.9}$$

where $H = p\beta\frac{S}{N} + \omega\beta\frac{L_1}{N} - (k+\mu+\mu_t)$ and $Q = -(r+\alpha+z+g+\mu)$

The characteristic equation of the model at disease free equilibrium is expressed as

$$[J_{0-\lambda I}] = 0$$

where J_0 is the Jacobian matrix (from the model) at disease free equilibrium, λ is the eigenvalue and I is the identity matrix.

Substituting disease free equilibrium point $(S^o, L_1^o, L_2^o, I^o, T^o) = (N, 0, 0, 0, 0)$ into Equation (5.2.9), minus the product of eigenvalue and identity matrix diagonally, we obtain the model matrix at disease free equilibrium as follows:

$$(J_0 - \lambda I) = \begin{pmatrix} -\mu-\lambda & 0 & 0 & -\beta & r \\ 0 & -c-\mu-\lambda & 0 & (1-p)\beta & g \\ 0 & 0 & -y-\mu-\lambda & 0 & z \\ 0 & c & y & p\beta-(k+\mu+\mu_t)-\lambda & \alpha \\ 0 & 0 & 0 & k & R \end{pmatrix} \tag{5.2.10}$$

where $R = -(r+\alpha+z+g+\mu)-\lambda$

From Equation (5.2.10), we form the characteristic equation, $[J_{0-\lambda I}] = 0$, as

$$(-\mu-\lambda)[(-c-\mu-\lambda)(-y-\mu-\lambda)(p\beta-k-\mu-\mu_t-\lambda)(-r-\alpha-z-g-\mu-\lambda)]$$

$$-c[(-y-\mu-\lambda)(p\beta-k-\mu-\mu_t-\lambda)(-r-\alpha-z-g-\mu-\lambda)] = 0$$

Simplifying the characteristic equation further, gives

$$(-y-\mu-\lambda)(p\beta-k-\mu-\mu_t-\lambda)(-r-\alpha-z-g-\mu-\lambda)[\mu(c+\mu)+\lambda(2\mu+c+\lambda)-c] = 0$$

From the simplified characteristic equation, we form the following four equations:

$$-(y+\mu)-\lambda = 0 \tag{5.2.11}$$

$$p\beta-(k+\mu+\mu_t)-\lambda = 0 \tag{5.2.12}$$

$$-(r+\alpha+z+g+\mu)-\lambda = 0 \tag{5.2.13}$$

$$\lambda^2+(2\mu+c)\lambda+\mu^2+c\mu-c = 0 \tag{5.2.14}$$

Using Equations (6.2.7) to (6.2.8), we can determine the eigenvalues that predict the stability of the disease free equilibrium. As mentioned earlier, disease free equilibrium is stable if all eigenvalues have negative real parts, and unstable if any of the eigenvalues is positive. Additionally, if one of the eigenvalues is zero then we cannot tell from stability analysis whether the disease free equilibrium is stable or unstable. Thus, considering Equations (6.2.7) to (6.2.8), the eigenvalues are:

$$\lambda_1 = -(y+\mu) < 0$$

$$\lambda_2 = p\beta-(k+\mu+\mu_t)$$

$$\lambda_3 = -(r+\alpha+z+g+\mu) < 0$$

$$\lambda_{4,5} = \frac{-(2\mu+c) \pm \sqrt{(2\mu+c)^2 - 4(\mu^2+c\mu-c)}}{2}$$

Here, we noted that λ_1 and λ_3 have negative real parts, and λ_2 has a positive real part if $p\beta > (k+\mu+\mu_t)$. For stability of the disease free equilibrium, we assume that $\lambda_{4,5}$ have negative real parts (i.e., $\lambda_4 < 0$ and $\lambda_5 < 0$). Disease free equilibrium is stable if $p\beta < (k+\mu+\mu_t)$ and unstable if $p\beta > (k+\mu+\mu_t)$, where $p\beta$ is the effective contact rate for susceptible individuals moving direct to active disease. On the other hand, disease free equilibrium is stable if the effective contact rate for susceptible individuals moving direct to active disease is less than the summation of case detection, natural death and disease death rates. Otherwise disease free equilibrium is unstable.

5.2.5 Sensitivity analysis

We conducted sensitivity analysis of the model for all parameters to explore TB progression influencing factors. We observed the impact of each parameter on the model output and its sensitivity. Since TB infection and disease progression depends on the host immunological status and virulence of the pathogen strain, our sensitivity analysis based on TB progression rate and immune response induced by natural MTB infection and post-treatment immune status.

5.3 Simulation results

Using data estimated from published literature, varying effective contact rate (ranging from 5 to 30 yr^{-1}) and computed or estimated values by matching infection and incidence data in South Africa (Table 5.1), we simulated Equation (5.2.1) numerically to explore the population impact of effective contact rate and post-treatment immune status on TB epidemiology. As mentioned earlier, the study was divided into three parts where we simulated the model when all treated individuals move to: (i) susceptible (i.e., $z = g = 0, r = 0.99\ yr^{-1}$) (ii) reinfected (i.e., $r = g = 0, z = 0.99\ yr^{-1}$) or (iii) newly infected state (i.e., $r = z = 0, g = 0.99\ yr^{-1}$). To be We performed the sensitivity analysis of these parameters and β In the model simulation, we used the initial assumption that $S = 100{,}000$, $L_1 = L_2 = T = 0$ and $I = 1$, implying that an infectious individual was introduced among $100{,}000$ fully susceptible individuals. The epidemic was observed for 700 years when $\beta = 5\ yr^{-1}$ and 200 years when $\beta \geq 10\ yr^{-1}$ so that the TB

epidemic stability point could be attained.

Here, we observed the number of individuals in all five states at stability point of a TB epidemic with increasing effective contact rate, and compared the number of newly infected and that of reinfected individuals. We also compared the number of active TB cases schematically when all treated individuals move to a susceptible, newly infected or reinfected state at stability point of a TB epidemic. We found that the number of newly infected cases increases when $\beta = 5$ to $\beta = 10\ yr^{-1}$ then decreases with increasing effective contact rate, while that of reinfected individuals increases in all values of effective contact rate (Tables 5.2, 5.3 and 5.4), implying that a large number of active TB cases might be contributed by repeatedly exposed individuals. The number of active TB individuals was increasing with increasing effective contact rate, but lower than that of newly infected and reinfected individuals. Of all five states, the number of treated individuals was noted to be the lowest, probably because treated individuals become either susceptible and move to a susceptible state or retain immunological memory and move to either a newly infected or reinfected state. We noted that as the effective contact rate increases, the number of susceptible individuals decreases dramatically with a steep slope until a stability point is attained, implying that effective contact rate is an important factor, which determines the likelihood of TB infection and disease in the community.

Observing the number of active TB cases when treated individuals move to a susceptible, newly infected or reinfected state, we noted the highest number of active TB cases when all treated individuals move to a susceptible state (Tables 5.2, 5.3 and 5.4). We went on to compare the number of active TB cases schematically when treated individuals move to a susceptible, newly infected or reinfected state and found that when all treated individuals become susceptible, the number of active TB cases becomes higher than moving to either a newly infected or reinfected state (Figure 5.5), perhaps because individuals moving to a newly infected or reinfected state have more protection due to immunological memory than susceptible individuals. These findings imply that treated individuals are at high risk of active disease acquisition if they become susceptible, probably because of immunological factors.

The time taken for a TB epidemic to reach the peak and stability points was noted to decrease with increasing effective contact rate in all cases, implying that effective contact rate is directly correlated with the force of infection. Here, we show that the number of active TB cases in the community is contributed by both newly infected and reinfected after developing TB disease, though TB prevalence might be driven by reinfection force, because the number of reinfected individuals becomes higher than that of newly infected individuals at stability point of a TB epidemic when $\beta \geq 20\ yr^{-1}$. Tables 5.2, 5.3 and 5.4 summarise results in Figures 5.2, 5.3 and 5.4, while Figure 5.5 compares TB cases as the impact of post-treatment immune status.

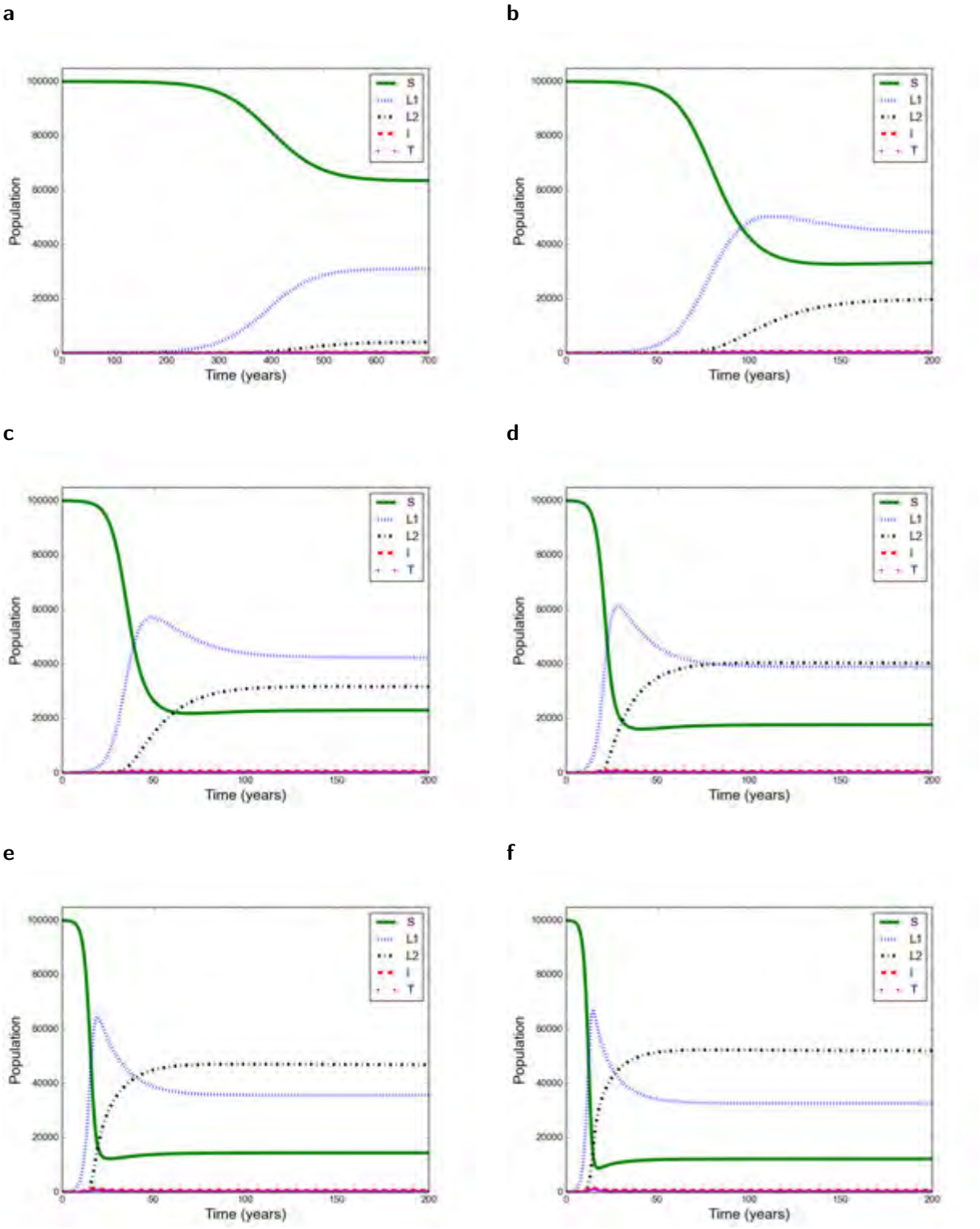

Figure 5.2: Numerical simulation of a mathematical model (Equation (5.2.1)) to explore the impact of effective contact rate when all treated individuals move to a susceptible state. (a) T moving to S when $\beta = 5\ yr^{-1}$. (b) T moving to S when $\beta = 10\ yr^{-1}$. (c) T moving to S when $\beta = 15\ yr^{-1}$. (d) T moving to S when $\beta = 20\ yr^{-1}$. (e) T moving to S when $\beta = 25\ yr^{-1}$. (f) T moving to S when $\beta = 30\ yr^{-1}$. Note: S = susceptible, L_1 = newly infected, L_2 = reinfected, I = active TB, T = treated.

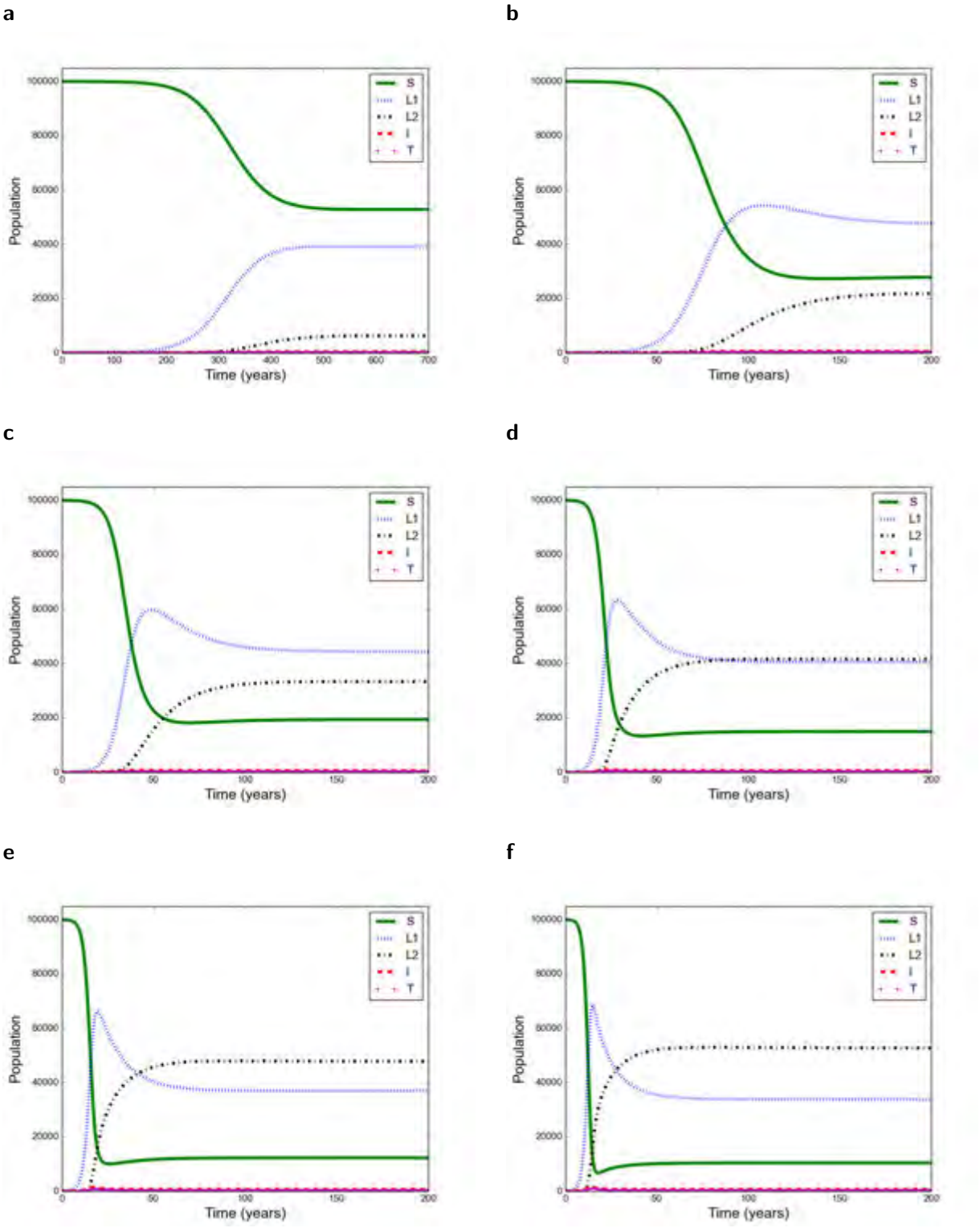

Figure 5.3: Numerical simulation of a mathematical model (Equation (5.2.1)) to explore the impact of effective contact rate when all treated individuals move to a newly infected state. (a) T moving to L_1 when $\beta = 5\ yr^{-1}$. (b) T moving to L_1 when $\beta = 10\ yr^{-1}$. (c) T moving to L_1 when $\beta = 15\ yr^{-1}$. (d) T moving to L_1 when $\beta = 20\ yr^{-1}$. (e) T moving L_1 when $\beta = 25\ yr^{-1}$. (f) T moving to L_1 when $\beta = 30\ yr^{-1}$. Note: S = susceptible, L_1 = newly infected, L_2 = reinfected, I = active TB, T = treated.

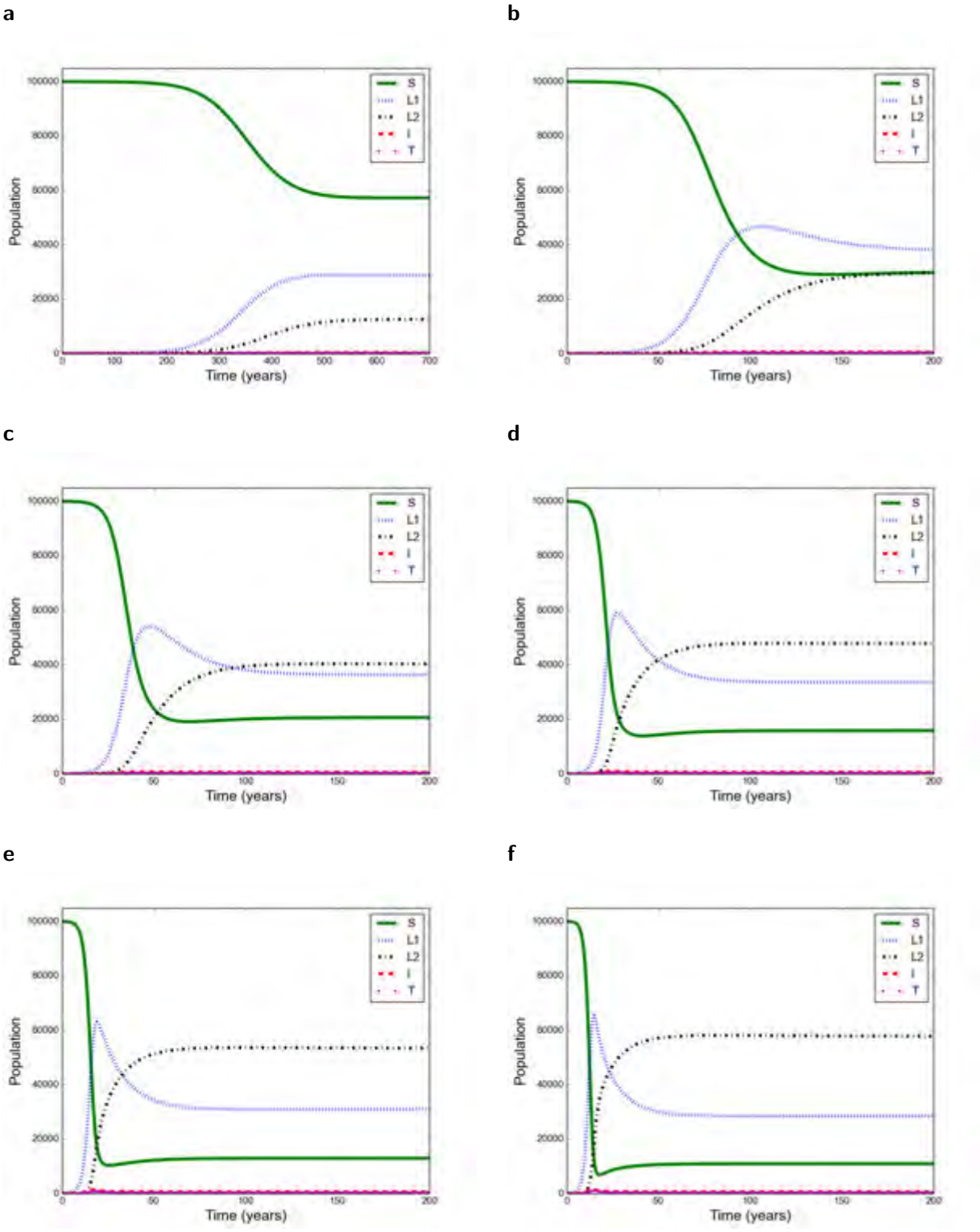

Figure 5.4: Numerical simulation of a mathematical model (Equation (5.2.1)) to explore the impact of effective contact rate when all treated individuals move to a reinfected state.
(a) T moving to L_2 when $\beta = 5\ yr^{-1}$. (b) T moving to L_2 when $\beta = 10\ yr^{-1}$. (c) T moving to L_2 when $\beta = 15\ yr^{-1}$. (d) T moving to L_2 when $\beta = 20\ yr^{-1}$. (e) T moving to L_2 when $\beta = 25\ yr^{-1}$. (f) T moving to L_2 when $\beta = 30\ yr^{-1}$. Note: S = susceptible, L_1 = newly infected, L_2 = reinfected, I = active TB, T = treated.

Table 5.2: Comparison of the number of individuals in all five states at stability point of a TB epidemic, when all treated individuals move to a susceptible state (Figure 5.2).

Effective contact rate	Susceptible	Newly infected	Reinfected	Treated	Active TB
5	62678	29732	2646	212	311
10	32142	43660	19017	330	484
15	21964	41517	30800	357	525
20	16607	37767	39375	371	545
25	13392	34821	45803	379	556
30	11250	31607	50892	382	561

Table 5.3: Comparison of the number of individuals in all five states at stability point of a TB epidemic, when all treated individuals move to a newly infected state (Figure 5.3).

Effective contact rate	Susceptible	Newly infected	Reinfected	Treated	Active TB
5	52232	37767	5089	197	289
10	27053	46607	20625	319	469
15	18482	43392	32142	351	515
20	14196	39375	40714	364	535
25	11250	35625	46607	371	545
30	9642	32946	51428	375	550

Table 5.4: Comparison of the number of individuals in all five states at stability point of a TB epidemic, when all treated individuals move to a reinfected state (Figure 5.4).

Effective contact rate	Susceptible	Newly infected	Reinfected	Treated	Active TB
5	56517	27589	11517	177	260
10	28928	37232	28392	298	438
15	19821	35089	39107	330	484
20	15000	32678	46607	344	505
25	12053	30000	52500	351	515
30	9910	27053	56785	354	520

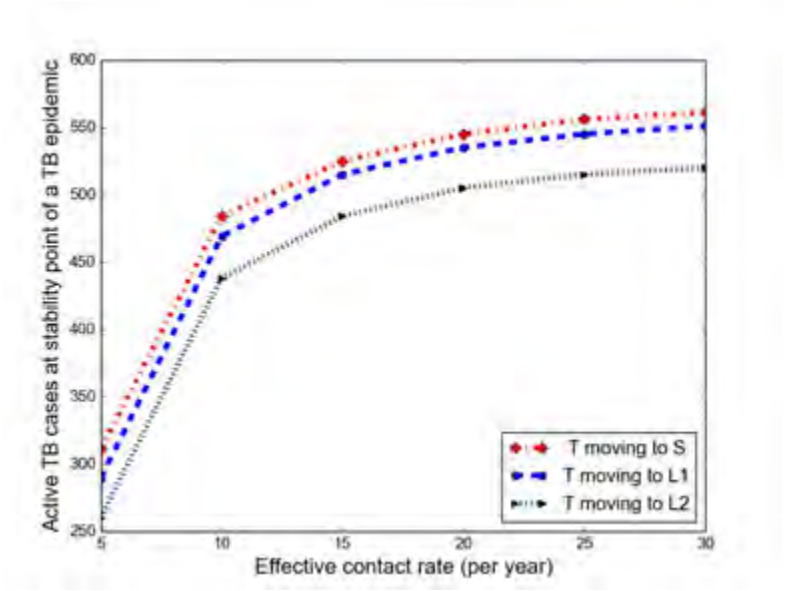

Figure 5.5: Active TB cases when all treated individuals move to either a susceptible, newly infected or reinfected state at stability point of a TB epidemic (Tables 5.2, 5.3 and 5.4).
TB becomes higher when treated individuals become susceptible than moving to either newly infected or reinfected. $S =$ susceptible, $L_1 =$ newly infected, $L_2 =$ reinfected, $T =$ treated.

5.4 Discussion

Using a mathematical model developed in this study, we investigated the impact of effective contact rate and post-treatment immune status on TB epidemiology, with the caveat that this is a simple model assuming a homogeneous population without age stratification and HIV. However, the model has major findings: Susceptible (S), newly infected (L_1), reinfected (L_2), active TB (I), and treated (T) individuals are all affected in a non-linear relationship with effective contact rate. While it is intuitive that the number of susceptible individuals declines with increasing effective contact rate the other states are more complex. When $\beta < 20$ then $L_1 > L_2$ if T move to either S or L_1 and when $\beta \geq 20$ then $L_2 > L_1$. Treatment and active TB rates are also non-linear, if effective contact rate decreases from 30 to 25 yr^{-1} then the decline in TB cases is $5/100,000$ but a reduction of 10 to 5 yr^{-1} produces a decline of $177(range, 173 - 180)/100,000$. This may explain the empiric finding that TB notification rates are relatively insensitive to moderate improvements in case finding in high burden settings. E.g. the Zamstar study and the Word Health Organisation (WHO) observation of very little data on the impact of enhanced case finding in high burdened settings [53]. This is also compatible with the modelling of TB transmission in South African prisons [109]. At high

effective contact rate (i.e., $\beta \geq 20$) there is a high proportion of cases from L_2 rather than L_1. This is compatible with the observation that $20-25\%$ of TB cases are re-treatment cases in high TB burden settings, such as Cape Town. Active TB can decline by 16% when individuals are multiply infected in low transmission settings with effective contact rate of $5\ yr^{-1}$, and 7% in high transmission transmission settings with effective contact rate of $30\ yr^{-1}$ compared to susceptible individuals (Figure 5.5). This implies that post-treatment immunological memory reduces the risk of active disease by $7-16\%$ compared to susceptible individuals.

The early peak values in TB rates demonstrate that there may be temporary peaks followed by apparent improvements in notifications when TB disease is introduced into a new susceptible population e.g. Eskimo epidemics [116]. The time course of TB epidemiology is long, and the status of the post-treatment state is something that prior models have ignored. Loss of protective factor of newly infected following treatment (or prophylaxis which is a form of treatment) could have major negative epidemiological consequences.

The findings in this study suggest that TB prevalence is driven by reinfection force, particularly in high TB burden settings. Though chemotherapy and prior natural MTB infection induce an immune response that reduces TB susceptibility [65], the number of reinfected individuals continues increasing dramatically. The source of reinfection strains is not clearly understood but the increasing number of reinfected individuals might be accelerated by the force of infection due to high effective contact rate and duration of exposure in congregate areas in particular. In conclusion, TB control strategies cannot only depend on medical recovery, extra effort is required, for example, reducing effective contact rates between infectious and susceptible individuals in the community. If post-treatment immune status can be improved by vaccination, it may significantly empower medical treatment.

Chapter 6

Impact of vaccination on TB control

Abstract

Despite the fact that a tuberculosis (TB) vaccine has been implemented globally, TB remains a public health concern that causes morbidity and mortality in the community. Here, we designed an age-structured mathematical model that incorporates vaccination for susceptible individuals (young age groups $[0-5)$ and $[5-15)$ years) to explore the impact of the vaccine on TB control in high TB burden settings, such as Cape Town. In order to explore the impact of the vaccine, the study was divided into two parts: (i) without vaccination and (ii) with vaccination, and we observed TB notification rates in different age groups. We schematically compared TB notification rates in the first case with the observed TB notification rates in Cape Town in 2009 so that to show if TB is decreasing or increasing. We found that in the first case, high rates of active TB were detected for the age groups $[0-5)$, $[15-25)$, $[35-45)$ and $[45-55)$ years with notification rates 592, 546, 531 and 569 per $100,000$ population, respectively. In the second case, when the vaccine was introduced in the population, active TB decreased for the age groups $[0-5)$, $[5-15)$ and $[15-25)$ years by 43.92%, 60.20% and 71.61%, respectively. The lowest TB notification rate was detected in the age group $[5-15)$ years in both cases. However, active TB remains high for the age groups $[25-35)$ to ≥ 75 years in both cases, suggesting that these age groups are at excessively high risk of developing TB disease. Results in the first case show that TB has increased for the age groups $[0-5)$, $[15-25)$, $[25-35)$, $[55-65)$, $[65-75)$ and ≥ 75 years, and decreased for the age groups $[35-45)$ and $[45-55)$ years, compared to the 2009 study. The findings in this study suggest that active disease progression depends on age and average duration of the waning of the vaccine effect.

6.1 Introduction

The Bacille Calmette Guerin (BCG) vaccine has been noted to induce immune protection against tuberculosis (TB) for about $0-80\%$ of individuals [65], whilst other studies demonstrated that vaccinated individuals are $70-80\%$ protected from TB disease [26, 50]. Furthermore, though there is no empirical data about BCG vaccine protection against TB infection, it is assumed that only 77% of the vaccinated individuals might be protected against TB disease [34]. Since they are not 100% protected, vaccinated susceptible individuals may acquire TB infection and develop active disease.

Prior infected individuals have greater defence mechanisms against TB than uninfected ones because the previous *Mycobacterium tuberculosis* (MTB) infection induces an immune response that reduces TB susceptibility [34, 65, 86]. For example, a study conducted in Norway in 1927 on the BCG vaccine, noted that vaccinated-uninfected and prior infected student nurses had a significantly lower risk of acquiring TB than unvaccinated and uninfected individuals [12]. Additionally, a study conducted by Vynnycky and Fine (1997) using an age-structured model and data from England and Wales, demonstrated that natural MTB infection confers a minimum protection of 16% and 41% against TB disease in a respective age group of 15 and over 20 years [34], which is a lower level of protection than that noted in the BCG vaccine $(0-80\%)$ [12, 65]. Furthermore, Andrews *et al* (2012) [91] estimated that the risk of developing active disease for the latently infected is 79% lower than uninfected individuals, implying that the immune protection induced by natural MTB infection is approximately equal to that of the BCG vaccine. The cause of greater diversity of the BCG vaccine and natural MTB induced immunity is not clearly understood, and more research is needed.

Despite the fact that vaccinated and medically recovered individuals acquire immunity that reduces TB susceptibility [86], they can be (re)infected and develop active disease if they become frequently exposed to infectious individuals in confined spaces and inhale airborne infectious particles, which are viable with potential for TB infection and disease. Furthermore, though latently infected individuals acquire immunity that prevents TB progression, they can develop active TB through either endogenous reactivation or exogenous reinfection if they interact with infectious individuals in confined spaces for long periods of exposure [65]. Since more than 60% of children become infected by the age of 16 years, there are only two ways that a vaccine can be useful in adolescents: first, if the vaccines provide superior immunity to natural MTB infection, perhaps through better cross-strain immunity, and second, if immunity conferred by natural MTB infection wanes. Though, natural MTB infection and the BCG vaccine induce an immune response that reduces TB susceptibility, it is not well understood

if the immunity conferred by natural MTB infection wanes, and there is no empirical study comparing the average duration of the waning of the immunity induced by natural MTB infection and that of the BCG vaccine.

Although it is not known if the BCG vaccine confers a superior immune response to natural MTB infection, the frequency of exposure to MTB reduces the efficacy of the BCG vaccine and airborne infectious particles dominate the immunological state of the host when they reach the threshold level [65]. The BCG vaccine improves natural immunity but does not reduce or improve immune response induced by the prior natural MTB infection. However, as mentioned earlier, natural MTB infection reduces BCG vaccine efficacy if vaccinated susceptible individual become frequently exposed to infectious individual(s) [65]. This reflects the fact that BCG vaccine efficacy becomes poor in high TB burden settings due to a high level of reinfection, and TB burden continues, regardless of vaccination. The BCG vaccine is thus more effective in low TB burden settings. The key question is, does the BCG vaccine induce a superior immune response that reduces active TB progression in all age groups?

Here, we use an age-structured mathematical model that incorporates vaccination for susceptible individuals (young age groups $[0-5)$ and $[5-15)$ years) to explore the impact of the vaccine on TB control in high TB burden settings, such as Cape Town. The study was divided into two parts: (i) without vaccination and (ii) with vaccination, and we observed TB notification rates in different age groups. We compared TB notification rates in this study with that observed in Cape Town in 2009 [102] to show if TB is increasing, decreasing or endemic in different age groups.

6.2 Methods

6.2.1 Model description and assumptions

For our study we preferred an age-structured model because, in reality, infection and disease rates vary in different populations depending on age and host immunological factors [34]. In order to explore the impact of the vaccine in different age groups, human immunodeficiency virus (HIV) infection and multi-drug resistant TB (MDR-TB) contributions are not incorporated in the design of the model. In the development of the model, we make an assumption that the BCG vaccine and prior MTB infection have the same protective factor, which reduces TB susceptibility. Furthermore, we assume that susceptible or vaccinated individuals develop active TB after latent TB acquisition, and treatment starts if the test indicates active disease.

The model is comprised of six states of susceptible individuals, $S(a,t)$ who are not yet infected but are at a high risk of acquiring infection; vaccinated individuals, $V(a,t)$ who are partially protected against TB disease; early latent TB, $E(a,t)$ who are primarily infected by MTB and are at high risk of developing TB disease after few years (< 5 years); late latent TB individuals, $L(a,t)$ with latent TB infection who take a long time (≥ 5 years) to develop TB disease through endogenous reactivation or revert to early latent TB through exogenous reinfection; active TB individuals, $I(a,t)$ with active disease who can transmit TB to susceptible individuals; and treated individuals, $T(a,t)$ who are cured by chemotherapy, and others are still on treatment.

6.2.2 Model design and development

Considering a and t as the variables denoting respectively age and time, we design the age-structured model as follows: New born individuals at a rate $\lambda(t)$, attain susceptibility and move to a susceptible state, where they get vaccinated with BCG vaccine at a rate $\theta(a)$. However, the vaccine wanes at a rate $\psi(a)$ after vaccination, let's say after a' years (usually $10-15$ years), and an individual becomes susceptible to TB [36]. In other words, for a vaccinated individual at age a, the vaccine wanes at age $a+a'$ and this individual again becomes susceptible to TB. When susceptible individuals come into contact with infectious individuals with the force of infection (FOI), $\Lambda(t) = \beta I(t)$, they acquire early latent TB, where β is the effective contact rate between infectious and susceptible individuals, and $I(t)$ is the number of infectious individuals. The vaccinated individuals become infected and move to either an early or late latent TB state depending on the infecting pathogen strain and the host acquired immune response. Early latent TB individuals progress to active TB at a rate $k(a)$ within few years after infection (< 5 years), and others move to late latent TB at a rate $\delta(a)$, depending on the host immune response and infecting pathogen strain. Late latent TB individuals move to active TB at a rate $p(a)$ through endogenous reactivation, and some become reinfected and revert to early latent TB. As mentioned earlier, the BCG vaccine and prior MTB infection induce an immune response, which reduces TB susceptibility. Thus, $y(a)(0 < y(a) < 1)$ is the protection by BCG vaccine and $z(a)(0 < z(a) < 1)$ is the protection by natural MTB infection from TB susceptibility. However, the protection factor from the vaccine is assumed to be approximately equal to that of natural MTB infection, such that $y(a) \approx z(a)$ [91]. Active TB individuals detected at a rate $c(a)$ move to a treated state, while some die from active disease at a rate μ_T. Furthermore, some active TB individuals recover naturally at a rate $f(a)$ and move to late latent TB due to immune retention. They are not infectious. Treated and successfully cured individuals may either become susceptible and move to a susceptible state at a rate $d(a)$ if the immune response wanes or become immune if they

retain immunological memory and move to a late latent TB state at a rate $r(a)$. However, due to incomplete treatment, treatment failure or immunological factors, some treated individuals retain infection and revert to active TB at a rate $\omega(a)$. We assume that in each state, there is a natural mortality rate of $\mu(a)$ as demonstrated in Figure 6.1. Note that rates are per year.

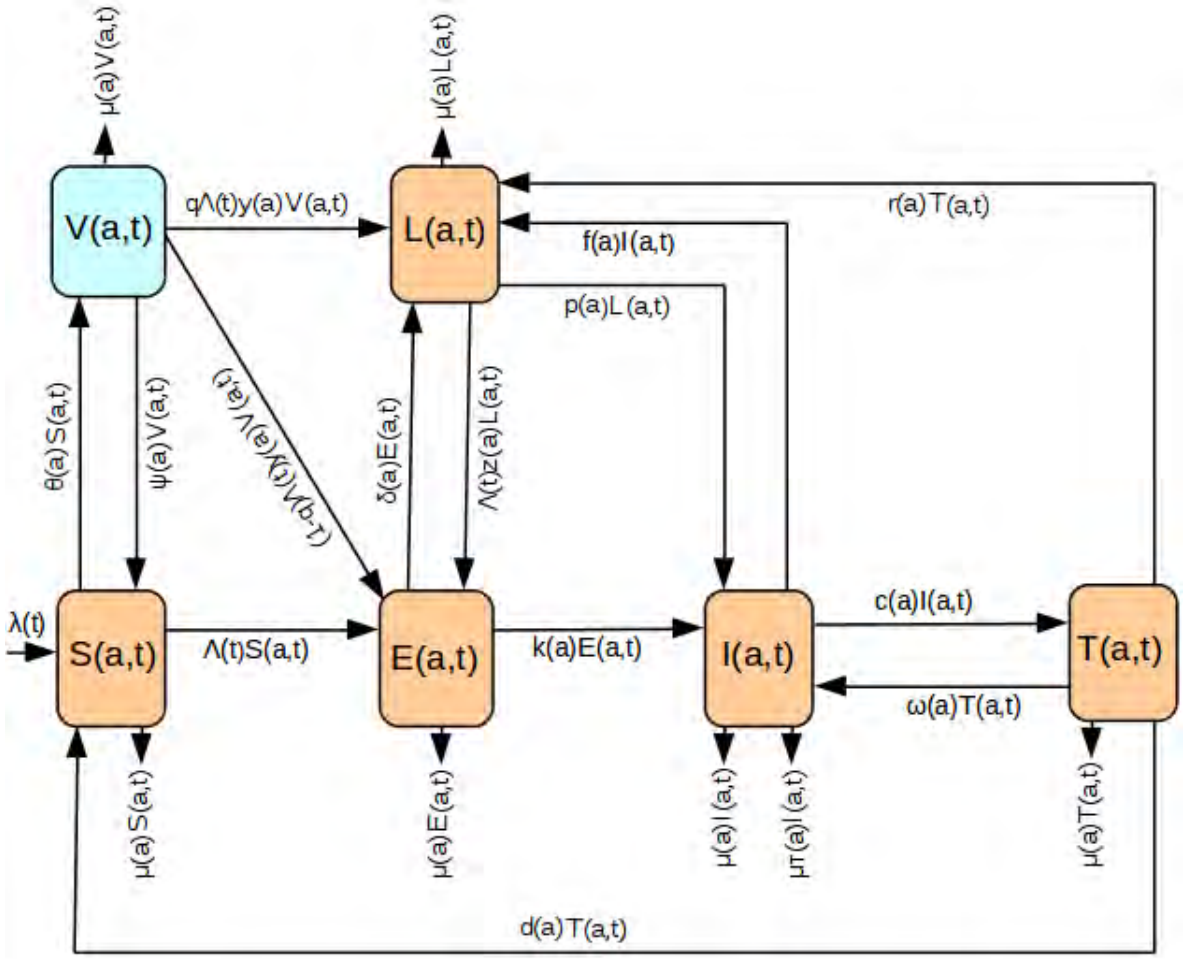

Figure 6.1: Age-structured model that incorporates vaccination, showing TB transmission. $S(a,t) =$ susceptible, $V(a,t) =$ vaccinated, $E(a,t) =$ early latent TB, $L(a,t) =$ late latent TB, $I(a,t) =$ active TB and $T(a,t) =$ treated individuals. Parameters are described in Table 6.1

From the model (Figure 6.1), we developed the mathematical model as follows:

$$\left.\begin{aligned}
\left(\tfrac{\partial}{\partial a}+\tfrac{\partial}{\partial t}\right)S(a,t) &= \lambda(t)-[\Lambda(t)+\theta(a)+\mu(a)]S(a,t)+\psi(a)V(a,t)\\
&\quad +d(a)T(a,t)\\
\left(\tfrac{\partial}{\partial a}+\tfrac{\partial}{\partial t}\right)V(a,t) &= \theta(a)S(a,t)-[\psi(a)+\Lambda(t)y(a)+\mu(a)]V(a,t)\\
\left(\tfrac{\partial}{\partial a}+\tfrac{\partial}{\partial t}\right)E(a,t) &= \Lambda(t)S(a,t)+(1-q)\Lambda(t)y(a)V(a,t)-[k(a)+\delta(a)\\
&\quad +\mu(a)]E(a,t)+\Lambda(t)z(a)L(a,t)\\
\left(\tfrac{\partial}{\partial a}+\tfrac{\partial}{\partial t}\right)L(a,t) &= q\Lambda(t)y(a)V(a,t)+\delta(a)E(a,t)-[\Lambda(t)z(a)+p(a)\\
&\quad +\mu(a)]L(a,t)+f(a)I(a,t)+r(a)T(a,t)\\
\left(\tfrac{\partial}{\partial a}+\tfrac{\partial}{\partial t}\right)I(a,t) &= k(a)E(a,t)-[c(a)+f(a)+\mu(a)+\mu_T(a)]I(a,t)\\
&\quad +p(a)L(a,t)+\omega(a)T(a,t)\\
\left(\tfrac{\partial}{\partial a}+\tfrac{\partial}{\partial t}\right)T(a,t) &= c(a)I(a,t)-[d(a)+\omega(a)+r(a)+\mu(a)]T(a,t)
\end{aligned}\right\} \quad (6.2.1)$$

where $\Lambda(t)=\beta I(t)$, which is the force of infection, β is an effective contact rate and $I(t)$ is the number of infectious individuals at any time t. Other parameters are described in Table 6.1, and corresponding values in Table

Table 6.1: Description of parameters used in Figure 6.1. Parameter values are demonstrated in Table 6.2.

Parameters	Description	Units
$\lambda(t)$	Birth rate at time t	yr^{-1}
β	Effective contact rate between infectious and susceptible individuals	yr^{-1}
$y(a)$	Protective factor due to vaccination	
$z(a)$	Protective factor due to prior natural MTB infection	
$\theta(a)$	Vaccination rate of age a from susceptible to vaccinated state	yr^{-1}
$\psi(a)$	Vaccine waning rate of age a from vaccinated to susceptible state	yr^{-1}
q	Probability of moving from vaccinated to late latent TB state	
$k(a)$	Progression rate of age a from early latent TB to active TB	yr^{-1}
$p(a)$	Endogenous reactivation rate of age a from late latent TB to active TB	yr^{-1}
$r(a)$	Rate of moving from treated to late latent TB state	yr^{-1}
$f(a)$	Rate of natural recovery from active TB	yr^{-1}
$\delta(a)$	Rate of moving from early latent TB to late latent TB as a function of age	yr^{-1}
$c(a)$	Case detection rate of age a from active TB to treated state	yr^{-1}
$\omega(a)$	Rate of treatment failure or relapse from treated to active TB	yr^{-1}
$d(a)$	Rate of moving from treated to susceptible state	yr^{-1}
$\mu(a)$	Natural mortality rate as a function of age	yr^{-1}
$\mu_T(a)$	TB mortality rate as a function of age	yr^{-1}

Table 6.2: Values of parameters described in Table 6.1. These values were estimated from published literature and South African statistics.

	age (years)									
parameters	$[0-5)$	$[5-15)$	$[15-25)$	$[25-35)$	$[35-45)$	$[45-55)$	$[55-65)$	$[65-75)$	≥ 75	reference
λ	0.0189	0	0	0	0	0	0	0	0	[17]
β	20.0	20.0	20.0	20.0	20.0	20.0	20.0	20.0	20.0	estimated
y	0.80	0.80	0.80	0.80	0.79	0.79	0.79	0.79	0.79	[65, 91]
θ	0.713	0.380	0	0	0	0	0	0	0	[36]
ψ	0.06	0.06	0.13	0.13	0.13	0.13	0.20	0.20	0.20	[27]
q	0.1	0.1	0.1	0.1	0.1	0.1	0.1	0.1	0.1	[65]
k	0.240	0.02	0.150	0.150	0.20	0.220	0.20	0.175	0.175	[71]
p	0.0002	0.0002	0.0002	0.0002	0.0002	0.0002	0.0002	0.0002	0.0002	[65]
r	2.0	2.0	2.0	2.0	2.0	2.0	2.0	2.0	2.0	computed
f	0.20	0.20	0.25	0.25	0.25	0.20	0.20	0.15	0.15	[27]
δ	0.2	0.2	0.2	0.2	0.2	0.2	0.2	0.2	0.2	estimated
c	0.61	0.61	0.61	0.61	0.61	0.61	0.61	0.61	0.61	[84]
ω	0.015	0.015	0.01	0.01	0.01	0.015	0.01	0.015	0.015	[63]
d	1.0	1.0	1.0	1.0	1.0	1.0	1.0	1.0	1.0	computed
μ	0.039	0.007	0.024	0.061	0.07	0.069	0.072	0.067	0.058	[18]
μ_T	0.075	0.075	0.075	0.075	0.075	0.075	0.2	0.5	0.5	[84]

Data computation and assumptions: Average duration of infectiousness (ρ) was assumed to be 6 months in all age groups, such that $\rho = 0.5$ yr. Thus, the rates of moving from treated to late latent TB (immune), $r(a)$, and susceptible, $d(a)$, in Table 6.2 were computed as follows: $r(a) = \frac{1}{\rho}$, and $d(a) = r(a)(1-\rho)$. Note: the square bracket indicates that the age is included, while the round bracket means it is not included.

6.2.3 Initial and boundary conditions

Assuming a full susceptible population, we use the boundary conditions as:

$$\frac{dS(0,t)}{dt} = \lambda(t)$$

Thus, at age $a = 0$ and time t, initial conditions are set as follows:

$$S(0,t) = \lambda(t), V(0,t) = E(0,t) = L(0,t) = I(0,t) = T(0,t) = 0$$

This implies that at age 0 and time t, disease free equilibrium is stable without vaccination, infection, active disease and treatment. Thus, the number of births corresponds to the small variation or change in the total number of individuals in the population aged 0 at time t, such

that

$$\frac{dN(0,t)}{dt} = \lambda(t),$$

implying that at age 0 and any time t, the number of susceptible individuals is equal to the total population as:

$$N(0,t) = S(0,t)$$

However, at age a and time $t = 0$, the following initial condition is fulfilled:

$$S(a,0) = S_0(a), V(a,0) = V_0(a), E(a,0) = E_0(a), L(a,0) = L_0(a), I(a,0) = I_0(a), T(a,0) = T_0(a)$$

At age a and time t, disease free equilibrium is unstable and the population is comprised of all six states, such that:

$$N(a,t) = S(a,t) + V(a,t) + E(a,t) + L(a,t) + I(a,t) + T(a,t),$$

implying that at any time t and age a, there are different age groups in the population from different states. Thus, summing up all equations in System (6.2.1), gives:

$$\left(\frac{\partial}{\partial a} + \frac{\partial}{\partial t}\right) N(a,t) = \lambda(t) - \mu(a)N(a,t) - \mu_T(a)I(a,t)$$

If μ_T is very small, such that $\mu_T \to 0$, we obtain:

$$\left(\frac{\partial}{\partial a} + \frac{\partial}{\partial t}\right) N(a,t) = \lambda(t) - \mu(a)N(a,t),$$

showing that the model is epidemiologically balanced.

6.2.4 Finite difference scheme and solution existence

In order to analyse the dynamics and different states of the system (6.2.1), we can explicitly express the time dependent solution, under the assumption that age depends on time, i.e., $a \equiv a(t)$. In this case, given a sufficiently smooth function $S(t, a(t)) \equiv S(t)$, we have:

$$\frac{dS}{dt} = \frac{\partial S}{\partial t}\frac{dt}{dt} + \frac{\partial S}{\partial a}\frac{da}{dt}$$

Letting $\frac{da}{dt} = 1$, we get:

$$\frac{dS}{dt} = \frac{\partial S}{\partial t} + \frac{\partial S}{\partial a}$$

Thus, for the system (6.2.1), the time dependent solution $(S(t),\ V(t),\ E(t),\ L(t),\ I(t),\ T(t))$ satisfies:

$$\left.\begin{aligned}
\tfrac{d}{dt}S(t) &= \lambda(t) - [\Lambda(t) + \theta_a(t) + \mu_a(t)]S(t) + \psi_a(t)V(t) + d_a(t)T(t)\\
\tfrac{d}{dt}V(t) &= \theta_a(t)S(t) - [\psi_a(t) + \Lambda(t)y_a(t) + \mu_a(t)]V(t)\\
\tfrac{d}{dt}E(t) &= \Lambda(t)S(t) + (1-q)\Lambda(t)y_a(t)V(t) - [k_a(t) + \delta_a(t) + \mu_a(t)]E(t)\\
&\quad + \Lambda(t)z_a(t)L(t)\\
\tfrac{d}{dt}L(t) &= q\Lambda(t)y_a(t)V(t) + \delta_a(t)E(t) - [\Lambda(t)z_a(t) + p_a(t) + \mu_a(t)]L(t)\\
&\quad + f_a(t)I(t) + r_a(t)T(t)\\
\tfrac{d}{dt}I(t) &= k_a(t)E(t) + p_a(t)L(t) - [c_a(t) + f_a(t) + \mu_a(t) + \mu_{T_a}(t)]I(t)\\
&\quad + \omega_a(t)T(t)\\
\tfrac{d}{dt}T(t) &= c_a(t)I(t) - [d_a(t) + \omega_a(t) + r_a(t) + \mu_a(t)]T(t)
\end{aligned}\right\} \qquad (6.2.2)$$

with $s_a(t) = s(a)$ for a given parameter $s(a)$ and initial conditions given by $S(0) = S_0(a)$, $V(0) = V_0(a)$, $E(0) = E_0(a)$, $L(0) = L_0(a)$, $I(0) = I_0(a)$ and $T(0) = T_0(a)$. Therefore, from the well known the Picard's existence theorem, the solution exists.

Here, we approximate the solution of the system of the partial differential equations in System (6.2.1) by estimating the partial derivative functions $\frac{\partial S}{\partial t}$ and $\frac{\partial S}{\partial a}$. In System (6.2.1), a and t are two independent variables denoting respectively age and time in a grid of equal intervals such that $\triangle a = \triangle t = h$, where h is a forward step interval and $-h$ indicates the backward step interval. We use Taylor series and apply truncation to form the backward-difference for partial derivatives. We prefer backward-difference rather than forward-difference because it projects the exact age and time in real life. Let us consider a grid as a function of age and time with equal intervals and use Taylor series in backward-difference as follows:

$$S(a-h,t) = S(a,t) - \frac{S'(a,t)h}{1!} + O(h^2), \qquad (6.2.3)$$

which can be written as

$$S(a-h,t) = S(a,t) - S'(a,t)h + O(h^2) \qquad (6.2.4)$$

Solving for $S'(a,t) = \frac{\partial S(a,t)}{\partial a}$ in Equation (6.2.4) and dividing by h both sides, we obtain:

$$\frac{\partial S(a,t)}{\partial a} = \frac{S(a,t) - S(a-h,t)}{h} + O(h) \tag{6.2.5}$$

For an error, $O(h)$ being very small (i.e., $O(h) \approx 0$), Equation (6.2.5) becomes:

$$\frac{\partial S(a,t)}{\partial a} \approx \frac{S(a,t) - S(a-h,t)}{h} \tag{6.2.6}$$

In numerical schemes for solving partial differential equations we assume a grid with discrete value $a_j = jh$ for $j = 1,2,\ldots,M$ and $t_n = nh$ for $n = 1,2,\ldots,N$. Assuming a grid with constant spacing as stated before, we take into account that $a_j - h = a_{j-1}$ and $t_n - h = t_{n-1}$ then Equation (6.2.6) can be expressed as:

$$\begin{aligned} \frac{\partial S(a_j,t_n)}{\partial a} &\approx \frac{S(a_j,t_n) - S(a_j-h,t_n)}{h} \\ &= \frac{S(a_j,t_n) - S(a_{j-1},t_n)}{h} \end{aligned} \tag{6.2.7}$$

using the same procedure and solving for $\frac{\partial S(a,t)}{\partial t}$, we obtain:

$$\begin{aligned} \frac{\partial (a_j,t_n)}{\partial t} &\approx \frac{S(a_j,t_n) - S(a_j,t_n-h)}{h} \\ &= \frac{S(a_j,t_n) - S(a_j,t_{n-1})}{h} \end{aligned} \tag{6.2.8}$$

Summing Equations (6.2.7) and (6.2.8), we obtain:

$$\begin{aligned} \left(\frac{\partial}{\partial a} + \frac{\partial}{\partial t}\right) S(a_j,t_n) &\approx \frac{S(a_j,t_n) - S(a_{j-1},t_n) + S(a_j,t_n) - S(a_j,t_{n-1})}{h} \\ &= \frac{2S(a_j,t_n) - \left[S(a_{j-1},t_n) + S(a_j,t_{n-1})\right]}{h} \end{aligned} \tag{6.2.9}$$

Thus, using discrete notation, such that $S(a_j,t_n) = S_j^n$, Equation (6.2.9) becomes:

$$\left(\frac{\partial}{\partial a} + \frac{\partial}{\partial t}\right) S(a_j,t_n) = \frac{2S_j^n - \left(S_{j-1}^n + S_j^{n-1}\right)}{h} \tag{6.2.10}$$

We can now design a numerical scheme to approximate the solution of System (6.2.1) of partial differential equations or better the initial boundary value of System (6.2.1). This scheme consists of solving the following system of linear equations:

$$\left.\begin{array}{l}
\frac{2S_j^n-\left(S_{j-1}^n+S_j^{n-1}\right)}{h}=\lambda^n-(\Lambda^n+\theta_j+\mu_j)S_j^n+\psi_jV_j^n+d_jT_j^n\\
\frac{2V_j^n-\left(V_{j-1}^n+V_j^{n-1}\right)}{h}=\theta_jS_j^n-(\psi_j+\Lambda^ny_j+\mu_j)V_j^n\\
\frac{2E_j^n-\left(E_{j-1}^n+E_j^{n-1}\right)}{h}=\Lambda^nS_j^n+(1-q)\Lambda^ny_jV_j^n-(k_j+\delta_j+\mu_j)E_j^n+\Lambda^nz_jL_j^n\\
\frac{2L_j^n-\left(L_{j-1}^n+L_j^{n-1}\right)}{h}=q\Lambda^ny_jV_j^n+\delta_jE_j^n-(\Lambda^nz_j+p_j+\mu_j)L_j^n+f_jI_j^n+r_jT_j^n\\
\frac{2I_j^n-\left(I_{j-1}^n+I_j^{n-1}\right)}{h}=k_jE_j^n+p_jL_j^n-(c_j+f_j+\mu_j+\mu_{Tj})I_j^n+\omega_jT_j^n\\
\frac{2T_j^n-\left(T_{j-1}^n+T_j^{n-1}\right)}{h}=c_jI_j^n-(d_j+\omega_j+r_j+\mu_j)T_j^n
\end{array}\right\} \quad (6.2.11)$$

Multiplying by h both sides in System (6.2.11) and simplify further by making the previous known initial condition the subject at right hand side, we obtain:

$$\left.\begin{array}{l}
(2+h(\Lambda^n+\theta_j+\mu_j))S_j^n-h(\psi_jV_j^n+d_jT_j^n)=h\lambda^n+S_{j-1}^n+S_j^{n-1}\\
(2+h(\psi_j+\Lambda^ny_j+\mu_j))V_j^n-h\theta_jS_j^n=V_{j-1}^n+V_j^{n-1}\\
(2+h(k_j+\delta_j+\mu_j))E_j^n-h(\Lambda^nS_j^n+(1-q)\Lambda^ny_jV_j^n+\Lambda^nz_jL_j^n)=E_{j-1}^n+E_j^{n-1}\\
(2+h(p_j+\Lambda^nz_j+\mu_j))L_j^n-h(q\Lambda^ny_jV_j^n+\delta_jE_j^n+f_jI_j^n+r_jT_j^n)=L_{j-1}^n+L_j^{n-1}\\
(2+h(c_j+f_j+\mu_j+\mu_{Tj}))I_j^n-h(k_jE_j^n+p_jL_j^n+\omega_jT_j^n)=I_{j-1}^n+I_j^{n-1}\\
(2+h(d_j+\omega_j+r_j+\mu_j))T_j^n-hc_jI_j^n=T_{j-1}^n+T_j^{n-1}
\end{array}\right\} \quad (6.2.12)$$

System (6.2.12), is a system of linear equations written in matrix form as

$$Ax=b \quad (6.2.13)$$

where A is a coefficient matrix, x is the variable matrix and b is a vector in System (6.2.12).

Hence, System (6.2.12) can be written in matrix form as follows:

$$\begin{pmatrix}
G & -h\psi_j & 0 & 0 & 0 & -hd_j\\
-h\theta_j & K & 0 & 0 & 0 & 0\\
-h\Lambda^n & h(q-1)\Lambda^ny_j & M & -h\Lambda^nz_j & 0 & 0\\
0 & -hq\Lambda^ny_j & -h\delta_j & Q & -hf_j & -hr_j\\
0 & 0 & -hk_j & -hp_j & R & -h\omega_j\\
0 & 0 & 0 & 0 & -hc_j & W
\end{pmatrix}
\begin{pmatrix}S_j^n\\V_j^n\\E_j^n\\L_j^n\\I_j^n\\T_j^n\end{pmatrix}=
\begin{pmatrix}h\lambda^n+S_{j-1}^n+S_j^{n-1}\\V_{j-1}^n+V_j^{n-1}\\E_{j-1}^n+E_j^{n-1}\\L_{j-1}^n+L_j^{n-1}\\I_{j-1}^n+I_j^{n-1}\\T_{j-1}^n+T_j^{n-1}\end{pmatrix} \quad (6.2.14)$$

where $G=2+h(\Lambda^n+\theta_j+\mu_j)$, $K=2+h(\psi_j+\Lambda^ny_j+\mu_j)$, $M=2+h(k_j+\delta_j+\mu_j)$, $Q=2+h(\Lambda^nz_j+p_j+\mu_j)$, $R=2+h(c_j+f_j+\mu_j+\mu_T)$ and $W=2+h(d_j+\omega_j+r_j+\mu_j)$.

System (6.2.14) can be solved using any known solver of systems of linear equations. Thus, using a Python package by applying data in Table 6.2 into System (6.2.14), we explored the impact of vaccination on TB control numerically as discussed in Section 6.3. In our simulation, we used step interval, $h = 0.05$.

6.3 Simulation results

We simulated the model numerically, while taking into consideration that each age group has its own parameters, which monitor TB dynamics. Furthermore, we consider that all age groups show an increasing TB notification rates over time. We therefore discretised the model to match the data and simplified it further into matrix form (Equation (6.2.14)) for easier coding and numerical simulation. Applying data estimated from published literature and computed values by matching infection and incidence data in South Africa (Table 6.2) in Equation (6.2.14), we simulated $100,000$ fully susceptible individuals in two different ways: (i) without vaccination (i.e., $\theta = 0$ for all age groups) and (ii) with vaccination (i.e., $\theta \neq 0$ for the age groups $[0-5)$ and $[5-15)$ years). We schematically compared TB notification rates in this study with the observed TB notification rates in Cape Town in 2009 [102] to determine whether TB is decreasing, increasing or endemic in different age groups.

The model detected TB notification rates in different age groups with different peaks in both cases (Figures 6.2a and 6.3a). In the first case (without vaccination), the highest TB notification rate peaked for the age group $[0-5)$ years with notification rate 592 per $100,000$ population because of immature immunity and higher TB progression rate than any other group. The second peak was observed for the age group $[45-55)$ years with notification rate 569 per $100,000$ population, followed by age groups $[15-25)$, $[25-35)$ and $[35-45)$ years with notification rates 546, 454 and 531 per $100,000$ population, respectively (Figure 6.2a). Comparing TB notification rates in the first part in this study with that observed in the 2009 study, we found that the shapes of the produced models in the two studies are the same, and TB notification rates are the same in the age group $[15-25)$ years. However, in this study, we noted higher TB notification rates for the age groups $[0-5)$, $[5-15)$ and $[25-35)$ years, and lower TB notification rates for the age groups $[35-45)$ and $[45-55)$ years than that reported in the 2009 study. Furthermore, we noted the difference in the two studies for the age groups $[55-65)$ to ≥ 75 years, where the 2009 study observed the decline of TB notification rates in these age groups, while the findings in this study show that TB notification rates remain high, probably because of different immunological memories and mortality rates in the two studies. On the other hand, the findings in this study suggest that TB has increased for the age groups

$[0-5)$, $[15-25)$, $[25-35)$, $[55-65)$, $[65-75)$ and ≥ 75 years, and decreased for the age groups $[35-45)$ and $[45-55)$ years, compared to the 2009 study (Figure 6.2b). This implies that TB mortality rate might be higher for some age groups in the 2009 study than the current study, probably because of treatment improvement. Furthermore, TB notification rates seem to be low in the 2009 for young age groups (age groups $[0-5)$ and $[5-15)$ years) because of vaccination impact compared to the model prediction in the first part in this study.

In the second case, when the vaccine was introduced in the population, active TB decreased for the age groups $[0-5)$ years by 43.92% (from 592 to 332), $[5-15)$ years by 60.20% (from 108 to 43) and $[15-25)$ years by 71.61% (from 546 to 155 per $100,000$ population) compared to non-vaccination prediction. However, regardless of vaccination, active TB remains remarkably high for the age groups $[25-35)$, $[35-45)$, $[45-55)$, $[55-65)$, $[65-75)$ and ≥ 75 years with notification rates 454, 531, 569, 471, 352 and 369 per $100,000$ population, respectively (Figure 6.3a), implying that the current vaccine may not have an impact on these age groups. Furthermore, these age groups are at excessively high risk of developing TB disease, probably because of the short average duration of the vaccine efficacy and some immunological factors. Comparing TB notification rates in the second part in this study with that observed in the 2009 study, we show that the model predicted lower TB notification rates for the age groups $[0-5)$, $[5-15)$ and $[15-25)$ years than the 2009 study (Figure 6.3b). We noted that TB notification rates for other age groups remain the same as predicted in the first part in this study.

We noted remarkably low TB notification rate in the age group $[5-15)$ years in both cases (with a notification rate of 108 if not vaccinated and 43 per $100,000$ population if vaccinated). However, low TB progression rate in this age group is not well understood, perhaps it is because of an active immune response that may fight against infectious particles. Furthermore, though there is no molecular empirical evidence, natural immunity and acquired immunity (from either the vaccine or MTB infection) may be stronger in this age group than any other age group. We noted lower active TB notification rate for old age groups $[65-75)$ and ≥ 75 years (with notification rates 352 and 369 per $100,000$ population, respectively) than productive age groups (Figures 6.2a and 6.2b). This is probably because effective contact rate and interactions, which are directly correlated with the force of infection are higher in productive age groups than in old age. Since TB cannot exist if individuals die, TB seems to be higher in young age groups than old age because of higher mortality rate in old age than young age groups. Furthermore, since MTB induce an immune response that reduces TB progression, old age group might have higher protection against active disease due to multiple infection than young age groups.

a

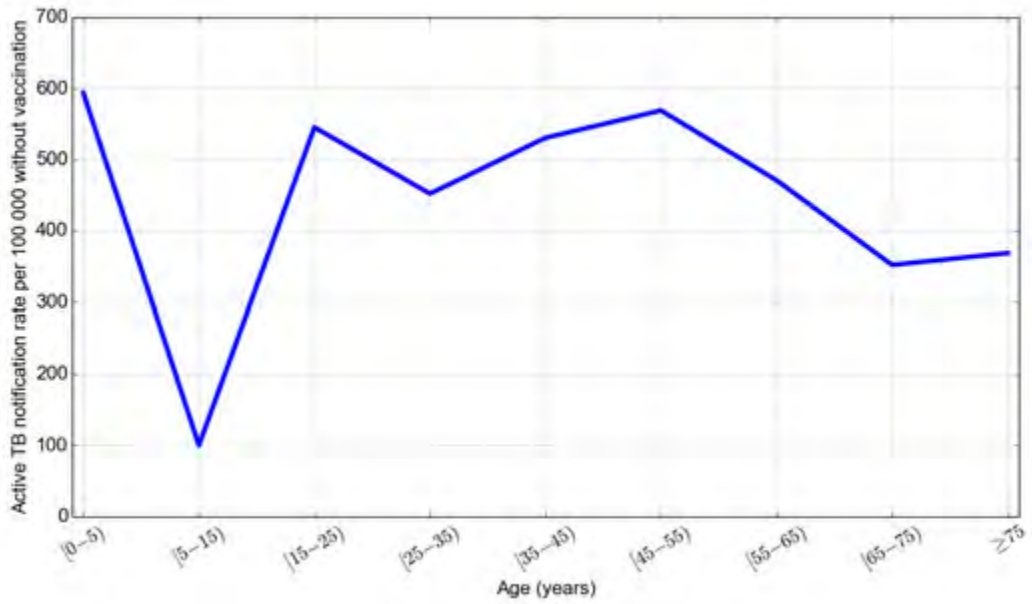

b

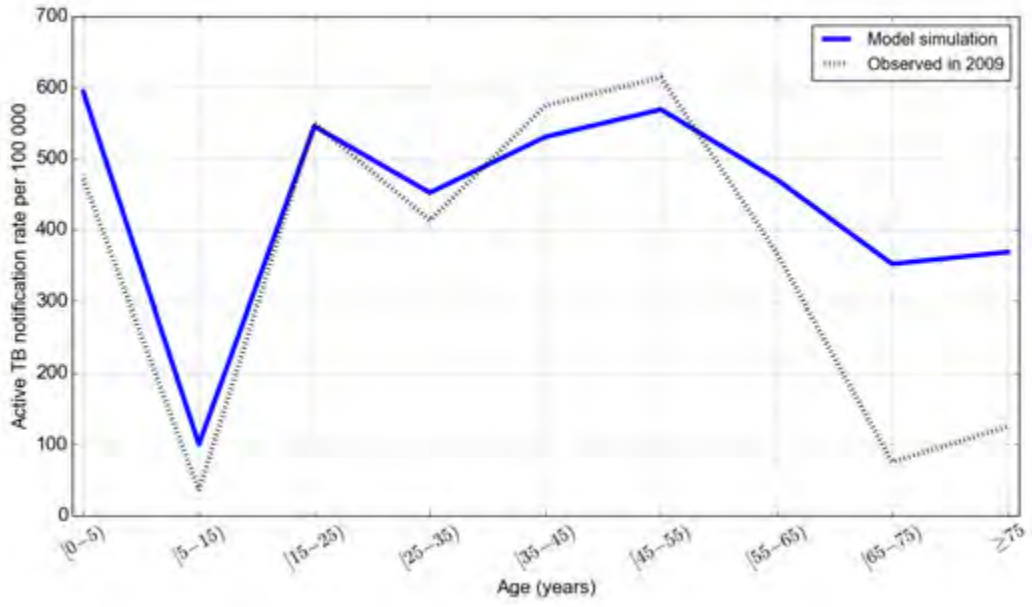

Figure 6.2: Model prediction TB notification rates without vaccination and the 2009 study. (a) Active TB notification rate per $100,000$ population without vaccination. (b) Comparison of TB notification rates observed in this study (model simulation without vaccination) and that observed in Cape Town in 2009.

a

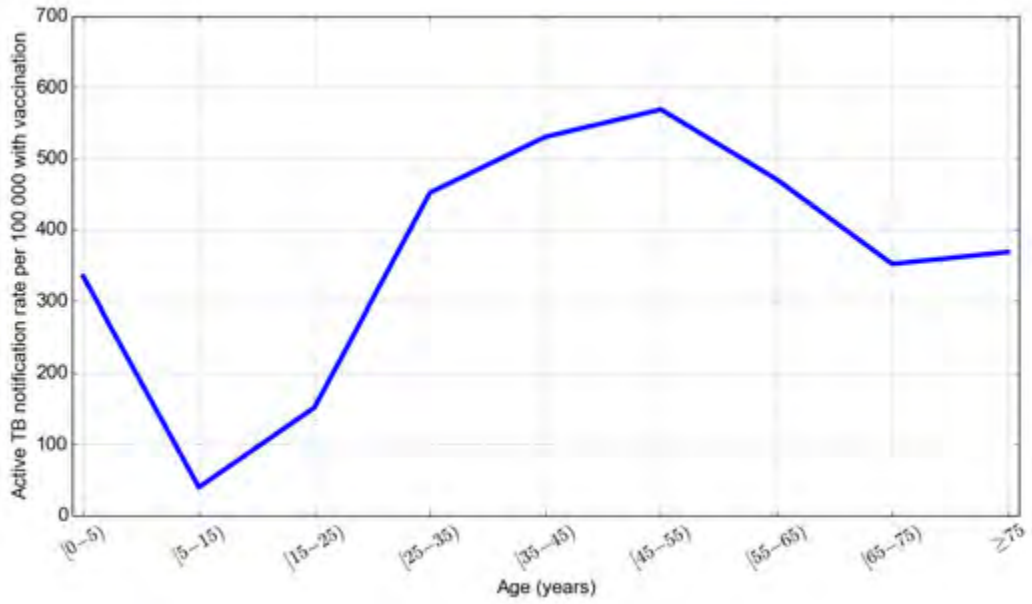

b

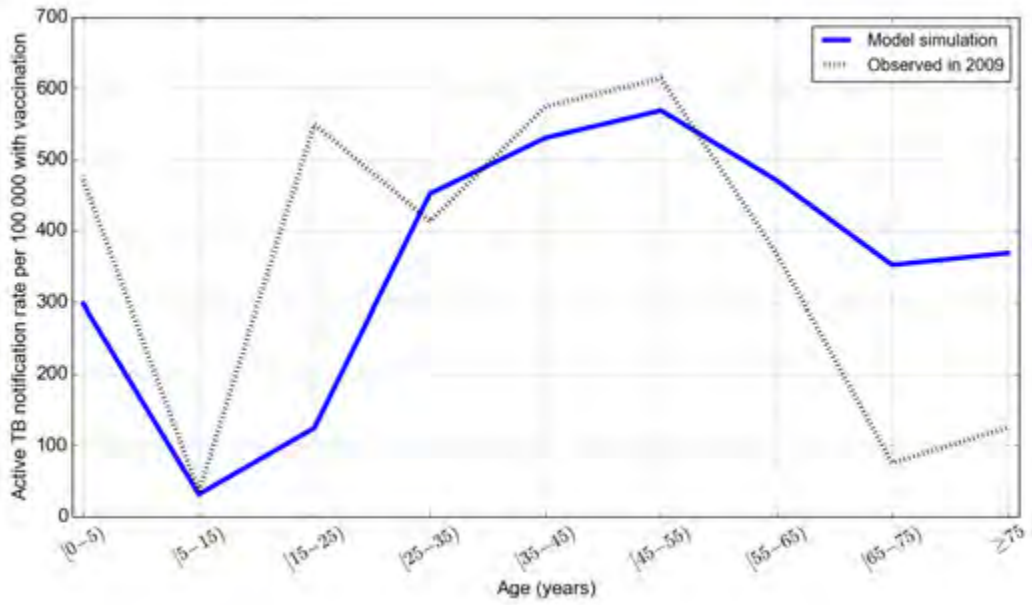

Figure 6.3: Model prediction TB notification rates with vaccination and the 2009 study. (a) Active TB notification rate per $100,000$ population with vaccination for the age groups $[0-5)$ and $[5-15)$ years. (b) Comparison of TB notification rates observed in this study (model simulation with vaccination) and that observed in Cape Town in 2009.

6.4 Discussion

We performed sensitivity analysis for all parameters of the model to explore factors influencing TB progression in different age groups. Since TB infection and disease progression depends on age and immunological memory status, our sensitivity analysis focused on TB progression rates and immune response induced by natural MTB infection and BCG vaccine.

Using an age-structured mathematical model developed in this study, we explored the impact of the vaccine on TB control in different age groups. Our findings suggest that active disease progression is different in different age groups. It is unclear what causes diversity of disease progression in different age groups, though immunity and average duration of the waning of the vaccine might be among the contributing factors. Since the BCG vaccine wanes after a limited range of years and individuals become susceptible to TB, it is plausible that a large number of TB cases among adults might be attributable to reinfection and reactivation [34, 65].

Since MTB hampers the effort of TB control, particularly in high TB burden settings by reducing the efficacy of the vaccine, the complement way is earlier diagnosis of TB cases in the community and treatment. However, due to poor diagnostic tools, which may give false-negative or positive results, in developing countries in particular, the most efficient form of control is the implementation of an efficacious TB vaccine, which combats MTB infection and prevents TB disease. Though the BCG vaccine and prior natural MTB infection confer almost the same immune protection against TB, the average duration of the waning of natural MTB induced immunity is not well understood, which makes the situation uncertain. Latently infected individuals are at higher risk of developing active disease through either endogenous reactivation or exogenous reinfection than vaccinated individuals. Thus, latently infected individuals should be vaccinated, especially in high TB burden settings.

Here, we show that TB progression is age dependent, perhaps because the strength of immunity and waning of the vaccine's efficacy are age dependent. To have a greater impact on TB control and achieve the WHO target of eliminating TB [80], the new vaccine should target age groups at high risk of TB infection and disease progression. Furthermore, in the control of endogenous reactivation in productive age, the average duration of the waning of the vaccine efficacy should be longer than that of the current vaccines. The findings in this study show that the current TB vaccine reduces disease progression in specific targeted age groups, but it does not control active disease progression 100%. This reiterates the need for early identification and treatment of TB cases to avoid new cases. We suggest that the new vaccine should be applicable for all age groups, while targeting age groups at high risk of disease progression for TB control.

Chapter 7

Conclusions

Tuberculosis (TB) incidence is still increasing worldwide, regardless of numerous TB interventions applied in different locations. Because of the high concentration of exhaled breath some of which is derived from infective sources, TB transmission in congregate locations, including households, schools, public transport, prisons and health care settings is remarkably high [32, 100, 109], especially in developing countries where poverty and HIV infection act as driving forces. The main reservoir of TB strains is not well understood but susceptible individuals usually become infected in these locations when they interact with infectious individuals and inhale airborne infectious particles for a prolonged period of exposure. Since unidentified TB cases and multi-drug resistant individuals expectorate massive numbers of airborne infectious particles, they are assumed to be one of the TB transmitting sources in the community.

Exhaled air contains a mixture of nitrogen, oxygen, carbon dioxide and water vapor. Carbon dioxide excretion as a surrogate for exhaled air is directly related to the oxygen consumption required for metabolic activity. The ratio of exhaled carbon dioxide to the oxygen consumption is defined by the respiratory quotient which is somewhat diet dependent but relatively constant at a value of 0.83 [7, 46]. The concentration of exhaled carbon dioxide is determined by the respiratory rate, which for an adult at rest is $8-10$ liters per minute. Therefore, for a normal adult at rest the carbon dioxide exhaled is $8-10$ liters of 4% $(40{,}000$ ppm) [7, 46]. Here, using carbon dioxide as a surrogate for exhaled air, we modified the Wells-Riley and the prior modified Wells-Riley models and obtained a more flexible mathematical model that predicts the risks of airborne infectious diseases, such as TB in multiple environments. We used this mathematical model to demonstrate TB transmission in some congregate settings, such as schools and prisons. Furthermore, we applied the model to guinea pig experimental data from previous *in vivo* studies to predict the probability of exposed guinea pigs acquiring infection in

these studies and quantified the number of infective organisms required to reach the alveolar to induce infection [67]. We believe that this is the first study to date to modify both the Wells-Riley and prior modified well-Riley models, and to apply the resulting model to the prediction of TB transmission and quantification of the number of infective organisms required to induce infection.

In contrast to the prior studies, including guinea pig experiment reports by Wells-Riley and others, we noted that susceptible individuals are not usually infected by a single airborne infectious particle [66]. This shows that TB infection is a somewhat complex scenario that incorporates respiratory deposition fraction, which determines the threshold level of airborne infectious particles needed at the host infective site. In other words, respiratory deposition fraction is correlated with airborne infectious particles, such that susceptible individuals usually become infected if surviving airborne infectious particles reach a threshold level to reach the relevant site and dominate the immunological state of the host [66].

Most studies show that ventilation plays a key role in the prevention of TB transmission but they don't quantify a specific value of air change per hour in each location or other dependent factors. To our knowledge, ventilation depends on various factors, including location, window(s) size, weather conditions, number of occupants and their physical activities in the given space. We believe that if these factors can be addressed and specific values of air change per hour can be quantified in each location, then improved ventilation can be among the best interventions for TB control. Furthermore, though some protective respirators have been used in some health care settings, their face-seal leakage, which is not specified hampers TB control efforts. Since HEPA filters are somewhat expensive, this means that the most affordable respirators are ineffective for TB control, which is why TB transmission is remarkably high in health care settings and other congregated areas.

Using a compartmental model developed in this study, we investigated the population impact of effective contact rate (β) and post-treatment on TB epidemiology. An infectious individual with varying effective contact rate (ranging from 5 to $30\ yr^{-1}$) was introduced among $100,000$ fully susceptible individuals and we observed the number of individuals in all five states at stability point of a TB epidemic. We found that the number of newly infected cases increases when $\beta = 5$ to $\beta = 10\ yr^{-1}$ then decreases with increasing effective contact rate, while that of reinfected individuals increases with increasing effective contact rate, implying that a large number of active TB cases might be repeatedly exposed individuals. We noted that the number of active TB becomes higher when all treated individuals move to a susceptible state than when they move to either a newly infected or reinfected state, probably because of immunological factors. The study shows that post-treatment immunological memory reduces the risk of TB

disease by $7-16\%$ compared to susceptible individuals. Using an age-structured model we developed that incorporates vaccination, we examined the impact of the vaccine on TB control in high TB burden settings, such as Cape Town. The model detected TB notification rates in different age groups with different peaks. We noted that the vaccine reduces TB progression for the age groups $[0-5)$ to $[15-25)$ years, and TB remains remarkably high for other age groups. This implies that TB progression depends on age and average duration of the waning of the efficacy of the vaccine.

In this study, we managed to explore TB transmission in the above outlined locations, showing that TB remains high in congregate settings. However, because of limited time, we didn't manage to visit other congregated areas, such as refugee camps and mining industries where TB prevalence might be remarkably high because of high population density, interaction, poor infrastructure, unidentified TB cases and TB co-infection with HIV. In our future work, we shall visit these locations and quantify environmental, biological and socio-economic factors correlated with TB prevalence and highlight preventive measures for TB control. Furthermore, we shall design and develop an age-structured mathematical model that incorporates TB and HIV co-infection for further investigation about TB transmission in high TB burden settings.

Rebreathed air volume from infectious individuals is an important factor that contributes to TB transmission in a community [100, 113]. The quantity of rebreathed air volume inhaled from others in enclosed spaces, such as prisons, health care settings and work places is remarkably high, which accelerates the fuel of airborne infectious diseases. Effective contact number is directly correlated with rebreathed air volume and has non-linear relationship with the period of infectiousness. Furthermore, airborne infectious particles viable with potential for TB infection have a complex relationship with the period of infectiousness and rebrethed air volume. The effective contact number and airborne infectious particles seem to have unidentified boundary values, which maintain a TB epidemic. In our future work, we shall use the derived equations in this study with addition of others to further identify and define boundary conditions required to maintain a TB epidemic within specific communities. The boundary conditions may be defined as the number of secondary cases infected by an index case in order to maintain a TB epidemic. The boundary conditions will vary by age and also between susceptible and previously infected individuals. The aim of this future work is to bring a TB epidemic under control by decreasing TB transmission in a community. Furthermore, the determination of boundary conditions required to maintain a TB epidemic will enable quantification of the targeted values of drivers of transmission, which will be required to break community transmission.

References

[1] Flugge C. (1897). Ueber luftinfection. Medical Microbiology and Immunology 25(1): 179-224.

[2] Myers J. A. (1930). The prevention of tuberculosis among nurses. The American Journal of Nursing 1361-1372.

[3] Wells W. F. (1955). Airborne contagion and air hygiene. an ecological study of droplet infections. Airborne Contagion and Air Hygiene. An Ecological Study of Droplet Infections.

[4] Sepkowitz K. A. (1994). Tuberculosis and the health care worker: a historical perspective. Annals of Internal Medicine 120(1): 71-79.

[5] Iseman M. D. (1995). Invited commentary on aerial dissemination of pulmonary tuberculosis. a two-year study of contagion in a tuberculosis ward. American Journal of Epidemiology 142(1): 1-2.

[6] Vesley D. L. (1995). Respiratory protection devices. American Journal of Infection Control 23(2): 165-168.

[7] Persily A. K. (1997). Evaluating building iaq and ventilation with indoor carbon dioxide. Transactions-American Society of Health Refrigerating and Air Conditioning Engineers 103: 193-204.

[8] Daniel T. M. (1998). The earliest history of tuberculosis in central-east africa: Insights from clinical records of the first twenty years of mango hospital and review of the relevant literature. Int J Tuberc Lung Dis 2: 1-7.

[9] Kendig N. (1998). Tuberculosis control in prisons [the eddie o'brien lecture]. The International Journal of Tuberculosis and Lung Disease 2(9s1): S57-S63.

[10] Nardell E. A. (1999). Air sampling for tuberculosis-homage to the lowly guinea pig. Chest 116(4): 1143-1145.

[11] Rieder H. L. (1999). Socialization patterns are key to the transmission dynamics of tuberculosis. Int J Tuberc Lung Dis 3(3): 177-178.

[12] Rieder H. L. (1999). *Epidemiological Basis of Tuberculosis Control (No. Ed. 1, pp. 1-162)*. International Union Against Tuberculosis and Lung Disease (IUATLD).

[13] Daniel T. M. (2004). The impact of tuberculosis on civilization. Infectious Disease Clinics of North America 18(1): 157-165.

[14] World Health Organization 2008. New laboratory diagnostic tools for tuberculosis control. Available at URL: http://www.who.int/tdr/publications/documents/diagnostic-tool-tb.pdf.

[15] Noeske J. (2012). TB control in prisons. INTECH open access publisher. Available at URL: http://www.intechopen.com/books/public-health-social-and-behavioral-health/tuberculosis-control-in-prisons.

[16] Braakhuis H. M. (2014). Particle deposition by size in human lung: Total, extrathoracic, tracheobronchial and alveolar. Particle and Fibre Toxicology 11(18): 1-125.

[17] South Africa Demographics Profile 2014. Available at url: http://www.indexmundi.com/south-africa/demographics-profile.html. Accessed: 20th June 2015.

[18] Statistics South Africa (2014). Mortality and causes of death in south africa, 2013: Findings from death notification. Statistics South Africa, Private Bag X44, Pretoria 0001.

[19] Fletcher H. A. and Schrager L. (2016). Tb vaccine development and the end tb strategy: importance and current status. Transactions of the Royal Society of Tropical Medicine and Hygiene 110(4):212-218. doi:10.1093/trstmh/trw016.

[20] Khan E. A. and Starke J. R. (1995). Diagnosis of tuberculosis in children: Increased need for better methods. Emerging Infectious Diseases 1(4): 115.

[21] Nardell E. A., Keegan J., Cheney S. A., and Etkind S. C. (1991). Airborne infection: theoretical limits of protection achievable by building ventilation. Am Rev Respir Dis 144: 302-306.

[22] Sanchez M. A. and Blower S. M. (1997). Uncertainty and sensitivity analysis of the basic reproductive rate: Tuberculosis as an example. American Journal of Epidemiology 145(12): 1127-1137.

[23] Asgharian B., Hofmann W., and Bergmann R. (2001). Particle deposition in a multiple-path model of the human lung. Aerosol Science and Technology 34(4): 332-339.

[24] Beggs C. B., Noakes C. J., Sleigh P. A., Fletcher L. A., and Siddiqi K. (2003). The transmission of tuberculosis in confined spaces: an analytical review of alternative epidemiological models. Int J. Tuberc Lung Dis 7(11): 1015–1026.

[25] Sereno A. B., Soares E. C. C., Lapa e Silva J. R., Nápoles A. M., Bialous S. A., Costa e Silva V. L. D., and Novotny T. E. (2012). Feasibility study of a smoking cessation intervention in directly observed therapy short-course tuberculosis treatment clinics in rio de janeiro, brazil. Revista Panamericana de Salud Pública 32(6): 451-456.

[26] Castillo-Chavez C. and Feng Z. (1998). Global stability of an age-structure model for TB and its applications to optimal vaccination strategies. Mathematical Biosciences 151(2): 135-154.

[27] Dye C., Gamett G. P., Sleeman K., and Williams B. G. (1998). Prospects for global tuberculosis control under the who dots strategy. Distr: General WHO/TB 98.251.

[28] Lawn S. D., Myer L., Edwards D., Bekker L. G., and Wood R. (2009). Short-term and long-term risk of tuberculosis associated with cd4 cell recovery during antiretroviral therapy in south africa. AIDS 23:1717-25.

[29] Lawn S. D., Bekker L. G., Middelkoop K., Myer L., and Wood R. (2006). Impact of HIV infection if epidemiology of tuberculosis in a peri-urban community in south africa: the need for age specific interventions. Clin Infect Dis 42: 1040-1047.

[30] Mohan D., Chopra A., and Sethi H. (2002). The co-occurrence of tobacco and alcohol in general population of metropolis delhi. The Indian Journal of Medical Research 116: 150-154.

[31] Van den Driessche P. and Watmough J. (2002). Reproduction numbers and sub-threshold endemic equilibria for compartmental models of disease transmission. Mathematical Biosciences 180(1): 29-48.

[32] Augustynowicz-Kopeć E., Jagielski T., Kozińska M., Kremer K., van Soolingen D., Bielecki J., and Zwolska Z. (2012). Transmission of tuberculosis within family-households. Journal of Infection 64(6): 596-608.

[33] Brooks-Pollock E., Cohen T., and Murray M. (2010). The impact of realistic age structure in simple models of tuberculosis transmission. Plos One 5(1): e8479.

[34] Vynnycky E. and Fine P. E. M. (1997). The natural history of tuberculosis: the implications of age-dependent risks of disease and the role of reinfection. Epidemiol. Infect 119: 183-201.

[35] Paul J. Edelson and Phypers M. (2010). TB transmission on public transportation: A review of published studies and recommendations for contact tracing. Travel Medicine and Infectious Disease 9: 27e31.

[36] Nyabadza F. and Winkler D. (2013). A simulation age-specific tuberculosis model for the cape town metropole. South African Journal of Science 109(910): 1-7.

[37] Talay F., Kumbetli Ş., and Dispensary E. T. (2008). Risk factors affecting the development of tuberculosis infection and disease in household contacts of patients with pulmonary tuberculosis. Turkish Respiratory Journal 9(1): 034-037.

[38] Wells W. F. and Stone W. R. (1934). On air-borne infection, study iii viability of droplet nuclei infection. Am J Epidemiol 20(3): 619-627.

[39] Centers for Disease Control and Prevention (CDC. (2013). Transmission of mycobacterium tuberculosis in a high school and school-based supervision of an isoniazid-rifapentine regimen for preventing tuberculosis - colorado, 2011-2012. MMWR. Morbidity and mortality weekly report 62(39): 805.

[40] Loudon R. G. and Roberts R. M. (1967). Droplet explusion from the respiratory tract. The American Review of Respiratory Disease 95(3): 435-442.

[41] Xiaolei G., Yuguo L., and Gabriel M. L. (2009). Ventilation control of indoor transmission of airborne diseases in an urban community. Indoor Built Environ 18(3): 205-218.

[42] Furuya H., Nagamine M., and Watanabe T. (2009). Use of a mathematical model to estimate tuberculosis transmission risk in an internet cafe. Environ Health Prev Med 14: 96-102.

[43] Lin H. H., Murray M., Cohen T., Colijn C., and Ezzati M. (2008). Effects of smoking and solid-fuel use on copd, lung cancer, and tuberculosis in china: a time-based, multiple risk factor, modelling study. The Lancet 372(9648): 1473-1483.

[44] Mahomed H., Ehrlich R., Hawkridge T., Hatherill M., Geiter L., Kafaar F., Abrahams D. A., Mulenga H., Tameris M., Geldenhuys H., Hanekom W. A., Verver S., and Hussey G. D. (2013). Screening for TB in high school adolescents in a high burden setting in south africa. Tuberculosis 93(3): 357-362.

[45] Baussano I., Williams B. G., Nunn P., Beggiato M., Fedeli U., and Scano F. (2010). Tuberculosis incidence in prisons: a systematic review. PLoS Medicine 7(12): e1000381.

[46] Emmerich S. J. and Persily A. K. (2001). State-of-the-art review of carbon dioxide demand controlled ventilation technology and application. NISTIR 6729.

[47] Hodgson M. J., Miller S. L., Li Y., McCoy W. F., Parsons S. A., Schoen L. J., and Sekhar C. (2009). ASHRAE position document on airborne infectious diseases.

[48] Horna-Campos O. J., Bedoya-Lama A., Romero-Sandoval N. C., and Martín-Mateo M. (2005). Risk of tuberculosis in public transport sector workers, lima, peru. Int J Tuberc Lung Dis 14(6): 714-719.

[49] Marais B. J., Obihara C. C., Warren R. M., Schaaf H. S., Gie R. P., and Bekker D. G. (2005). The burden of childhood tuberculosis: a public health perspective. Int J Tuberc Lung Dis 9(12): 1305–1313.

[50] Nainggolan J., Supian S., Supriatna A. K., and Anggriani N. (2013). Mathematical model of tuberculosis transmission with reccurent infection and vaccination. In Journal of Physics: Conference Series (Vol. 423, No. 1, p. 012059). IOP Publishing.

[51] Noakes C. J. and Sleigh P. A. (2009). Mathematical models for assessing the role of airflow on the risk of airborne infection in hospital wards. J R Soc Interface 6: S791-800.

[52] Padilla-Carlin D. J., McMurray D. N., and Hickey A. J. (2008). The guinea pig as a model of infectious diseases. Comparative Medicine 58(4): 324-340.

[53] Kranzer K., Houben R. M., Glynn J. R., Bekker L. G., Wood R., and Lawn S. D. (2010). Yield of hiv-associated tuberculosis during intensified case finding in resource-limited settings: a systematic review and meta-analysis. The Lancet Infectious Diseases 10(2): 93-102.

[54] Lönnroth K., Williams B. G., Stadlin S., Jaramillo E., and Dye C. (2008). Alcohol use as a risk factor for tuberculosis – a systematic review. Public Health 8: 289.

[55] Middelkoop K., Bekker L. G., Myer L., Dawson R., and Wood R. (2008). Rates of tuberculosis transmission to children and adolescents in a community with a high prevalence of HIV infection among adults. Clinical Infectious Diseases 47(3): 349-355.

[56] Middelkoop K., Mathema B., Myer L., Shashkina E., Whitelaw A., Kaplan G., Kreiswirth B., Wood R., and Bekker L-G. (2014). Transmission of TB in a high HIV prevalent south african community. Journal of Infectious Diseases: (Epub ahead of print).

[57] Middelkoop K., Bekker L. G., Morrow C., and Wood R. (2009). Childhood tuberculosis infection and disease: a spartial and temporal transmission analysis in south african township. S Afr Med J 99: 738-743.

[58] Gammaitoni L. and Nucci M. C. (1997). Using a mathematical model to evaluate the efficacy of TB control measures. Emerg Infect Dis 3: 335-342.

[59] Riley R. L., Mills C. C., Nyka W. Weinstock N., Storey P. B., Sultan L. U., Riley M. c., and Wells W. F. (1959).

[60] Riley R. L., Mills C. C., O'Grady F., Sultan L. U., Wittstadt F., and Shivpuri D. N. (1962). Infectiousness of air from a tuberculosis ward. ultraviolet irradiation of infected air: Comparative infectiousness of different patients. Am Rev Respir Dis 85: 511–525.

[61] Baker M., Das D., Venugopal K., and Howden-Chapman P. (2007). Tuberculosis associated with household crowding in a developed country. J Epidemiol Community Health 62: 715–721.

[62] Blower S. M., Mclean A. R., Porco T. C., Small P. M., Hopewell P. C., Sanchez M. A., and Moss A. R. (1995). The intrinsic transmission dynamics of tuberculosis epidemics. Nature Medicine 1(8): 815-821.

[63] Blower S. M., Mclean A. R., Porco T. C., Small P. M., Hopewell P. C., Sanchez M. A., and Moss A. R. (1995). The intrinsic transmission dynamics of tuberculosis epidemics. Nature Medicine 1(8): 815-821.

[64] Gomes M. G. M., Rodrigues P., Frank M. Hilker F. M., Mantilla-Beniers N. B., Muehlen M., Paulo A. C., and Medley G. F. (2007). Implications of partial immunity on the prospects for tuberculosis control by post-exposure interventions. Journal of Theoretical Biology 248: 608–617.

[65] Gomes M. G. M., Franco A. O., Gomes M. C., and Medley G. F. (2004). The reinfection threshold promotes variability in tuberculosis epidemiology and vaccine efficacy.

Proceedings of the Royal Society of London. Series B: Biological Sciences 271(1539): 617-623.

[66] Issarow C. M., Mulder N., and Wood R. (2015). Modelling the risk of airborne infectious disease using exhaled air. Journal of Theoretical Biology 372: 100-106.

[67] Issarow C. M., Wood R., and Mulder N. (2016). Seminal mycobacterium tuberculosis in vivo transmission studies: Reanalysis using probabilistic modelling. Mycobact Dis 6: 217. doi:10.4172/2161-1068.1000217.

[68] Lygizos M., Shenoi S. V., Brooks R. P., Bhushan A., Brust J. C., Zelterman D., and Friedland G. H. (2013). Natural ventilation reduces high TB transmission risk in traditional homes in rural kwazulu-natal, south africa. BMC Infectious Diseases 13(1): 300.

[69] Mehra M., Cossrow N., Kambilli C., Underwood R., Makkar R., and Potluri R. (2013). Assessment of tuberculosis burden in china using a dynamic disease simulation model. Int J Tuberc Lung Dis 17(9): 1186-1194.

[70] Murray M., Oxlade O., and Lin H. H. (2011). Modeling social, environmental and biological determinants of tuberculosis. Int J Tuberc Lung Dis 15(6): S64-S70.

[71] Blaser N., Zahnd C., Hermans S., Salazar-Vizcaya L., Estill J., Morrow C., and Wood R. (2015). Tuberculosis in cape town: An age-structured transmission model. Epidemics 14: 54-61.

[72] Classen C. N., Warren R., Richardson M., Hauman J. H., Gie R. P., Ellis J. H., and Beyers N. (1999). Impact of social interactions in the community on the transmission of tuberculosis in a high incidence area. Thorax 54(2): 136-140.

[73] Rudnick S. N. and Milton D. K. (2003). Risk of indoor airborne infection transmission estimated from carbon dioxide concentration. Indoor Air 13(3): 237-245.

[74] Sze To G. N. and Chao C. Y. H. (2010). Review and comparison between the wells–riley and dose-response approaches to risk assessment of infectious respiratory diseases. Indoor Air 20(1): 2-16.

[75] Diekmann O., Heesterbeek J. A. P., and Roberts M. G. (2009). The construction of next-generation matrices for compartmental epidemic models. Royal Society Interface 7(47): 873–885.

[76] Matuka O., Singh T. S., Bryce E., Yassi A., Kgasha O., Zungu M., Kyaw K., Malotle M., Renton K., and O'Hara L. (2015). Pilot study to detect airborne mycobacterium tuberculosis exposure in a south african public healthcare facility outpatient clinic. Journal of Hospital Infection doi: 10.1016/j.jhin.2014.11.013.

[77] Medical Research Council of South Africa. Technical specifications for uvgi equipment requested as donation for tuberculosis research. Available at URL: http://www.mrc.ac.za/hr/docs/airfacility.pdf. Accessed 23rd June 2015.

[78] Word Health Organization. Guidance for national tuberculosis programmes on the management of tuberculosis in children. WHO/HTM/TB/2006.371.

[79] Word Health Organization. Who policy on TB infection control in health-care facilities, congregate settings and households. WHO/HTM/TB/2009.41.

[80] Word Health Organization. Global tuberculosis report 2012. WHO/HTM/TB/2012.6.

[81] World Health Organization. Tuberculosis in prisons 2014. Available at URL: http://www.who.int/tb/challenges/prisons/story$_1$/en/.

[82] World Health Organization. Global tuberculosis report 2013. WHO/HTM/TB/2013.11.

[83] World Health Organization. Global tuberculosis report 2014. WHO/HTM/TB/2014.08.

[84] World Health Organization. Global tuberculosis report 2015. WHO/HTM/TB/2015.22.

[85] World Health Organization. Global tuberculosis report 2016. WHO/HTM/TB/2016.13.

[86] Fennelly K. P. and Jones-López E. C. (2015). Quantity and quality of inhaled dose predicts immunopathology in tuberculosis. Frontiers in Immunology 6.

[87] Johnstone-Robertson S. P., Mark D., Morrow C., Middelkoop K., Chiswell M., Aquino L. D., and Wood R. (2011). Social mixing patterns within a south african township community: implications for respiratory disease transmission and control. American Journal of Epidemiology kwr 251.

[88] Chen P-S. and Li C-S. (2008). Concentration profiles of airborne mycobacterium tuberculosis in a hospital. Aerosol Science and Technology 42(3): 194-200.

[89] Andrews J. R., Hatherill M., Mahomed H., Hanekom W. A., Campo M., Hawn T. R., Wood R., and Scriba T. J. (2015). The dynamics of quantiferon-TB gold in-tube conversion and reversion in a cohort of south african adolescents. Am J Respir Crit Care Med 191(5): 584-91.

[90] Andrews J. R., Morrow C., and Wood R. (2012). Modeling the role of public transportation in sustaining tuberculosis transmission in south africa. American Journal of Epidemiology 177(6): 556-561.

[91] Andrews J. R., Noubary F., Walensky R. P., Cerda R., Losina E., and Horsburgh C. R. (2012). Risk of progression to active tuberculosis following reinfection with mycobacterium tuberculosis. Clinical Infectious Diseases 54(6): 784-791.

[92] Andrews J. R., Morrow C., Walensky R. P., and Wood R. (2014). Integrating social contact and environmental data in evaluating tuberculosis transmission in a south african township. Journal of Infectious Diseases 210(4): 597-603.

[93] Escombe A. R., Moore D. A., Gilman R. H., Pan W., Navincopa M., Ticona E., Martinez C., Caviedes L., Sheen P., Gonzalez A., Noakes C. J., Friedland J. S., and Evans C. A. (2008). The infectiousness of tuberculosis patients coinfected with HIV. PLoS Med 5: e188.

[94] Escombe A. R., Moore D. A., Gilman R. H., Navincopa M., Ticona E., Mitchell B., and Evans C. A. (2009). Upper-room ultraviolt light and negative air ionization to prevent tuberculosis transmission. PLoS Medicine 6(3): e100004.

[95] Roberts J. R., Mason B. W., Paranjothy S., and Palmer S. R. (2012). The transmission of tuberculosis in schools involving children 3 to 11 years of age. Pediatric Infectious Disease 31(1): 82-84.

[96] Wood R., Johnstone-Robertson S., and Uys P. (2010). Tuberculosis transmission to young children in a south african community: Modelling household and community infection risks. Clin Infect Dis 51(4): 401-408.

[97] Wood R., Johnstone-Robertson S., Uys P., Hargrove J., Middelkoop K., Lawn S. D., and Bekker L. G. (2010). Tuberculosis transmission to young children in a south african community: Modeling household and community infection risks. Clinical Infectious Diseases 51(4): 401–408.

[98] Wood R., Liang H., WU H., Middelkoop K., Oni T., Rangaka M. X., Wilkinson R. J., Bekker L. G., and Lawn S. D. (2009). Changing prevalence of tuberculosis infection with increasing age in high burden townships in south africa. Int J Tuberc Lung Dis 14(4): 406-412.

[99] Wood R., Morrow C., Barry 3rd C. E., Bryden W. A., Call C. J., Hickey A. J., Rodes C. E., Scriba T. J., Blackburn J., Issarow C., Mulder N., Woodward J., Moosa A., Singh

V., Mizrahi V., and Warner D. F. (2016). Real-time investigation of tuberculosis transmission: Developing the respiratory aerosol sampling chamber (RASC). PloS One 11(1): e0146658.

[100] Wood R., Morrow C., Ginsberg S., Piccoli E., Kalil D., Sassi A., and Andrews J. R. (2014). Quantification of shared air: A social and environmental determinant of airborne disease transmission. PloS One 9(9): e106622.

[101] Wood R., Johnstone-Robertson S., and Bekker L. G. (2011). Tuberculosis control has failed in south africa - time to reappraise strategy. S Afr Med J 101: 111-114.

[102] Wood R., Lawn S. D., Caldwell J., Kaplan R., Middelkoop K., and Bekker L. G. (2011). Burden of new and recurrent tuberculosis in a major south african city stratified by age and HIV-status. plos One 6(10): e25098.

[103] Wood R., Racow K., Bekker L. G., Morrow C., Middelkoop K, Mark D., and Lawn S. D. (2012). Idoor social networks in a south africa township: Potential contribution of location to tuberculosis transmission. plos One 7(6): e39246.

[104] Yusuf H. R., Braden C. R., Greenberg A. J., Weltman A. C., Onorato I. M., and Valway S. E. (1997). Tuberculosis transmission among five school bus drivers and students in two new york counties. Pediatrics 100(3): e9-e9.

[105] Dharmadhikari A. S., Mphahlele M., Stoltz A., Venter K., Mathebula R., Masotla T., and Nardell E. A. (2012). Surgical face masks worn by patients with multidrug-resistant tuberculosis: Impact on infectivity of air on a hospital ward. American Journal of Respiratory and Critical Care Medicine 185(10): 1104-1109.

[106] Dharmadhikari A. S., Basaraba R. J., Van Der Walt M. L., Weyer K., Mphahlele M., Venter K., and Nardell E. A. (2011). Natural infection of guinea pigs exposed to patients with highly drug-resistant tuberculosis. Tuberculosis (Edinb) 91(4): 329-38.

[107] Hermans S., Boulle A., Caldwell J., Pienaar D., and Wood R. (2015). Temporal trends in tb notification rates during art scale-up in cape town: an ecological analysis. Journal of the International AIDS Society 18(1).

[108] Hermans S., Horsburgh Jr C. R., and Wood R. (2015). A century of tuberculosis epidemiology in the northern and southern hemisphere: the differential impact of control interventions. PloS One 10(8): e0135179.

[109] Johnstone-Robertson S., Lawn S. D., Welte A., Bekker L. G., and Wood R. (2011). Tuberculosis in a south african prison - a transmission modelling analysis. SAMJ: South African Medical Journal 101(11): 809-813.

[110] Verver S., Warren R. M., Beyers N., Richardson M., van der Spuy G. D., Borgdorff M. W., and van Helden P. D. (2005). Rate of reinfection tuberculosis after successful treatment is higher than rate of new tuberculosis. American journal of Respiratory and Critical Care Medicine 171(12): 1430-1435.

[111] Verver S., Warren R. M., Munch Z., Richardson M., van der Spuy G. D., and Borgdorff M. W. (2004). Proportion of tuberculosis transmission that takes place in households in a high incidence area. Lancet 363: 212e4.

[112] Cohen T., Colijn C., Finklea B., and Murray M. (2007). Exogenous re-infection and the dynamics of tuberculosis epidemics: local effects in a network model of transmission. Journal of the Royal Society Interface 4(14): 523-531.

[113] Richardson E. T., Morrow C. D., Kalil D. B.and Bekker L. G., and Wood R. (2014). Shared air: A renewed focus on ventilation for the prevention of tuberculosis transmission. PloS One 9(5): e96334.

[114] A New Tool to Diagnose Tuberculosis: The Xpert MTB/RIF Assay. Available at url: https://www.cdc.gov/tb/publications/factsheets/pdf/xpertmtbrifassayfactsheet$_final$.pdf. Accessed: 04th Nov 2016.

[115] van Zyl-Smit R. N., Allwood B., Stickells D., Symons G., Abdool-Gaffar S., Murphy K., and Richards G. A. (2013). South african tobacco smoking cessation clinical practice guideline. SAMJ: South African Medical Journal 103(11): 869-876.

[116] Comstock G. W., Baum C., and Snider Jr D. E. (1979). Isoniazid prophylaxis among alaskan eskimos: A final report of the bethel isoniazid studies 1, 2. American Review of Respiratory Disease 119(5): 827-830.

[117] Li Y., Leung G. M., Tang J. W., Yang X., Chao C. Y. H., Lin J. Z., and Yuen P. L. (2007). Role of ventilation in airborne transmission of infectious agents in the built environment–a multidisciplinary systematic review. Indoor Air 17(1): 2-18.